TITLE:
INTEGRATED SEDIMENT APPROACH AND IMPACTS OF CLIMATE CHANGE ON RESERVOIR SEDIMENTATION(Dissertation_全文)

AUTHOR(S):
CHUTACHINDAKATE, CHADIN

CITATION:
CHUTACHINDAKATE, CHADIN. INTEGRATED SEDIMENT APPROACH AND IMPACTS OF CLIMATE CHANGE ON RESERVOIR SEDIMENTATION. 京都大学, 2009, 博士(工学)

ISSUE DATE:
2009-09-24

URL:
https://doi.org/10.14989/doctor.k14934

RIGHT:
許諾条件により本文は2010-03-24に公開

京都大学学術情報リポジトリ
KURENAI 紅
Kyoto University Research Information Repository

INTEGRATED SEDIMENT APPROACH AND IMPACTS OF CLIMATE CHANGE ON RESERVOIR SEDIMENTATION

JULY 2009

CHUTACHINDAKATE CHADIN

INTEGRATED SEDIMENT APPROACH AND IMPACTS OF CLIMATE CHANGE ON RESERVOIR SEDIMENTATION

By

Chadin CHUTACHINDAKATE

A dissertation submitted in partial fulfillment of the requirements for the degree of Doctor of Philosophy

Examination Committee: Prof. Tetsuya SUMI (Chairperson)
Prof. Takeshi TAMURA
Prof. Masaharu FUJITA

Nationality: Thai
Previous Degree: Master of Engineering
Water Engineering and Management
Asian Institute of Technology
Thailand

Kyoto University
Department of Civil and Earth Resource Engineering
Japan

July 2009

Acknowledgements

First of all I would like to express my sincere gratitude to Prof. Tetsuya Sumi, my advisor, without his valuable advice and guidance; it was hardly possible to complete this work. I would like to thank my advisor so much to give me the good chance and best experience to study in Kyoto University, Japan. Working at this laboratory, I feel that I am working at home or here, it likes my 2nd home.

A sincere gratitude also goes to Prof. Takeshi Tamura for his valuable suggestion, support, kindness guidance both study life and daily life in Kyoto.

I would like to express my profound gratitude to Prof. Masaharu Fujita, my committee member for his helpful comments and valuable suggestions.

Sincere thanks attend to Dr. Junichi Kobayashi for his helpful suggestion, friendly and kindly support me about my research and also my life style in Japan.

Sincere thanks also attend to Dr. Hitoshi Yashikawa and Dr. Jun Saito for their suggestion about Japanese culture and tradition. Also warm thanks go to all students of the Applied Mechanics Laboratory, Department of Civil and Earth Resources Engineering, Kyoto University and Laboratory of Socio and Eco Environment Risk Management, Water Research Center, Disaster Prevention Research Institute (DPRI), Kyoto University for their support and friendship. Sincere thanks go to Dr. Yasuhiro Takemon and Dr. Sameh Kantoush for their suggestion and support my research.

Sincere thanks are extended to NEWJEC, Osaka branch office; it was hardly to complete some part of my research if it's without this internship work. Sincere thanks are extended to all staffs and members of river engineer group for their willingness to supply the necessary data, teach me how to work and give me the good memory about office's environment.

Sincere thanks are also extended to Managawa dam office, Fukui Prefecture, for their willingness to supply the necessary data for analysis in this study.

Also sincere thanks are extended to Japanese Government which sponsored the MEXT scholarship for my study at Kyoto University, Japan.

I would like to express my love and respect to my Thai and Japanese friends, seniors and juniors here in Kyoto University for extending helping hand to complete the study. Especially to Mr. Thamrongsak Suwanishwong my good friend, I would like to share this Ph.D. degree to him too.

Finally, I would like to express my sincere gratitude to my parents, brother and sisters for their love, help and support which made possible to pursue my study.

Abstract

Nowadays the sediment becomes one significant problem to reservoir watershed and it is effect and related to reservoir operation system. As the research topic, an integrated sediment approach and impacts of climate change on reservoir sedimentation, there are three main parts demonstrated in this research that all parts are related together with sediment point of view. Annual sediment depositing volume in reservoir was estimated by general soil loss equation but the efficiency was not acceptable. The first part of this study shows that the efficiency is improved by using general soil loss equation with sediment transport model. The second part is about monitoring the sediment inflow to reservoir. The important parameter to operate the reservoir is turbidity concentration of flow into dam, in the second part the suspended sediment concentration was predicted by real time therefore the reservoir operation to release turbid flow will get more efficiency. For last part, in the next future year sediment yield and water resources on the study area were investigated by extrapolated temperature and rainfall data then the results will be useful for long term reservoir operation system.

First part, the integrated sedimentation was used to model an annual depositing sediment volume in reservoir. Sediment system in watershed includes not only sediment yield but also sediment transportation along the rivers. In this study, the Geographic Information System (GIS) incorporated with sediment yield model can be assisted to enhance the evaluation estimation of soil erosion. Surface erosion on Managawa river basin is then computed with the Modified Universal Soil Loss Equation (MUSLE) and it is verified to reflect the hydrological processes to which it will be able to estimate soil losses. In the sediment transport routing module, total load equation is applied to carry sediment from soil surface erosion to deposit in Managawa dam. According to annual accumulation sediment volume data in Managawa reservoir during 1981 – 2004, the establish model and simulation results are satisfied. The efficiency of the Modified Universal Equation with sediment routing in rivers is more than the simple Modified Universal Equation.

Second part, the real time suspended sediment concentration forecasting was used for monitoring the turbidity flow on the upstream of reservoir. The sediment flow into the reservoir is a factor for decision support in real time reservoir operation therefore the serious area of sediment erosion of Managawa river basin, Japan is monitored by suspended sediment gauge. The hourly suspended sediment concentration at Okumotani station; the upstream of Managawa reservoir, was monitored and estimated by the artificial neural network (ANN) model that the input data were rainfall data and its products. This artificial neural network (ANN) was calibrated and validated by using recently suspended sediment data on heavy rainfall events from December 2006 to January 2008. Choosing an appropriate neural network structure and providing field data to that network for training purpose are address by using a constructive back propagation algorithm. Rainfall and its products; the computed discharge from rainfall runoff model and rainfall intensity, were applied as inputs to neural network. It is demonstrated that the artificial neural network (ANN) is capable of modeling the hourly suspended sediment

concentration with good accuracy and the neural network model has efficiency more than the multiple linear regression (MLR) model and the sediment rating curve (SRC) model.

Last part, the effects of climate change on water resources and sediment yield were investigated by climate change scenarios which the main meteorological data were rainfall and temperature data. Historic trends of temperature and precipitation on Managawa river basin were detected by parametric and nonparametric tests. The daily mean temperature data from 1981 to 2008 at Ono station, Fukui prefecture was the representative of temperature on the study area. The hourly rainfall data from 1981 to 2008 were obtained by Managawa dam office processed with the reliability of data and weighted data. From monotonic and step trend tests, the temperature trend was found herein to follow a clear and steady trend every month. The average annual temperature exhibited an increasing trend with a magnitude 0.4 ºC per decade. Application of the Mann-Kendall and Mann-Whitney test for rainfall time series on Managawa river basin showed no step change and no monotonic trend in Managawa precipitation. The average annual precipitation exhibited a decreasing trend with a magnitude 52 mm per decade. The weather generating models both temperature and rainfall expressed the high efficiency for validation step. The generated weather series 2009 - 2060; temperature and precipitation height, for future climatic conditions can be inputted into the soil loss equation to investigate the change in sediment sources and extrapolated rainfall can be inputted to rainfall runoff model to investigate the change in runoff for future climate change condition. The sediment yield rate should be reduced because of the decrease in precipitation.

Table of Contents

CHAPTER	TITLE	PAGE
	Title Page	i
	Acknowledgements	iii
	Abstract	iv
	Table of Contents	vi
	List of Tables	viii
	List of Figures	ix
	List of Illustrations	xi
1	Introduction	1
	1.1 Description of study area	1
	1.2 Problem statement	4
	1.3 Objectives	5
	1.4 Scope and limitation of this study	5
2	Literature review	7
	2.1 Hydrologic and hydrodynamic models	7
	2.2 Sediment yield model	8
	2.3 Sediment prediction model	10
	2.4 Climate change model	13
3	Rainfall runoff model	16
	3.1 Theoretical of NAM model	16
	3.2 Data collection and analysis for rainfall runoff model	22
	3.3 Results analysis	25
	3.4 Conclusions	29
4	Hydrodynamics model	30
	4.1 Theoretical of HD model	30
	4.2 Data collection and analysis for hydrodynamics model	37
	4.3 Results analysis	42
	4.4 Conclusions	45
5	Integrated sedimentation model	46
	5.1 Sediment yield model	46
	5.2 Sediment transport model	48
	5.3 Integrated sedimentation model	49
	5.4 Results analysis	53
	5.5 Discussion and conclusions	55
6	Sediment prediction model	59
	6.1 Artificial neural network model	60
	6.2 Multiple linear regression model	70

Table of Contents (Continued)

CHAPTER	TITLE	PAGE
	6.3 Sediment rating curve model	70
	6.4 Data measurement and location	71
	6.5 Results analysis	73
	6.6 Discussion and conclusions	77
7	Effects of climate change on water resources and sediment yield	81
	7.1 Climate change information	81
	7.2 Data collection and processing	82
	7.3 Analysis of long term trends in meteorological variables	84
	7.4 Weather generating model	89
	7.5 Impact of global warming on water resources	93
	7.6 Discussion and conclusions	96
8	Summary, conclusions and recommendation	98
	8.1 Summary	99
	8.2 Conclusions	101
	8.3 Recommendation	103
	References	105
	Appendixes	109

List of Tables

TABLE	TITLE	PAGE
1.1	The properties of Managawa dam, Sasougawa dam and Kumokawa dam	3
3.1	Calibration parameters and default hypercube search space	21
3.2	Rain gauge station and available hourly rainfall data	22
3.3	Thiessen Parameters	24
3.4	NAM model parameters	25
3.5	Statistical Performance Indices of NAM Model Calibration and Verification	27
4.1	List of stream flow station and recording year in the upstream of Managawa River Basin	38
4.2	Location of each cross section	41
4.3	Roughness coefficient of bed material	43
4.4	Statistical performance index during flood period of HD Model calibration and verification	43
5.1	Topographic information of each sub-basin	53
5.2	Annual average soil surface erosion from MUSLE	54
5.3	Observed and computed sediment volume, 1981-2004, in Managawa Dam	55
6.1	Correlation coefficients between input variables and suspended sediment	74
6.2	Performances of neural networks	75
6.3	Performances of neural networks, multiple linear regression and sediment rating curve models	77
7.1	The gauge stations used in this study and their record length	82
7.2	Statistics for the annual temperature and precipitation time series	86
7.3	Partitions of the temperature and rainfall time series	87
7.4	t-test results of step trend for temperature and rainfall time series	87
7.5	Mann-Whitney test results of step trend for temperature and rainfall time series	88
7.6	Monotonic trend test for temperature and rainfall time series	88
7.7	Monotonic trend test for rainfall time series during dry season and wet season	89
7.8	The lag-one autocorrelation coefficient of temperature for each Month	91
7.9	Monthly statistical parameters for temperature (1981-2008)	93
7.10	Monthly statistical parameters for rainfall (1981-2008)	94
7.11	Annual average soil surface erosion from MUSLE (2009-2060)	96

List of Figures

FIGURE	TITLE	PAGE
1.1	Managawa river basin	1
1.2	Flood control chart	2
1.3	Capacity of the reservoir	2
1.4	Scope of the study	6
3.1	NAM Model Concept	16
3.2	Structure of the NAM model	18
3.3	The consistency of rainfall station record in the upstream of Managawa river basin by using Double Mass Curve	23
3.4	Thiessen Polygon of this study area	24
3.5	Annual weighting rainfall on Mangawa river basin	25
3.6	Comparison between observe and computed discharge data in 2004	27
3.7	Comparison between observe and computed discharge data in 2003	28
3.8	Comparison between observe and computed discharge data in 2002	28
4.1	Diagram of MIKE 11 HD model setup	30
4.2	Cross Section Divided in a Series of Rectangular Channels	33
4.3	Channel Section with Computational Grid	34
4.4	Centered 6-points Abbott Scheme	35
4.5	Centering of Continuity Equation in 6-point Abbott Scheme	35
4.6	Centering of Momentum Equation in 6-point Abbott Scheme	36
4.7	Selected stream flow stations in the upstream of Managawa dam, UTM coordinate	38
4.8	Locations of river cross sections in Managawa river basin, UTM coordinate	39
4.9	Cross sections of beginning and ending of each branch	40
4.10	Annual rainfall at Managawa river basin from 1981 – 2004	42
4.11	Comparison between observe and computed water level at Nagashima station, 2004	44
4.12	Comparison between observe and computed water level at Nagashima station, 2002	44
4.13	Comparison between observe and computed water level at Nagashima station, 1998	45
5.1	Sub-basins in this study	47
5.2	Location that sediment yield of each sub-basin from MUSLE supplied to the main river system	48
5.3	Land use in 1976, 1987, 1991 and 1997	50
5.4	Scope of this part study	51
5.5	Hydrodynamic boundary condition diagram	52
5.6	Sediment distribution curve of 4 samplings in Managawa Dam, 1998	52

List of Figures (Continued)

FIGURE	TITLE	PAGE
5.7	Sensitivity analysis of grain size diameter effect to accumulation sediment volume in 1995	53
5.8	Annual rainfall, observed and computed accumulation sediment volume	56
5.9	Relationship between Annual Discharge and Annual Rainfall, 1981-2004	57
5.10	Relationship between Annual Discharge and Computed Sediment Volume	57
5.11	Relationship between Annual Discharge and Observed Sediment Volume	58
6.1	Typical Three Layers Neural Network Architecture	60
6.2	Flowchart of Calculation Process in Back Propagation Neural Network Model	65
6.3	Flowchart of Back Propagation Training and Testing Process	66
6.4	Sigmoid Logistics Activation Function with Its Derivative	67
6.5	Artificial Neural with Activation Function	70
6.6	Turbidity measuring equipment: Compact-HTW JFE-Alec Electron Co.Ltd	71
6.7	Suspended Sediment Gauge located at Okumotani catchment	72
6.8	Intake at the Okumotani power station	72
6.9	Weir at Okumotani station	73
6.10	Comparisons between the observed and computed suspended sediment concentration of each model; case 13, 19, 21, 25 and 26 respectively	77
7.1	Maximum, minimum and average monthly rainfall at Managawa river basin; 1981-2008	83
7.2	Maximum, minimum and average monthly temperature at Ono station; 1981-2008	83
7.3	Annual average temperature, 10 year moving average and average temperature before and after 1995	86
7.4	Annual average rainfall, 10 year moving average and average Rainfall	86
7.5	Validation results of the temperature generating model	91
7.6	Validation results of precipitation generating model	93
7.7	Generated mean temperature for the future year	94
7.8	Generated annual precipitation height for the future year	95

List of Illustrations

CQOF	the overland flow runoff coefficient ($0 \leq CQOF \leq 1$)
TOF	the threshold value for overland flow ($0 \leq TOF \leq 1$)
CKIF	the time constant for interflow
TIF	the root zone threshold value for interflow ($0 \leq TIF \leq 1$)
OF	the overland flow (mm/hour)
OF_{min}	the upper limit for linear routing
TG	the root zone threshold value for groundwater recharge ($0 \leq TG \leq 1$)
EI	Efficiency Index
SR	the variation explained by the model
ST	total variation of the discharge
SE	sum of square errors
Qi	observed discharge at time i
Qm	mean value of observed discharge
Fi	calculated discharge at time i
N	number of data points
Q_{op}	observed peak
Q_{sp}	simulated peak
$Q_{o,i}$	observed value at time step i
$Q_{s,i}$	simulated value at time step i
T_{op}	time of observed peak
T_{sp}	time of simulated peak
n	number of time steps
ρ	the density
H	the depth
b	the width
$\bar{u}$	the average velocity along the vertical
α	the vertical velocity-distribution coefficient
q	lateral inflow
A_{0j}	the surface area between grid point j-1 and j
A_{0j+1}	the surface area between grid point j and j+1
$\Delta 2x_j$	the distance between point j-1 and j+1
Y	the sediment yield on a given day (ton)
Q_s	the surface runoff (mm)
q_p	the peak runoff rate (m^3/s)
A_{area}	area (km^2)
K	the USLE soil erodibility factor
C	the USLE cover and management factor
P	the USLE support practice factor
LS	the USLE topographic factor
$CFRG$	the coarse fragment factor
q_p	the peak runoff rate (m3/s)
c	the runoff coefficient
i	the rainfall intensity (mm/hr)
A_{eo}	the observed soil loss for event e

List of Illustrations (Continued)

A_{ep}	the predicted soil loss
$A_{\ln m}$	the mean value of $\ln(A_{eo})$ for all the events selected
$W_{ji,m}(n)$	weight of the effect received by j^{th} unit in layer m caused by i^{th} unit in layer (m-1) at n^{th} iteration.
$O_{j,m}$	output of the j^{th} element in layer m (m=1,2,…,L)
I_i	i^{th} element of the input
t_j	j^{th} element of the desired output (target)
n_m	number of units in the m^{th} layer
$\delta_{j,m}$	the value of δ for neuron j in layer m
t_j	target value of neuron j in output layer
$O_{j,m}$	output of neuron j in layer m
$N_{j,m}$	Net of neuron j in layer m
$\theta_{j,m}$	bias value for neuron j in layer m
η	learning parameter
α	momentum constant
$W_{ji,m}(n)$	weight value between node j in layer m and node i at n iteration
$W_{ji,m}(n+1)$	weight value between node j in layer m and node i at n+1 iteration
$\Delta W_{ji,m}(n)$	weight change between node j in layer m and node I at n iteration.
$\Delta W_{ji,m}(n+1)$	weight change between node j in layer m and node I at n+1 iteration
SS	suspended sediment concentration
R	rainfall
T	temperature
A	rainfall in two hours
D	the absolute of discharge changing
RMSE	root mean square error
t_k	the temperature on day *k*
μ_T	the mean temperature for a period (1 month)
σ_T	the standard deviation of temperature during that period
ρ_{1T}	the lag-one autocorrelation coefficient of temperature during that period
υ_k	the random standard normal variation
S_{T_j}	the coefficient of the linear regression equation relating mean temperature in month *j* to time (year)
$\bar{\mu}'_{T_j}$	the mean value of mean temperature in month *j*
ρ'_{T_j}	the autocorrelation coefficient of mean temperature values between months *j* and *j-1*
y_0	the initial year of generation
υ_{ij}	the random standard normal variation
p_t	the precipitation height on day *t*
u_t	the random variable between 0 and 1

CHAPTER 1
Introduction

Nowadays there are so many existing dams in the world and the number of construction of new dams is reducing therefore it is necessary to improve operation and management system or reconstruction of existing dams. Because of climate change and human activities on the reservoir watershed, the sediment becomes one of big problem on reservoir area. Sedimentation; sediment yield and sediment transport, and sediment management are important factors to reservoir operation and management. In this study, the Managawa river basin is the representative of the watershed to study on sediment problem.

1.1 Description of study areas

1.1.1 Case study in Japan: Managawa river basin

Managawa Dam constructed during 1965-1977 in Fukui prefecture is located at latitude 35º 55' 50" N and longitude 136º 32' 31" E. Managawa Dam is a multi-propose concrete arch dam with 127.5 m height, 357 m width and 115 MCM capacity designed for irrigation, water supply and power generation where Managawa river is a tributary of Kuzurui river which the dam configuration is shown in Table 1.1.

Catchment area above the dam is about 223.7 km^2 that the mean elevation is 830 m above mean sea level and land slope is about 0.45. Since there are Kumokawa Dam and Sasougawa Dam situated on up stream of Managawa Dam as shown in Figure 1.1**,** sediment will be captured by those dams but Kumokawa Dam has been filled full by sediment. Therefore sediment supply to Managawa Dam is also generated from watershed above Kumokawa Dam. During the study period, 1981-2006, the average annual rainfall is 2391 mm. The area is covered by forest where accounts for 94% area of total watershed. The major soil types in the study area are sandstone, mudstone and conglomerate (Managawa Dam office, 2005).

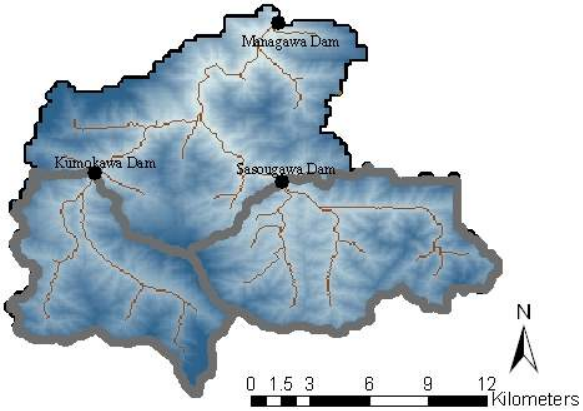

Figure 1.1: Managawa river basin

- The main purposes of Managawa dam

(1) Flood control

The maximum capacity for flood inflow to this dam is about 2,700 m^3/s as shown in Figure 1.2 and it will release water to downstream by small effect to downstream during flood event.

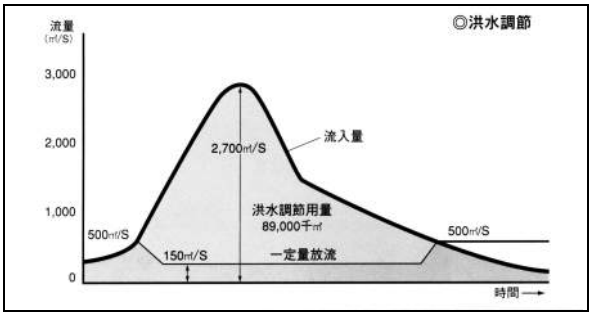

Figure 1.2: Flood control chart

(2) Ecology system at down stream area

The dam operation rule or water release pattern of this dam is trying to keep the ecology system at down stream alive.

(3) Electric generating

Hydropower plant located on this dam can generate the maximum electric about 14,000 kW.

Company:	Fukui prefecture corporate agency
Waterway type:	Conduit diameter 2.80 m. and 2.2 km. long
Capacity:	66,421 MWH
Output:	Peak time 14,000 kW Normal time 680 kW
Water discharge:	Peak time 15.0 m^3/s Normal time 3.37 m^3/s
Net head:	Peak time 109.80 m. Normal time 118.0 m.

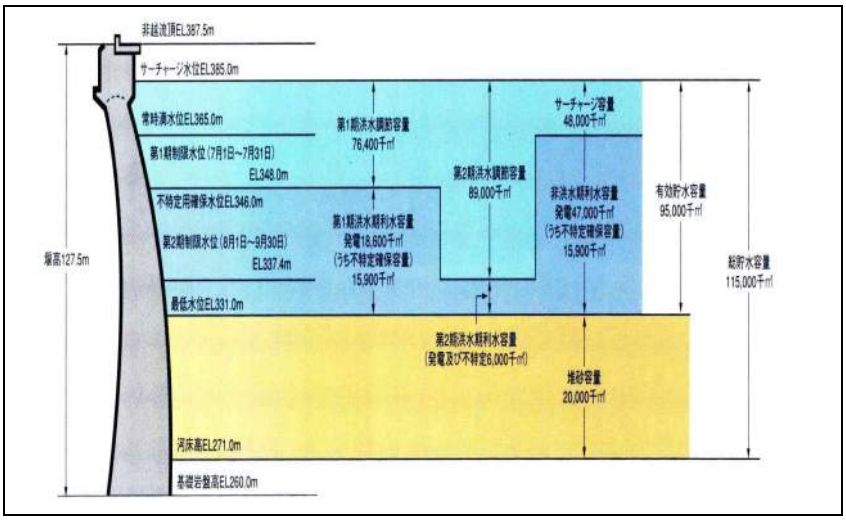

Figure 1.3: Capacity of the reservoir

However the properties of Managawa dam and the upstream dams; Sasougawa dam and Kumokawa dam, are shown in the table below.

Table 1.1: The properties of Managawa dam, Sasougawa dam and Kumokawa dam

	Managawa dam	Sasougawa dam	Kumokawa dam
Purposes	Flood control Electricity Irrigation	Flood control Electricity Irrigation	Sediment prevention Electricity
Water use ratio	Electricity 0.5% Others 99.5%	Electricity 26% Others 74%	Electricity 54% Others 46%
Start operation	S52.10	S31.11	S31.12
Manager	The Ministry of Land, Infrastructure and Transport	Fukui prefecture	Fukui prefecture
Crest Level	EL365.0m	EL528.0m	EL534.0m
Watershed area	223.7 km^2	70.7 km^2	55.8 km^2
Water body area	2.93 km^2	2.34 km^2	0.18 km^2
Normal capacity	115,000,000 m^3	58,806,000 m^3	1,490,000 m^3
Storage capacity	95,000,000 m^3	52,243,000 m^3	－
Lowest water level	EL 331.0m	EL 485.0m	EL 528.0m
Water storage height	34.0m	35.5m	－
計画水位高	EL 331.0m	EL 485.0m	EL 534.0m
Dead storage	20,000,000 m^3	3,500,000 m^3	1,490,000 m^3
Dam type	Concrete parabolic arch dam with central spill way	Gravity dam	Concrete arch dam
Structure	Length 357 m. Height 127.5 m.	Length 215 m. Height 76 m. Spill way at 68 m.	Length 95 m. Height 39 m. Spill way at 33 m.
Volume of dam	507,000 m^3	225,520 m^3	19,000 m^3
Remarks			This dam is fully filled by sediment.

1.1.2 Case study in Thailand

Nowadays, the sediment problem in Thailand is not serious but there are some studies, research and sediment protection work in that country. This study will show some sediment work case in Thai reservoirs. There are 2 department corresponding with dam operation and management in Thailand; Royal Irrigation Department (RID) and Electricity Generating Authority of Thailand (EGAT). The dams belonged to EGAT are more considered and there are many research about sediment depositing volume in EGAT dams because it is necessary to protect their conduits from sediment to take water from reservoir to turbine. In case of RID, the most of RID dams are smaller than EGAT dams therefore sediment will be easy to fill up to dead storage level so some RID dams were researched to get the sediment depositing volume.

1.2 Problem statement

Sediment is the important problem in some watershed especially on mountainous area as Japan. The sediment on the mountain or up stream of river basin is carried to deposit at the flat plane area or behind of hydraulic structures as weir or dam. In Japan, the depositing sediment volume in some dams is surveyed every year and it's costly to measuring the reservoir's bottom profile. There are many physical and numerical models to find out an annual depositing sediment volume in reservoir. If the efficiency of the computer modeling is high and acceptable, it will not be necessary to measure the reservoir's bottom profile every year. In one part of this study, I try to improve the efficiency of soil loss equation on reservoir watershed to get more accuracy results matching with observed data.

On the up stream of dam, there are suspended sediment gauges installed to get the sediment concentration carried in river. Normally the automatic equipment for measuring bed load is not available therefore in Japan we can estimate that the bed load is about 30% of suspended load in unit weight. Therefore we can estimate the annual total sediment load to flow into reservoir if the annual suspended sediment load is known. To improve reservoir operation and protect the damage from sediment flowing to reservoir, it is necessary to install suspended sediment gauge at the upstream of reservoir and at the mouth of the high rate of sediment yield area. It will be helpful to design the operation if the recently sediment inflow to dam is known. Therefore in one part of this study the suspended sediment concentration is predicted by real time modeling.

Presently, global warming is the well known topic and it causes to change the climate all area in the world. This study tries to find out the effect of climate change to water resources on the representative area; Managawa river basin. It will be helpful for reservoir management if the impacts of climate change on water resources in reservoir watershed are known.

1.3 Objectives

In each reservoir watershed, the considered river basin for management is divided into three parts as upstream of reservoir, reservoir body and downstream of reservoir. This research is mainly concentrated on the upstream of reservoir and reservoir management. The sediment problem in reservoir watershed is the main topic for this research and the purposes of this study are followed.

- To compute the annual depositing sediment volume in reservoir by using soil erosion model and sediment transportation model.
- To predict the suspended sediment concentration flowing into the reservoir that this predicted output will be helpful for improving the reservoir operation system.
- To consider the effect of global warming or impact of climate change to hydrology and reservoir operation system.
- To consider and improve the reservoir operation system.

1.4 Scope and limitation of the study

The models used to apply to river basin management on this research area are tools for sedimentation and sediment management considerations as followed.

- Rainfall - Runoff model
- Hydrodynamic model
- Sediment Transport model
- Sediment Yield model
- Integrated Sedimentation model
- Hourly Suspended Sediment model
- Climate change model effect to water resources and sediment yield

The rainfall runoff model in this study was applied by NAM model concept and 1D Hydrodynamic model was applied for water discharge routing on the study area. I used Modified Universal Soil Loss Equation (MUSLE) to compute the sediment yield then sediment was transported in river which we applied total load equation for modeling. About sediment prediction model, this study used Artificial Neural Network (ANN) model to predict suspended sediment concentration in the river then compare the results of neural network with Multi Linear Regression (MLR) model and Sediment Rating Curve (SRD) model. Climate change effects to water resources and sediment yield on the study area investigated by applying the results of the weather generating model to input rainfall runoff model and sediment yield model.

The flow charge of the scope of this study is shown in Figure 1.4.

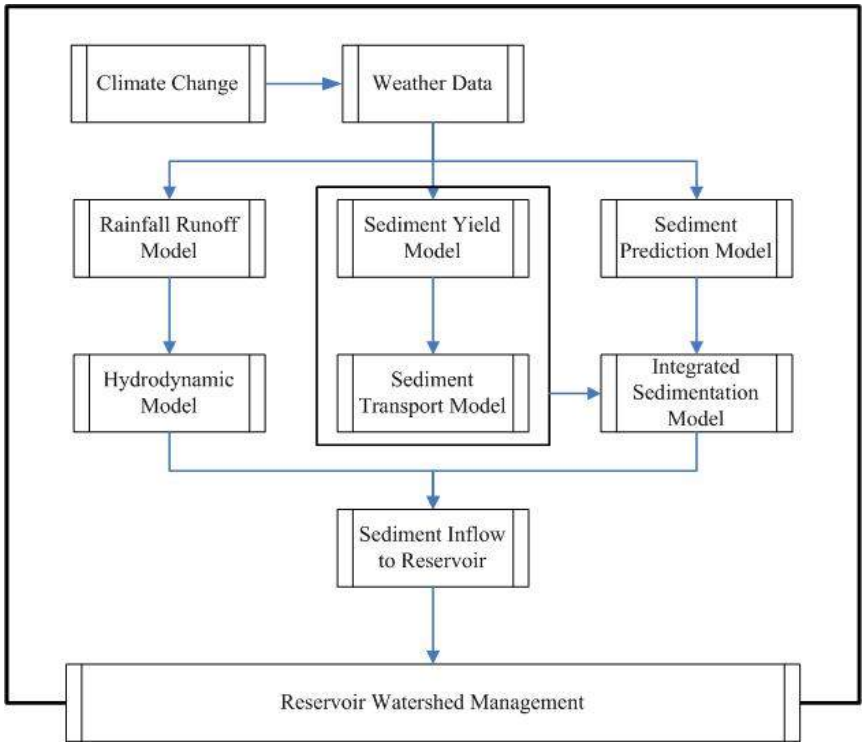

Figure 1.4: Scope of the study

CHAPTER 2
Literature Review

In this Chapter, it will be explained about historical of the related researches with the sedimentation and sediment management models which are rainfall runoff model, hydrodynamic model, sediment yield model, sediment transport model, artificial neural network model, multiple linear regression model, sediment rating curve model, meteorological variables' trends and weather generating model.

2.1 Hydrologic and hydrodynamic models

Both of hydrologic and hydrodynamic models are the basic models for water resources processing and management. In this study, there was using the rainfall runoff model and hydrodynamic model to transform rainfall to runoff then it would be routed along the river.

- Rainfall runoff model

Rainfall runoff estimation from a watershed is of vital importance as these values are required in most hydrologic analysis for the purpose of water resources planning, flood forecasting, pollution control and many other applications. Modeling the rainfall-runoff process is a complex activity as it is influenced by a number of implicit and explicit factors such as precipitation distribution, evaporation, transpiration, abstraction, watershed topography, and soil types. The runoff discharges and flow rates at a river sites varies greatly throughout the course of a year, depending on seasonal rainfall, watershed characteristics and many other parameters. These variables greatly increase the modeling effort and time and in turn provide ample opportunities for research endeavors.

Various models have been developed to solve the rainfall runoff relationship in engineering research and practices. The widely known rainfall runoff models identified are the Rational Method (McPherson, 1969), Soil Conservation Service-Curve Number Method (Maidment, 1993), and Green and Ampt Method (Green, 1911). The more complex models which should provide better runoff estimation are continuously being researched and developed. Some of the complex models identified are Genetic Danish MIKE11 NAM (1972). The choice and validity of the model depends on the type of problem, the data availability and the decision to be made.

In this study, NAM model processed on MIKE 11, DHI software was selected to explain hydrological processing on Managawa river basin because the model application is available and obtained data as rainfall, evaporation and water discharge is suitable and matching with this model. In more detail, it will be shown in next Chapter, Rainfall runoff model.

- Hydrodynamic Model

For simulating hydrodynamic flows, water quality, and sediment transport in estuaries, rivers, irrigation systems, channels, and other water bodies, the most advanced, powerful, and comprehensive 1-D dynamic flow model that is MIKE11 which has been used since 1979 by consulting firms and government reviewing agencies worldwide. It can be used for detailed design, management, and operation of both simple and complex river and channel systems. In addition, it can be used to simulate storm water runoff and progressive inundation from river overflows and coastal storm surges.

In this study, HD model processed on MIKE 11, DHI software was selected to explain routing and hydrodynamic processing along the river on Managawa catchment because the model application is available and obtained data as rainfall, water depth, water velocity and water discharge is suitable and matching with this model. It will be descript again in Chapter 4; Hydrodynamic model.

2.2 Sediment Yield

There are many researches about sediment yield application with Modified Soil Loss Equation (MUSLE) as descript below.

K.F. Golson el at. (2000) Evaluating modified rainfall erosivity factors in the Universal Soil Loss Equation. The Universal Soil Loss Equation (USLE) has undergone numerous modifications and revisions to enhance its ability to estimate soil loss cause by erosion in agriculture lands. There is still a considerable amount of uncertainty surrounding the use of the USLE as well as some of its modifications. This research examines the prediction capabilities of two very similar modifications that were made to the USLE's rainfall erosivity (R) factor; they are termed the Modified Universal Soil Loss Equation (MUSLE) and the Onstad-Foster Equation.

I. Sumathi el at. (2002) Using GIS for facilitating sediment yield estimation. In the study, the Geographic Information System (GIS) combined with the sediment yield model can enhance the evaluation of soil erosion estimation. Geographic Information System with the Modified Universal Soil Loss Equation (MUSLE) was used to estimate sediment yield on a Ebbaned watershed of Lower Bhavani Catchment, Nilgiris district, India.

S.H. Sadeghi (2004) Application of MUSLE in prediction of sediment yield in Iranian. The Amameh catchment was selected to check the applicability of sediment estimation model for the agro-climatic conditions of Iran. The MUSLE was selected for application on this catchment. The efficiency of the model for sediment yield prediction was assessed. In the process, a constrained type of MUSLE was developed, which is more suitable than the original MUSLE for the study area.

E. Chen el at. (2004) Effects of distribution-based parameter aggregation on a spatially distributed agricultural nonpoint source pollution model. This study investigated how

model structure and input data representation affect sediment predictions made using the Soil and Water Assessment Tool (SWAT). The study focused on the integration of two specific components of SWAT: the Modified Universal Soil Loss Equation (MUSLE) and the hydrologic response unit (HRU). This study indicates that greater attention should be made to structuring the data inputs to match the underlying assumptions of sub-models within SWAT.

F. Imaizumi el at. (2005) Relationship between sediment supply and transport processes in Miyagawa dam catchment. This study investigated timing and volume of sediment supply and transport based on aerial photo interpretation and volume of sediment deposits behind the dam in Miyagawa dam catchment.

C.L. Shieh el at. (2005) Sediment yield model for a watershed: a case study of Choushui River, Taiwan. This study descript that the cause of sediment yielding was not only from surface erosion but also from rainfall-induced land slide. Surface erosion was computed with the MUSLE equation and the rainfall-induced landslide was computed by using the Utsuogi empirical relation. The results also show the great contributions of rainfall-induced landslide to sediment yield that have been confirmed by field observations in mountainous area of Taiwan.

R. Bhattarai el at. (2007) Estimation of soil erosion and sediment yield using GIS at catchment scale. In this study, a GIS-based method has been applied for the determination of soil erosion and sediment yield in a small watershed in Mun river basin, Thailand. The method involves spatial disintegration of the catchment into homogenous grid cells to capture the catchment heterogeneity. The gross soil erosion in each cell was calculated using Universal Soil Loss Equation (USLE) by carefully determining its various parameters.

S.H. Sadeghi el at. (2007) Conformity of MUSLE estimates and erosion plot data for storm-wise sediment yield estimation. In this study, the conformity of mathematical model of the MUSLE for the estimation of storm-wise sediment yield in plots was examined at Matash Ranch in norther Iran. The results of the study verified the disability of the model in sound prediction of sediment yield on storm basis for the study area.

S.H.R. Sadeghi (2007) Applicability of the Modified Universal Soil Loss Equation for prediction of sediment yield in Khanmiraza watershed, Iran. This study aims to estimate the sediment yield due to storm rainfall and runoff at the outlet of the Khanmiraza watershed located in western Iran. The estimation was made for six storm events using the Modified Universal Soil Loss Equation (MUSLE). The results of this study demonstrated the efficiency of the MUSLE in estimating storm-associated sediment yield except one storm event in the study area with a high level of agreement and non-significant differences between mean estimated and measured value in the study storm events.

- Modified Universal Soil Loss Equation (MUSLE)

There exist many kinds of soil erosion models, both physical models and empirical models and also there are many useful numerical formulas to predict annual sediment yield. The most popular soil erosion equation is Universal Soil Loss Equation (USLE). Simple empirical methods such as Universal Soil Loss Equation (USLE) (Musgrave, 1947; Wishchmeier and Smith, 1965), Revised Universal Soil Loss Equation (RUSLE) (Renard et al., 1991) or Modified Universal Soil Loss Equation (MUSLE) (Williams, 1975) are frequently used for estimation of surface erosion and sediment yield from catchment areas. In Modified Universal Soil Loss Equation (MUSLE), the rainfall energy factor is replaced with a runoff factor and optimizes hydrologic process of sediment yield thus these improve the sediment yield prediction.

- SWAT model

The Soil and Water Assessment Tool (SWAT) is a long term distributed parameter model, designed to predict the impact of land management practice in a watershed (Arnold et al., 1998). In this study, the SWAT ArcView interface (DiLuzio et al., 2001) was used to write SWAT input files from GIS data layers. SWAT model calculates soil erosion caused by rainfall-runoff process using MUSLE. The model is a modified form of the USLE. The difference between the two approaches that in MUSLE rainfall energy factor is replaced with a runoff factor which represents energy used in detaching and transporting sediment. SWAT model requires a Digital Elevation Model (DEM) from which it determines the drainage network and divides the basin into sub-basins defined by grid cells, spatially related one to another, that each has geographic position in the watershed defined by surface topography.

This study applies SWAT model only to find out the soil erosion of each sub-basin at each outlet point. In more detail about this sediment yield, it will be explain in Chapter 5; Integrated sedimentation model.

2.3 Sediment Prediction

In literature review, there are so many studies about sediment forecasting model by using neural network that it will be shown below.

H.K. Cigizoglu (2000) Suspended sediment estimation for river using artificial neural networks and sediment rating curves. In this study, a comparison is made between artificial neural networks (ANNs) and sediment rating curves for two rivers with very similar catchment areas and characteristics in the north of England. In particular, an ANN approach can give information about the structure of events which is impossible to achieve with sediment rating curves. The ANN estimates are compared also with corresponding classical regression ones and found to be significantly superior.

H.M. Nagy el at. (2002) Prediction of sediment load concentration in rivers using artificial neural network model. An artificial neural model is used to estimate the natural

sediment discharge in rivers in terms of sediment concentration. This is achieved by training the network to extrapolate several natural streams data collected from reliable sources. In verification, the estimated sediment concentration values agree well with the measured ones.

Ozgur Kisi (2005) Suspended sediment estimation using neuro-fuzzy and neural network approaches. The neuro-fuzzy (NF) and neural network (NN) models are established for estimating current suspended sediment values using the stream flow and antecedent sediment data. The sediment rating curve and multi-linear regression are also applied to the same data. The daily stream flow and suspended sediment data for two stations; Quebrada Blanca station and Rio Valenciano station, operated by the US Geological Survey were used as case studies. Based on comparison of the results, it is found that the NF model gives better estimates than the other techniques.

Avnash Agarwal el at. (2005) ANN-based sediment yield models for Vamsadhara river basin, India. In this study, most universal accepted feed-forward error back-propagation artificial neural network models, supported by batch and pattern learning, daily, weekly, ten-daily and monthly sediment yield were developed for the Vamsadhara river basin of India. The generalized pattern learned models for different time scales were compared with linear transfer function models and it was found that the pattern learned models developed with generalization through cross validation were superior in general, except weekly for the study area.

H.K. Cigizoglu el at. (2006) Generalized regression neural network in modeling river sediment yield. In this study another ANN algorithm, generalized regression neural network, GRNN, was used in river suspended sediment estimation. The neural networks are trained using daily river flow and suspended sediment data belonging to Juniata catchment in USA. Also the estimated and observed sediment sums are examined in addition to two previously mentioned performance criteria. The ANN estimations are found significantly superior to conventional method results.

H.K. Cigizoglu el at. (2006) Methods to improve the neural network performance in suspended sediment estimation. The effect of employment of different methods of suspended sediment estimation by artificial neural networks was the concern of this study. The range dependent neural network (RDNN) was found to be superior to conventional ANN applications, where only a single network is trained considering the entire training data set. It was seen that both low and high observed sediment values were closely approximated by the RDNN.

Yun-Mei Zhu el at. (2007) Suspended sediment flux modeling with artificial neural network: An example of the Longchuanjiang river in the upper Yangtze catchment, China. Artificial neural network (ANN) was used to model the monthly suspended sediment flux in the Longchuanjiang river, the upper Yangtze catchment, China. It is demonstrated that ANN is capable of modeling the monthly suspended sediment flux with fair good accuracy when proper variables and their lag effect on the suspended sediment flux are used as inputs.

Emrah Dogan el at. (2007) Estimation of total sediment load concentration obtained by experimental study using artificial neural networks. The main purpose of this study is to establish an effective model which includes nonlinear relations between dependent (total sediment load concentration) and independent (bed slope, flow discharge and sediment particle size) variables. The results show that ANN model is found to be significant superior to total sediment transport equations.

Ozgur Kisi (2007) Constructing neural network sediment estimation models using a data-driven algorithm. Artificial neural network (ANN) models are designed for suspended sediment estimation using statistical pre-processing of the data. The result of the study indicates that the statistical pre-processing of the data could significantly reduce the effort and computational time required in developing an ANN model.

Raveen K. Rai el at. (2008) Event-based sediment yield modeling using artificial neural network. In this study, a back propagation feed forward artificial neural network (ANN) model was developed for the computation of event-based temporal variation of sediment yield from the watersheds. The model was developed from the storm event data registered over the two small watershed and the responses were computed in term of runoff hydrographs and sedimentographs. ANN based model results better agreement that the linear transfer function model for the computation of runoff hydrographs and sedimentographs for both the watersheds.

- *Artificial Neural Network Model*

Artificial neural network (ANN) is a type of empirical model. It is derived from the researches on the nature of the human brain (Muller et al., 1995). Hydrologic applications of artificial neural network (ANN) include the modeling of daily rainfall-runoff-sediment yield process, snow-rainfall process, assessment of stream's ecological and hydrological responses to climate change, rainfall-runoff forecasting, ground water quality prediction and ground water remediation. Artificial neural network (ANN) can be applied to predict the monthly, weekly and daily suspended sediment in the catchment by relating it to average rainfall, temperature, rainfall intensity and water discharge (Yun-Mei Zhu, 2007). Because of its ability to simulate nonlinear complex system without any priori assumption about the processes involved, artificial neural network (ANN) provides a promising alternative for the conventional empirical and physical models in sediment modeling.

This study is an attempt to predict an hourly suspended sediment concentration on the river by using back propagation artificial neural network with hydrologic and hydrodynamic data as inputs of network.

In more detail about model and the results of artificial neural network compared with multiple linear regression and sediment rating curve, it will be explained in Chapter 6; Sediment prediction model.

2.4 Climate change model

Mikhail A. Semenov (1997) Use of a stochastic weather generator in the development of climate change scenarios. Climate change scenarios with a high spatial and temporal resolution are required in the evaluation of the effects of climate change on agricultural potential and agricultural risk. This study on the sensitivity of crop models and climatic extremes has clearly demonstrated that changes in variability can have more profound effects on crop yield and on the probability of extreme weather events than simple changes in the mean values. The stochastic weather generator used in this study, LARS-WG, has been validated across Europe and has been shown to perform well in the simulation of different weather statistics, including those climatic extremes relevant to agriculture.

Vaclav Dvorak el at. (1997) Climate change hydrology and water resources impact and adaptation for selected river basins in the Czech Republic. The objective of this research is to study potential impacts of climate change on hydrological system and water resources, four river basins have been selected in the territory of the Czech Republic and to simulate potential changes in runoff, three hydrological models have been applied using incremental and GCM scenario; BILAN, SACRAMENTO and CLIRUN models. Results of the assessments and concluded with suggestions for possible general adaptation policy options, efficient water demand management and protection of water resources.

Brent Frakes el at. (1999) An evaluation of two hydrologic models for climate change scenarios. In this study, a black box artificial neural network (ANN) model was compared to a distributed parameter conceptual Geographic Information System based Hydrologic Modeling System (GIS-HMS). Both models computed daily direct surface runoff in four sub-basins of the west branch of Susquehanna river basin, Pennsylvania and were evaluated with five objective functions. Overall, results were comparable between models.

Alan F. Hamlet el at. (1999) Effects of climate change on hydrology and water resources in the Columbia river basin. In this study, the implications future climate change predictions derived from four global climate models (GCMs) were used to evaluated possible future changes to Pacific Northwest climate, the surface water response of the Columbia river basin and the ability of the Columbia river reservoir system to meet regional water resources objectives.

Pao-Shan Yu el at. (2002) Impact of climate change on water resources in southern Taiwan. This study investigates the impact of climate change on water resources in southern Taiwan. The historical trends of meteorological variables were detected using a non-parametric statistical test. The analytical results indicate that the transition probabilities of daily precipitation occurrence significantly influence precipitation generation and generated runoff for future climatic conditions in southern Taiwan was found to rise the wet season and decline during the dry season.

Z.X. Xu el at. (2003) Monotonic trend and step changes in Japanese precipitation. In this study, both parametric t-test and nonparametric Mann-Kendall and Mann-Whitney techniques are applied to the spatially averaged precipitation time series over Japan. The results indicate that although several step changes occurred in Japanese precipitation, the time series did not exhibit significant evidence of monotonic trend during the past century.

Niklas S. Christensen el at. (2004) The effects of climate change on the hydrology and water resources of the Colorado river basin. The potential effects of climate change in this study are assessed by comparing simulated hydrologic and water resources scenarios derived from down scaled climate simulation of the US Department of Energy National Center for Atmospheric Research Parallel Climate Model (PCM) to scenarios driven by observed historical (1950-1999) climate.

Van Thanh Van Nguyen (2005) Downscaling methods for evaluating the impacts of climate change and variability on hydrological regime at basin scale. This paper provides an overview of various down scaling methods that could be used for assessing the potential impacts of climate change and variability on hydrological regime. Two popular statistical downscaling (SD) methods based on the Statistical Downscaling Model (SDSM) and the Stochastic Weather Generator (LARS-WG) were selected for testing their feasibility in the simulation of hydrologic processes.

Chen Ya-Ning el at. (2007) Effects of climate change on water resources in Tarim river basin, Northwest China. In this paper, the effects of climate change on water resources in Tarim river basin were investigated based on hydrology, temperature and precipitation data from past 50 years. The long term trends of hydrological time series were detected using both parametric and nonparametric techniques. The results showed that the temperature increased by 1ºC over the past 50 years and the average annual precipitation exhibited an increasing trend with magnitude of 6.8 mm per decade.

Mohammed Sharif el at. (2007) Improve K-Nearest neighbor weather generating model. In this paper, a modified approach is developed that allows nearest neighbor re-sampling with perturbation of the historic data. The approach is demonstrated through application to the upper Thames river basin in Ontario. Daily weather variables were simulated at multiple stations in and around the basin. Analysis of the simulated data demonstrated the ability of the model to reproduce important statistical parameters of the observed data series while allowing perturbations to the observed data point.

H. Thodsen el at. (2008) The influence of climate change on suspended sediment transport in Danish river. In this study, climate change induced changes in suspended sediment transport are modeled for five scenarios on the basis of modeled changes in land used and land cover for two Danish river catchments. The results showed that the suspended sediment transport increases during winter months as a result of the increase river discharge cause by increase in precipitation, and decreases during summer and early autumn months.

D. Mbano el at. (2009) Impacts of rainfall and forest cover change on runoff in small catchments: case study of Mulunguzi and Namadzi catchment areas in southern Malawi. In this study, annual seasonal and monthly series of rainfall and river discharge of catchments were analyzed for trends using the nonparametric Mann-Kendall static and Sens slope estimator. Further, Linear regression and the RainRU model were applied to establish whether the relationship between rainfall and runoff in two catchments has changed.

In more detail about the future trends of meteorological variables and weather generating models, it will be explained in Chapter 7; Effects of climate change on water resources and sediment yield.

CHAPTER 3
Rainfall Runoff Model

The rainfall runoff model is a hydrological model. For river basin management, rainfall runoff model is basically used to predict discharge from precipitation data. In this study, the NAM model is selected for calculating the discharge flowing into reservoirs.

3.1 Theoretical description of NAM Model

NAM is an abbreviation of the Danish "Nedbor-Afstromings Model", meaning precipitation runoff model. The NAM model is so called deterministic, conceptual, lumped type model with moderate input data requirement.

Being a lumped model, NAM treats each subcatchment as one unit, the parameters and variables are thus representing average value for the entire subcatchment.

A conceptual model like NAM model, shown in Figure 3.1, is based on physical structures and equation used together with semi empirical ones. Thus, some of the parameters can be evaluated from physical catchment data, but the final parameter estimation must be performed by calibration applying concurrent input and output time series.

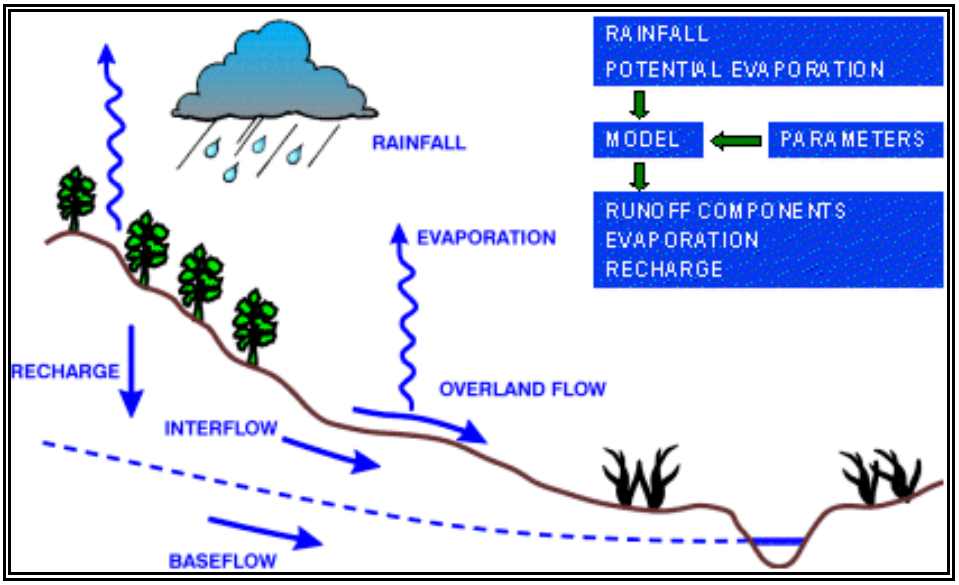

Figure 3.1: NAM Model Concept (Source: DHI)

NAM simulates the rainfall-runoff process in rural catchments as shown in Figure 3.2. It operates by continuously accounting for the moisture content in four different and mutually interrelated storage; snow storage, surface storage, root zone storage, and groundwater storage, which represent physical elements of the catchment.

Model input:

- Model parameters
- Initial conditions; In general it is recommended to disregard the first 3-6 month of the NAM simulation in order to eliminate the influence of erroneous initial conditions.
- Meteorological data; rainfall, evapotranspiration, temperature and radiation (optional)
- Stream flow data for model calibration and validation; the final parameter estimation must be performed by calibration against time series of hydrological observations.

Model providing:

- Input and editing of rainfall-runoff data and computational parameters required for rainfall-runoff modeling
- Specification of rainfall/runoff time series. Time series are specified on the time-series page within the RR editor
- Calculation of weighted rainfall by use of a weighting of different rainfall stations in order to obtain representative catchment rainfall
- Digitizing of catchment boundaries and rainfall stations in a graphical display (Basin View) including automatic calculation of catchment areas and mean area rainfall weights
- Presentation of results. Specification of discharge stations used for calibration and presentation of results

3.1.1 Model Structure

A conceptual model like NAM is based on physical structures and equations used together with semi-empirical ones. Being a lumped model, NAM treats each catchment as a single unit. The parameters and variables represent, therefore, average values for the entire catchment. As a result, some of the model parameters can be evaluated from physical catchment data, but the final parameter estimation must be performed by calibration against time series of hydrological observations.

The model structure is shown in Figure 3.2. It is an imitation of the land phase of the hydrological cycle. NAM simulates the rainfall-runoff process by continuously accounting for the water content in four different and mutually interrelated storages that represent different physical elements of the catchment. These storages are:

- Snow storage
- Surface storage
- Lower or root zone storage
- Groundwater storage

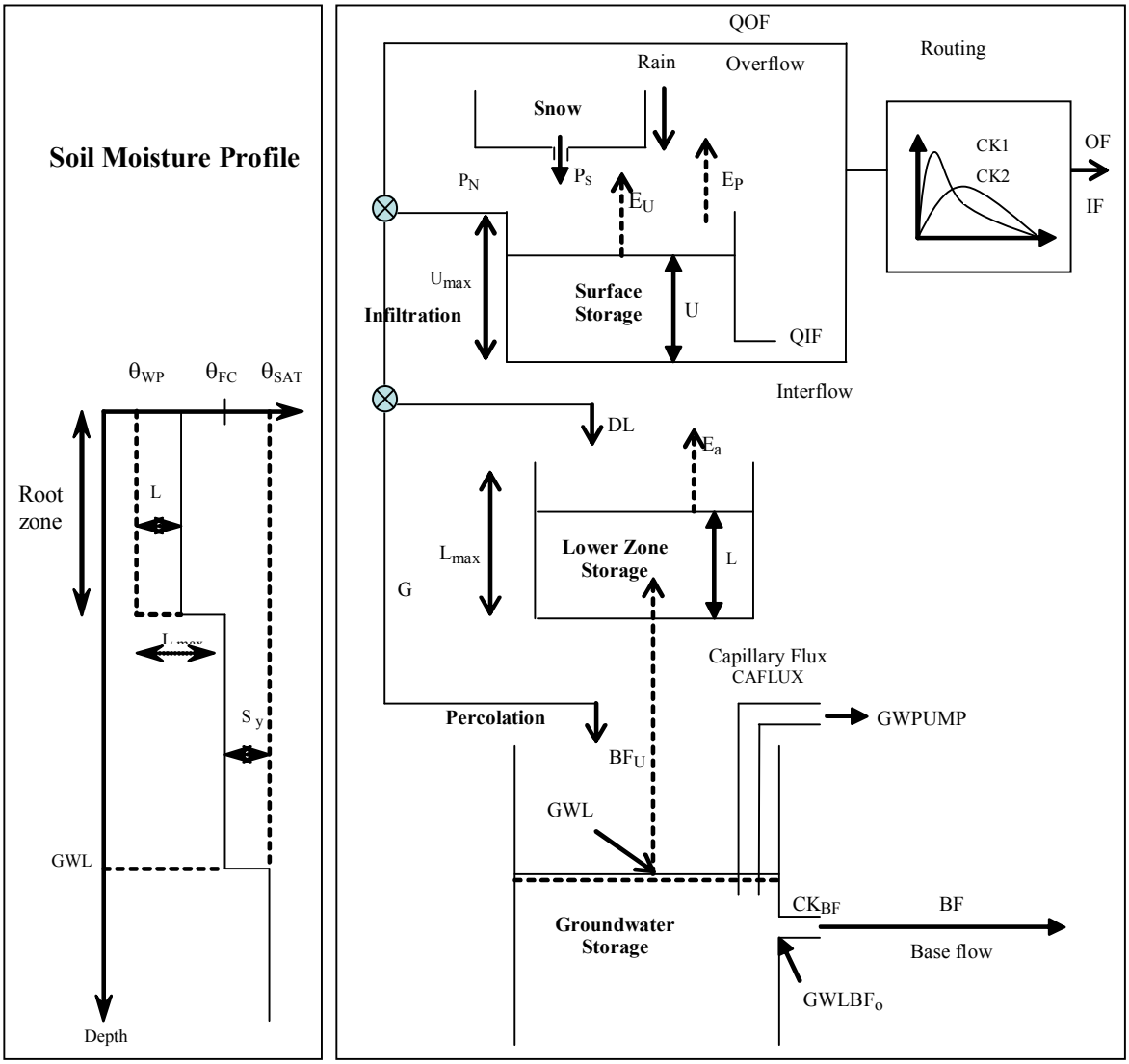

Figure 3.2: Structure of the NAM model (Source: DHI, 2000)

In addition NAM allows treatment of man-made interventions in the hydrological cycle such as irrigation and groundwater pumping.

Based on the meteorological input data NAM produces catchment runoff as well as information about other elements of the land phase of the hydrological cycle, such as the temporal variation of the evapotranspiration, soil moisture content, groundwater recharge, and groundwater levels. The resulting catchment if split conceptually into overland flow, interflow and baseflow components.

3.1.2 Basic Modeling Components

Surface storage

Moisture intercepted on the vegetation as well as water trapped in depressions and in the uppermost, cultivated part of the ground is represented as surface storage. U_{max} denotes the upper limit of the amount of water in the surface storage.

The amount of water, U, in the surface storage is continuously diminished by evaporative consumption as well as by horizontal leakage (interflow). When there is the maximum surface storage, some of the excess water, P_N, will enter the streams as overland flow, whereas the remainder is diverted as infiltration into the lower zone and groundwater storage.

Lower zone or root zone storage

The soil moisture in the root zone, a soil layer below the surface from which the vegetation can draw water for transpiration, is represented as lower zone storage, L_{max} denotes the upper limit of the amount of water in this storage.

Moisture in the lower zone storage is subject to consumptive loss from transpiration. The moisture content controls the amount of water that enters the groundwater storage as recharge and the interflow and overland flow components.

Evapotranspiration

Evapotranspiration demands are the first met at the potential rate from the surface storage. If the moisture content U in the surface storage is less than these requirements (U<Ep), the remaining fraction is assumed to be withdrawn by root activity from the lower zone storage at an actual rate E_a. E_a is proportional to the potential evapotranspiration and varies linearly with the relative soil moisture content, L/L_{max} of the lower zone storage

$$Ea = (Ep - U)\frac{L}{L_{max}} \tag{3.1}$$

Overland flow (QOF)

When the surface storage spills, i.e. when $U>U_{max}$, the excess water P_N gives rise to overland flow as well as to infiltration. QOF denotes the part of P_N that contributes to overland flow. It is assumed to be proportional to P_N and to vary linearly with the relative soil moisture content, L/L_{max} of the lower zone storage

$$QOF = \begin{cases} CQOF\,\dfrac{L/L_{max} - TOF}{1 - TOF} & \text{for } L/L_{max} > TOF \\ 0 & \text{for } L/L_{max} \le TOF \end{cases} \tag{3.2}$$

Where CQOF is the overland flow runoff coefficient ($0 \le CQOF \le 1$)

TOF is the threshold value for overland flow ($0 \le TOF \le 1$)

The proportion of the excess water P_N that does not run off as overland flow infiltrates into the lover zone storage. A portion, ΔL, of the water available for infiltration, (P_N-QOF), is assumed to increase the moisture content L in the lower zone storage. The remaining amount of infiltrating moisture, G, is assumed to percolate deeper and recharge the groundwater storage.

Interflow

The interflow contribution, QIF, is assumed to be proportional to U and to vary linearly with the relative moisture content of the lower zone storage.

$$QIF = \begin{cases} CKIF \dfrac{L/L_{max} - TIF}{1 - TIF} & \text{for } L/L_{max} > TIF \\ 0 & \text{for } L/L_{max} \le TIF \end{cases} \qquad (3.3)$$

where CKIF is the time constant for interflow, and TIF is the root zone threshold value for interflow ($0 \le TIF \le 1$)

Interflow and Overland flow routing

The interflow is routed through two linear reservoirs in series with the same time constant CK_{12}. The overland flow routing is also based on the linear reservoir concept but with a variable time constant

$$CK = \begin{cases} CK_{12} & \text{for } OF < OF_{min} \\ CK_{12} & \text{for } OF \ge OF_{min} \end{cases} \qquad (3.4)$$

Where OF is the overland flow (mm/hour), OF_{min} is the upper limit for linear routing (=0.4 mm/hr), and β =0.4.

The constant β =0.4 corresponds to using the Manning formula for modeling the overland flow. Equations (3.4) ensures in practice that the routing of real surface flow is kinematic, while subsurface flow being interpreted by NAM as overland flow (in catchments with no real surface flow component) is routed as a linear reservoir.

Groundwater recharge

The amount of infiltrating water G recharging the groundwater storage depends on the soil moisture content in the root zone

$$G = \begin{cases} (P_N - QOF)\dfrac{L/L_{max} - TG}{1 - TG} & \text{for } L/L_{max} > TG \\ 0 & \text{for } L/L_{max} \le TG \end{cases} \qquad (3.5)$$

where TG is the root zone threshold value for groundwater recharge ($0 \le TG \le 1$)

Soil moisture content

The lower zone storage represents the water content within the root zone. After apportioning the net rainfall between overland flow and infiltration to groundwater, the remainder of the net rainfall increased the moisture content L within the lower zone storage by the amount ΔL

$$\Delta L = P_N - QOF \quad (3.6)$$

Baseflow

The base flow BF from the groundwater storage is calculated as the out flow from a linear reservoir with time constant CK_{BF}

3.1.3 Model Calibration and Calibration Parameters

In the NAM model, the parameters and variables as shown with range of calibration parameters in Table 3.1 represent average values for the entire catchment. While in some case a range of likely parameter values can be estimated, it is not possible, in general, to determine the values of the NAM parameters on the basis of the physiographic, climatic and soil physical characteristic of the catchment, since most of the parameters are of an empirical and conceptual nature. Thus, the final parameter estimation must be performed by calibration against time series of hydrological observations.

Table 3.1: Calibration parameters and default hypercube search space

Parameter	*Unit*	*Lower bound*	*Upper bound*
U_{max}	mm.	5	35
L_{max}	mm.	50	400
CQOF	-	0	1
CKIF	hours	200	2000
$CK_{1,2}$	hours	3	72
TOF	-	0	0.9
TIF	-	0	0.9
TG	-	0	0.9
CK_{BF}	hours	500	5000

Source : MIKE11-Reference Manual-DHI Software (2002)

3.1.4 Calibration Objectives and Evaluation Measures

The following objectives are usually considered in the model calibration

1. A good agreement between the average simulated and observed catchment runoff (i.e. a good water balance)
2. A good overall agreement of the shape of the hydrograph
3. A good agreement of the peak flows with respect to timing, rate and volume
4. A good agreement for low flow

3.2 Data collection and data analysis for rainfall runoff model

3.2.1 Hourly Rainfall Data

The available hourly rainfall data from Managawa dam office are shown in Table 3.2. There are 8 rain gauge stations located on this watershed as named Akio, Sasougawa dam, Nukumi, Heikedaira, Nagajima, Managawa dam, Kumanoko and Kumogawa dam.

Table 3.2: Rain gauge station and available hourly rainfall data

Station Name	***Lat. (N)***	***Long. (E)***	***Hourly Rainfall Data (from year)***
Managawa dam	35º54'12"	136º32'26"	1967
Nakajima	35º52'41"	136º30'27"	1967
Kumokawa dam	35º50'51"	136º27'26"	1973
Heikedaira	35º49'56"	136º29'16"	1978
Kumanoko	35º49'38"	136º26'19"	1967
Nekumi	35º47'59"	136º28'53"	1977
Sasougawa dam	35º50'38"	136º32'57"	1965
Akiu	35º50'03"	136º35'43"	1976

Managawa dam started to operation from 1981 so the rainfall-runoff model in this study is considered after Managawa dam operation started.

Reliability of rainfall data

For checking the consistency of data for selected rainfall stations, the Double Mass Curve method are used for yearly rainfall data during 1992-2003. As for the analysis, it is found that rainfall data for selected stations are found satisfactory, showing straight line in below Figure 3.3.

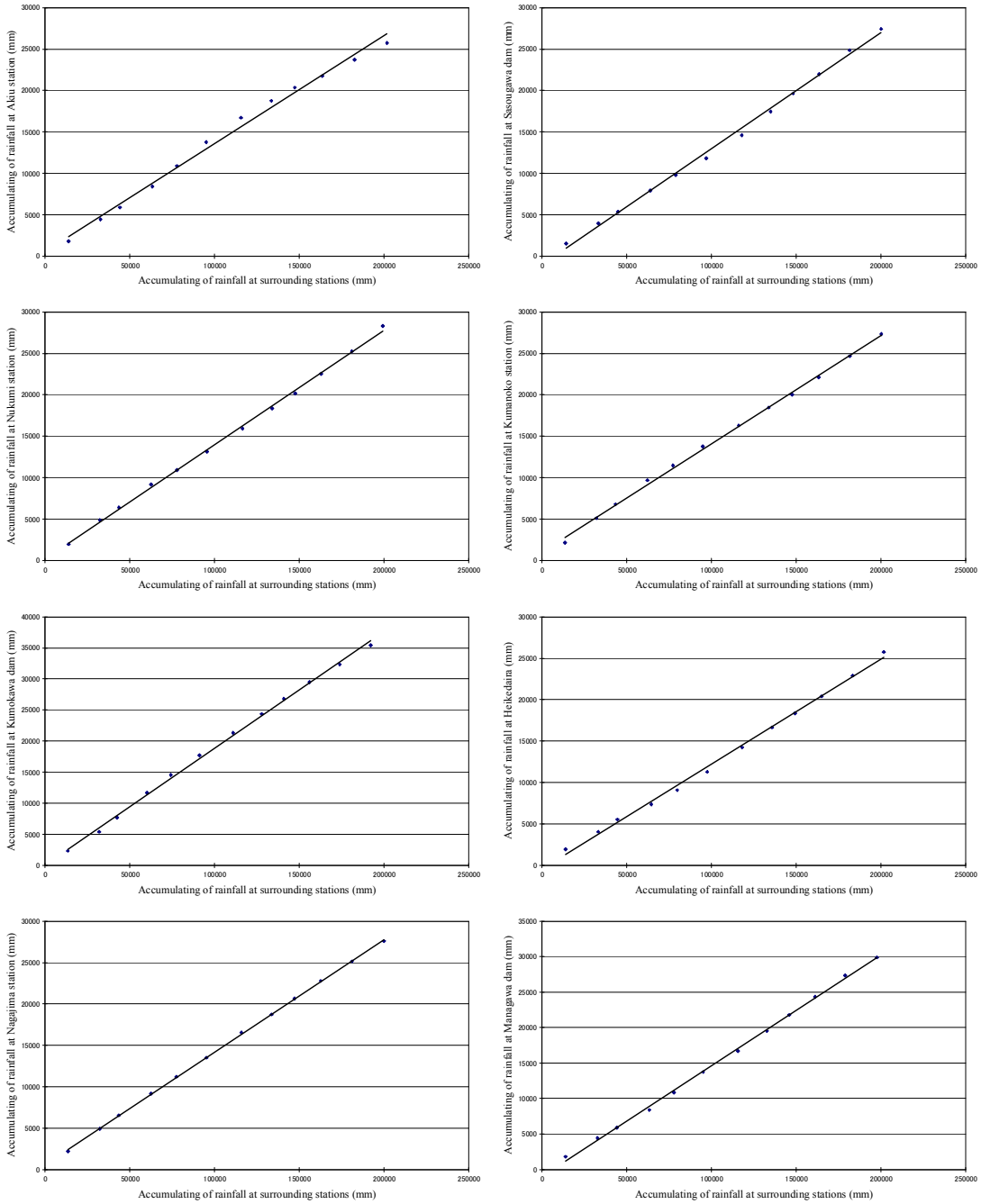

Figure 3.3: The consistency of rainfall station record in the upstream of Managawa river basin by using Double Mass Curve (1992-2003)

Thiessen Polygon

The method of mean areal precipitation computation in this study is by Thiessen method. This method assigns an area called a Thiessen polygon to each rainfall gauge. Thiessen polygon of each gauge is the region for which if we choose any point at random in the polygon, that point is closer to this particular gauge than to any other gage. In effect, the

precipitation surface is assumed to be constant and equal to the gage value throughout the region. Thiessen polygon of this study area is shown in Figure 3.4 and Thiessen parameters are in Table 3.3.

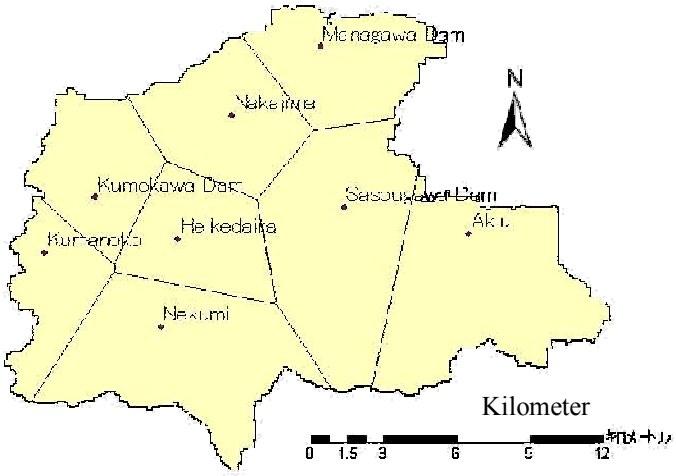

Figure 3.4: Thiessen Polygon of this study area

Table 3.3: Thiessen Parameters

Station	***Area (km^2)***	***Parameter***
Akio	41.9	0.187
Sasougawa dam	39.3	0.176
Nekumi	35.2	0.157
Heikedaira	19.7	0.088
Nagajima	28.1	0.126
Managawa dam	19.8	0.088
Kumakawa	17.5	0.078
Kumokawa dam	22.3	0.100
Total	223.8	1.000

3.2.2 Evaporation

Daily evaporation in Managawa river basin, there is one weather station located at Managawa dam site and the evaporation data is available on paper base from 1994 – 2004. Each year during winter season; December, January, February and March, they do not collect this kind of data. The annual evaporation rate on this river basin is about 800 mm.

3.2.3 Water discharge

Hourly discharge data flowing into Managawa dam is available from 1981 and this study was applying the discharge flowing into Managawa dam to calibrating the rainfall runoff model; NAM model.

3.3 Result analysis

3.3.1 Calibration and Verification

Annual rainfall on this study is about 2,400 mm. Followed the historic rainfall data as shown in Figure 3.5, the heavy rainfall years were used for calibration and verification the model. This study applied the recently rainfall data in year 2004 for calibrating the model then the data in year 2002 and 2003 were used for verification step.

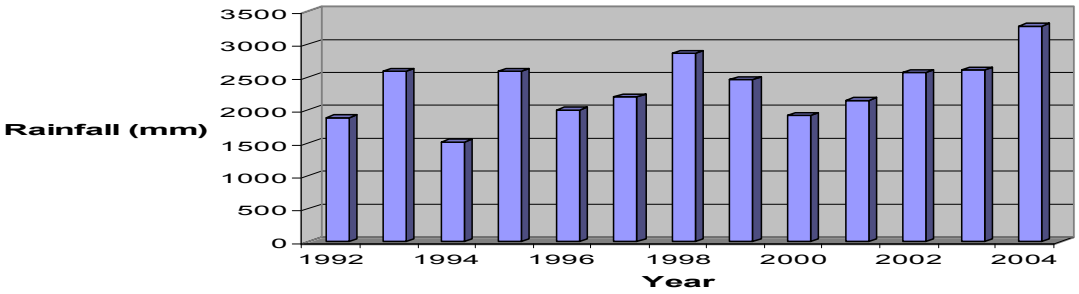

Figure 3.5: Annual weighting rainfall on Mangawa river basin

Managawa catchment area is 224 km^2. The rainfall data of each station are summarized and weighted with parameters in Table 3.3 to input of model. Auto calibration was used to adjust each parameters of NAM model then considered the hydrograph and changed some parameters by appropriation between calculated and collected data and reduce the error or increase efficiency of the model. NAM model parameters as in Figure 3.2 are given in the table below.

Table 3.4: NAM model parameters

Parameters	***Value***
Umax	15.3
Lmax	117
CQOF	0.373
CKIF	602.1
CK1.2	10.2
TOF	0.412
TIF	0.518
TG	0.773
CKBF	2303
Carea	1
Sy	0.1
GWLBF0	10
GWLBF1	0

3.3.2 Efficiency of Rainfall Runoff model

The efficiency of NAM model is considered as efficiency index (EI), peak error, volume error, peak time error and plotted hydrograph.
Efficiency Index (EI):

Where

$$EI = \frac{SR}{ST} \tag{3.7}$$

$$SR = ST - SE \tag{3.8}$$

$$ST = \sum_{i=1}^{N} (Q_i - \bar{Q})^2 \tag{3.9}$$

$$SE = \sum_{i=1}^{N} (Q_i - F_i)^2 \tag{3.10}$$

EI is Efficiency Index

SR is variation explained by the model

ST is total variation of the discharge

SE is sum of square errors

Q_i is observed discharge at time i

$\bar{Q}$ is mean value of observed discharge, $\bar{Q} = \frac{1}{N}\sum_{i=1}^{N} Q_i$

F_i is calculated discharge at time i

N is number of data points

Peak error : $\frac{Q_{op} - Q_{sp}}{Q_{sp}}$ (3.11)

Volume error : $\frac{\sum_{i=1}^{n} (Q_{o,i} - Q_{s,i})}{\sum_{i=1}^{n} Q_{o,i}}$ (3.12)

Peak time error : T_{op}-T_{sp} (3.13)

Where

Q_{op} is observed peak
Q_{sp} is simulated peak
$Q_{o,i}$ is observed value at time step i
$Q_{s,i}$ is simulated value at time step i
T_{op} is time of observed peak
T_{sp} is time of simulated peak
n is number of time steps

Table 3.5: Statistical Performance Indices of NAM Model Calibration and Verification

Error Estimation	***Calibration***	***Verification***	
	2004	***2002***	***2003***
Efficiency Index (%)	92.8	82.5	84.7
Peak error	0.138	-0.211	-0.333
Volume error	0.524	0.695	0.605
Peak time error (day)	0	0	0

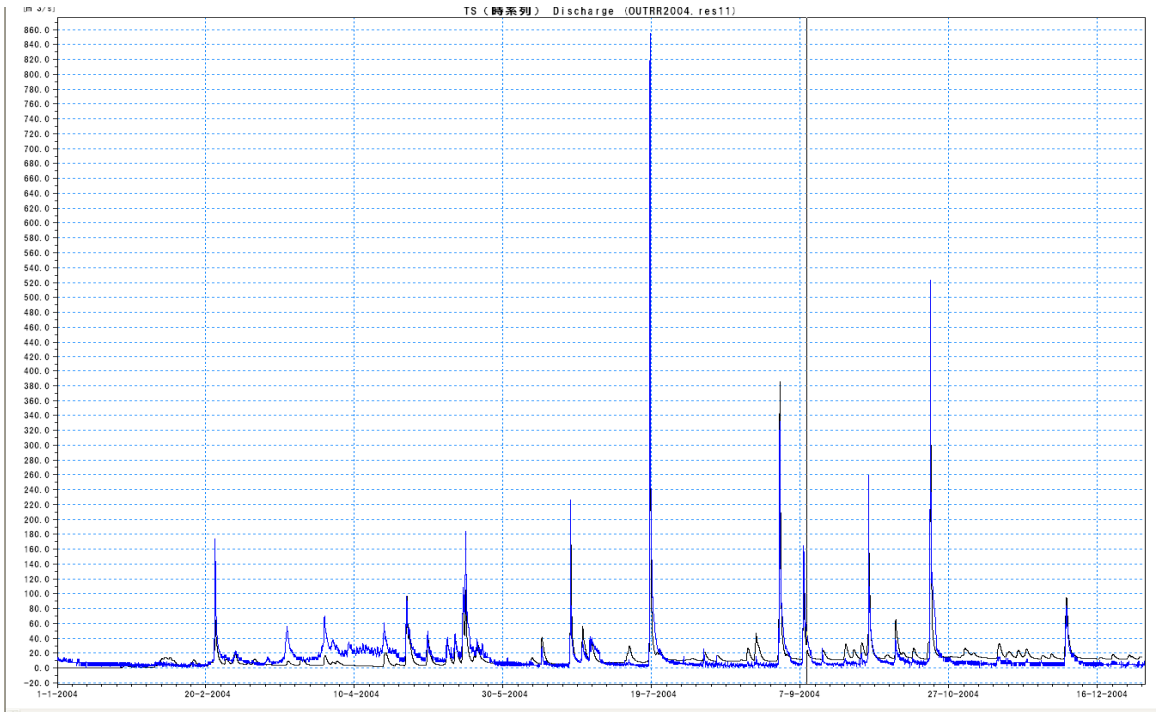

Figure 3.6: Comparison between observe and computed discharge data in 2004

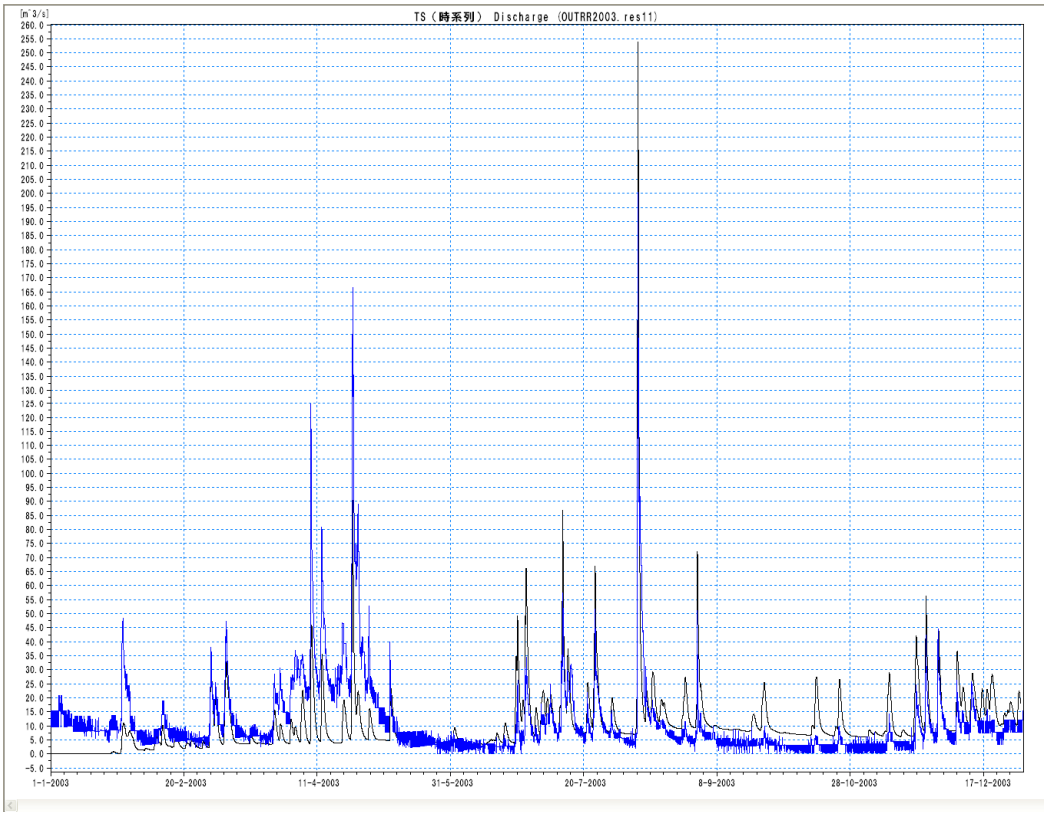

Figure 3.7: Comparison between observe and computed discharge data in 2003

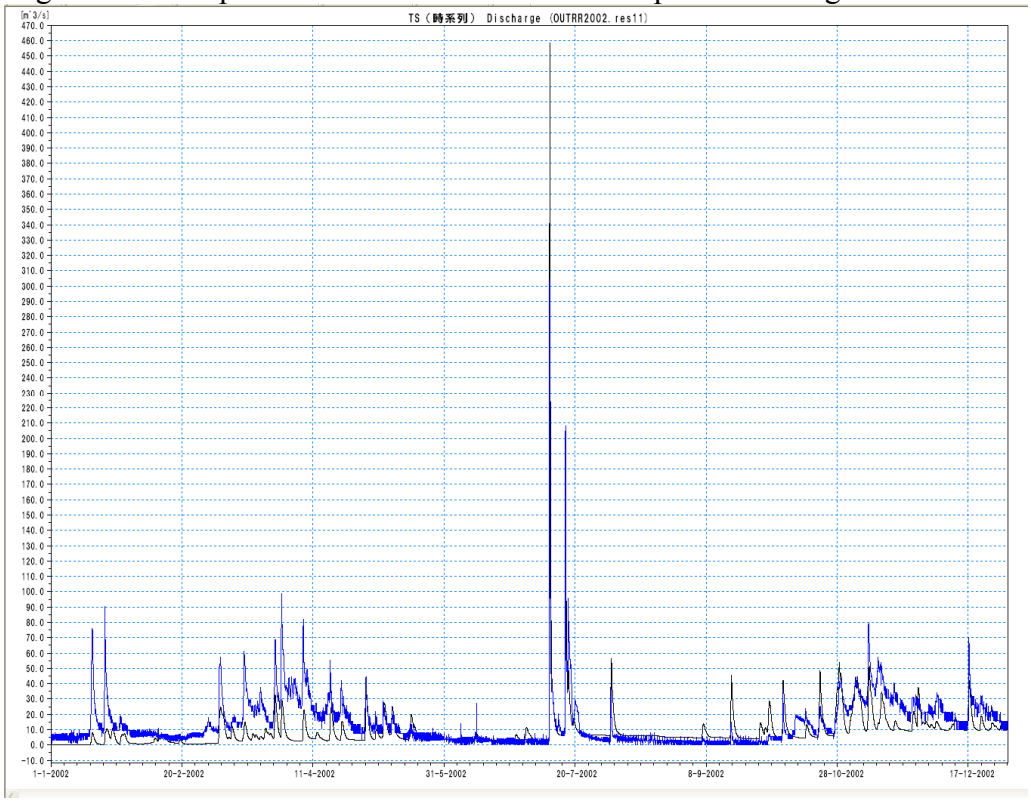

Figure 3.8: Comparison between observe and computed discharge data in 2002

From the efficiency of the model, the calibration efficiency is about 92 %, the verification efficiency is about 83% as shown in Table 3.5. The peak time of simulated hydrograph is same with observed one, the trend of simulated curve is quite match with observed one as shown in Figure 3.6 – 3.8. The results are very satisfactory for calibration and verification in term of time to peak, shape of hydrograph, and volume. The shapes of simulated hydrograph match well with the observed hydrograph and the statistical performances are tabulated.

3.4 Conclusions

The rainfall runoff model in this study is NAM model. The calibration and verification steps expressed the efficiency of model and these parameters set is good acceptable. Because the high flow or flood event is the significant problem on river basin, it was necessary to train and calibrate the rainfall runoff model and their parameters by the heavy rainfall years. The rainfall runoff model is the most basic model for water resources management. This study will apply this model and it's parameters with integrated sedimentation model, suspended sediment concentration prediction model and extrapolation data by climate change effect in the next chapters.

CHAPTER 4
Hydrodynamic Model

4.1 Theoretical of HD Model

The hydrodynamic module uses an implicit, finite difference scheme for the computation of unsteady flows in the rivers and estuaries. The module can describe sub-critical as well as supercritical flow conditions through a numerical scheme which adapts according to the local flow conditions which is shown the diagram of MIKE11 model setup in Figure 4.1.

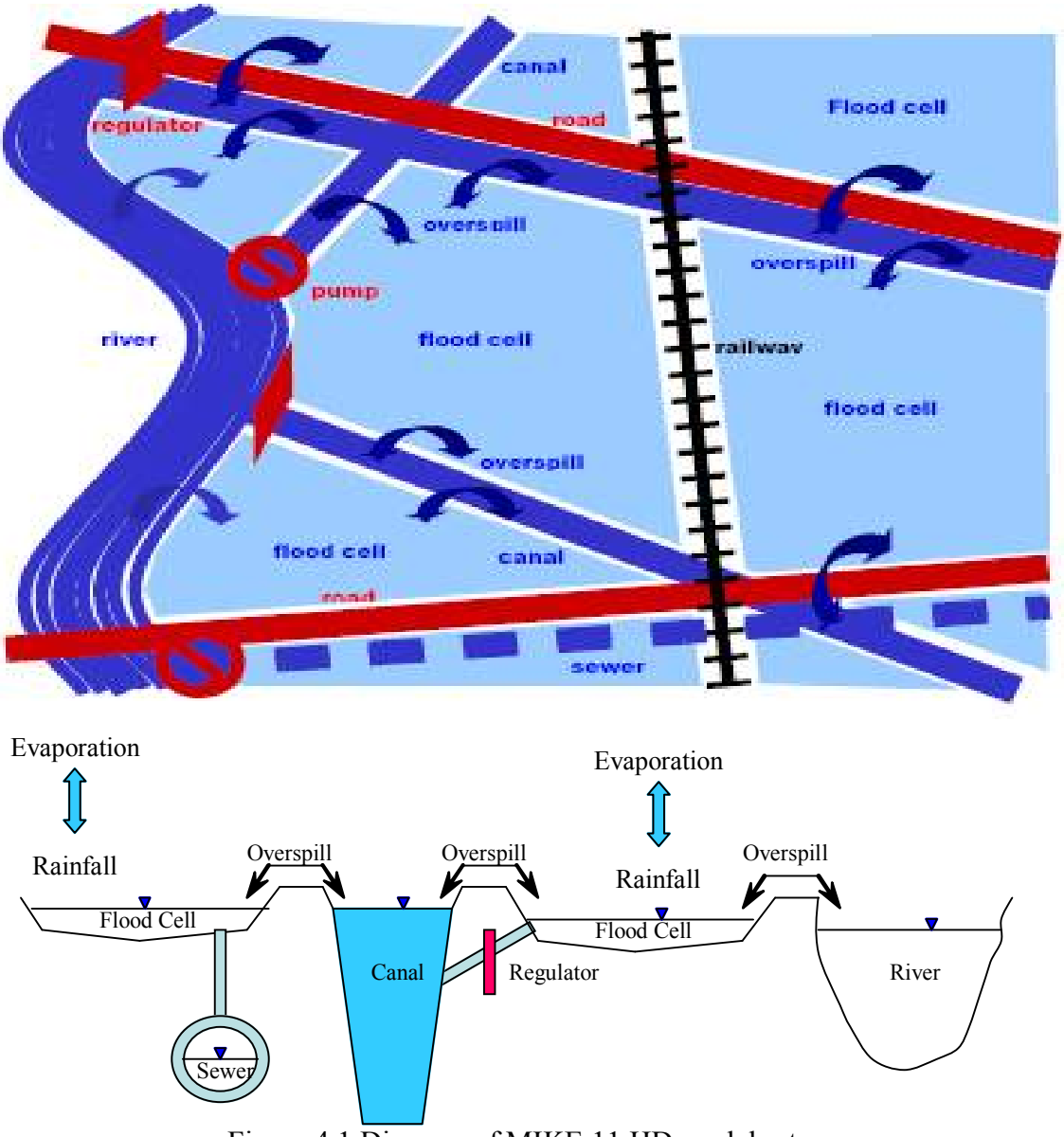

Figure 4.1 Diagram of MIKE 11 HD model setup

The formulations can be applied to looped networks and quasi two-dimensional flow simulation on flood plains. The computational scheme is applicable for vertically homogeneous flow conditions extending from steep river flows to tidal influenced estuaries. The complete non-linear equations of open channel flow (Saint-Venant) can be solved numerically between all grid points at specified time intervals for given boundary conditions. In addition to this fully dynamic description, a choice of other flow descriptions is available:

Higher-order, fully dynamic
- Diffusive wave
- Kinematic wave
- Quasi-steady state
-Kinematic routing (Muskingum, Muskingum-Cunge)

MIKE11_HD applied with the dynamic wave description solves the vertically integrated equations of conservation of continuity and momentum, based on the following assumptions:

- The water is incompressible and homogeneous, i.e. negligible variation in density.
- The bottom-slope is small, thus the cosine of the angle it makes with the horizontal may be taken as 1.
- The wave lengths are large compared to the water depth. This ensures that the flow everywhere can be regarded as having a direction parallel to the bottom, i.e. vertical accelerations can be neglected and a hydrostatic pressure variation along the vertical can be assumed
- The flow is subcritical.

- Model input:

- Model parameters; bed resistance, velocity distribution coefficient (α), DELH coefficient, DELHS coefficient, Delta coefficient (δ), ESP coefficient, FroudeExp, FroudeMax, Inter1Max, MaxlterSteady, NODE compatibility, NoITER, THETA, Zeta Min
- Initial conditions
- Boundary conditions; constant values of h or Q, time varying values of h or Q, a relationship between h and Q
- Cross Sections

3.1.5 Saint Venant Equations

For the rectangular cross section with a horizontal bottom and a constant width, the conservation of mass and momentum can be expressed as follows (in the instance neglecting friction and lateral inflows):

Conservation of mass:

$$\frac{\partial(\rho Hb)}{\partial t} = -\frac{\partial(\rho Hb\bar{u})}{\partial x} \tag{4.1}$$

Conservation of momentum:

$$\frac{\partial(\rho Hb\bar{u})}{\partial t} = -\frac{\partial\left(\alpha\rho Hb\bar{u}^2 + \frac{1}{2}\rho gbH^2\right)}{\partial x} \tag{4.2}$$

Where ρ is the density, H is the depth, b is the width, $\bar{u}$ is the average velocity along the vertical and α is the vertical velocity-distribution coefficient.

Introducing the bottom slope, I_b, and allowing for the channel width to vary will give rise to two more terms in the momentum equation. These terms describe the projections in the flow direction of the reactions of the bottom and side-walls to the hydrostatic pressure. The momentum equation now becomes:

$$\frac{\partial(\rho Hb\bar{u})}{\partial t} = -\frac{\partial\left(\alpha\rho Hb\bar{u}^2 + \frac{1}{2}\rho gbH^2\right)}{\partial x} + \frac{\partial b}{\partial x}\frac{\rho gH^2}{2} - \rho gHbI_b \tag{4.3}$$

$$= -\frac{\partial(\alpha\rho Hb\bar{u}^2)}{\partial x} - b\frac{\partial\left(\frac{1}{2}\rho gH^2\right)}{\partial x} - \rho gHbI_b$$

When the water level, h, is introduced into the relationship instead of water depth:

$$\frac{\partial h}{\partial x} = I_b + \frac{\partial H}{\partial x} \tag{4.4}$$

And the equations are divided by ρ, the conservation laws of mass and momentum becomes:

$$\frac{\partial(Hb)}{\partial t} = -\frac{\partial(Hb\bar{u})}{\partial x} \tag{4.5}$$

$$\frac{\partial(Hb\bar{u})}{\partial t} = -\frac{\partial(\alpha Hb\bar{u}^2)}{\partial x} - Hbg\frac{\partial h}{\partial x} \tag{4.6}$$

These equations can be integrated to describe the flow through cross sections of any when divided up into a series of rectangular cross sections as shown in Figure 4.2. According to the previous assumptions $\partial h/\partial x$ is constant across the channel and no exchange of momentum occurs between the subchannels. If the integrated across sectional area is called A and the integrated discharged Q, and B is the full width of the channel, then:

$$A = \int_0^B Hdb \tag{4.7}$$

$$Q = \int_0^B H\bar{u}\,db = \bar{u}A \tag{4.8}$$

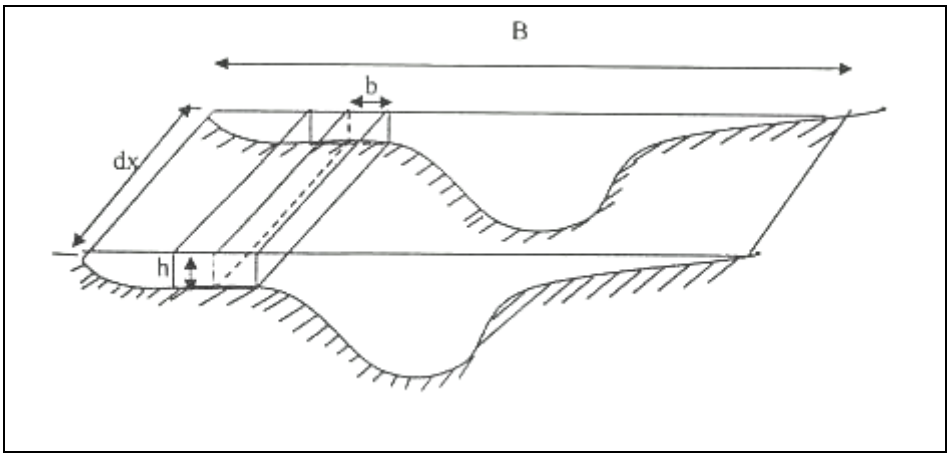

Figure 4.2: Cross Section Divided in a Series of Rectangular Channels

Integrating the mass and momentum conservation equations and introducing Equation (4.7) and (4.8) yields:

$$\frac{\partial Q}{\partial x} + \frac{\partial A}{\partial t} = 0 \tag{4.9}$$

$$\frac{\partial Q}{\partial t} + \frac{\partial\left(\alpha \frac{Q^2}{A}\right)}{\partial x} + gA\frac{\partial h}{\partial x} = 0 \tag{4.10}$$

Including the hydraulic resistance, e.g. using the Chezy description and the lateral inflow; q, into these equations leads to the basic equations used in MIKE 11:

$$\frac{\partial Q}{\partial x} + \frac{\partial A}{\partial t} = q \tag{4.11}$$

$$\frac{\partial Q}{\partial t} + \frac{\partial\left(\alpha \frac{Q^2}{A}\right)}{\partial x} + gA\frac{\partial h}{\partial x} + g\frac{Q|Q|}{C^2 AR} = 0 \tag{4.12}$$

3.1.6 Solution Scheme

The solution to the combined system of equations at each time step is performed according to the procedure outlined below. The solution method is the same for each model level (kinematics, diffusive, dynamic).

The transformation of equation (4.11) and (4.12) in Saint Venant Equations to a set of implicit finite difference equations is performed in a computational grid consisting of alternating Q and h points i.e. points where the discharge, Q and water level, h, respectively, are computed at each time step (see Figure 4.3). The computational grid is generated automatically by the model on the basis of the user requirements. Q-points are always placed midway between h-points may differ. The discharge will, as a rule, be defined as positive in the positive x-direction (increasing chainage).

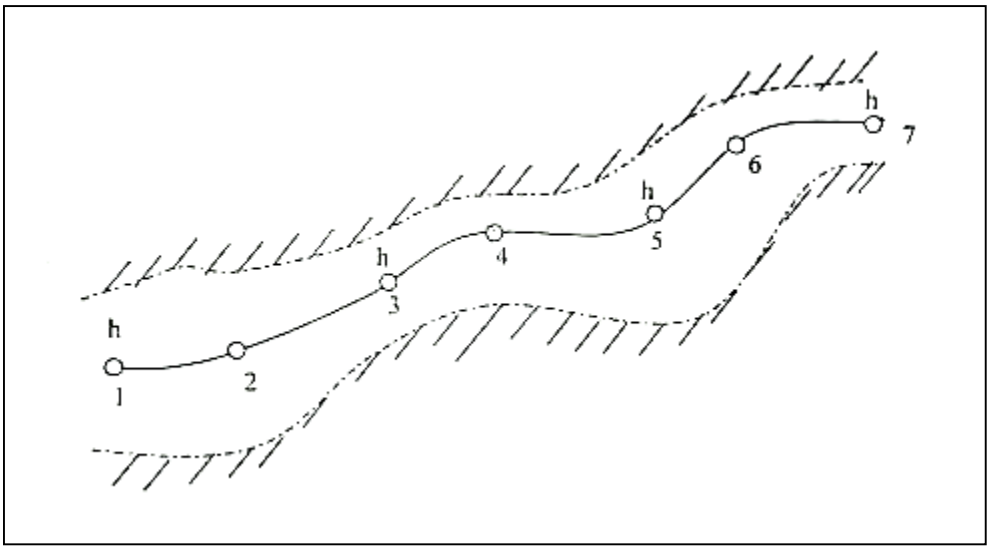

Figure 4.3: Channel Section with Computational Grid

The adopted numerical scheme is a 6-points Abbott-scheme as shown in Figure 4.4.

Continuity Equation

In the continuity equation the storage width, b_s, is introduced as:

$$\frac{\partial A}{\partial t} = b_s \frac{\partial h}{\partial t} \tag{4.13}$$

giving:

$$\frac{\partial Q}{\partial x} + b_s \frac{\partial h}{\partial t} = q \tag{4.14}$$

where q is lateral inflow

As only Q has derivative with respect to x, the equation can easily be centered at an h-point (see Figure 4.5).

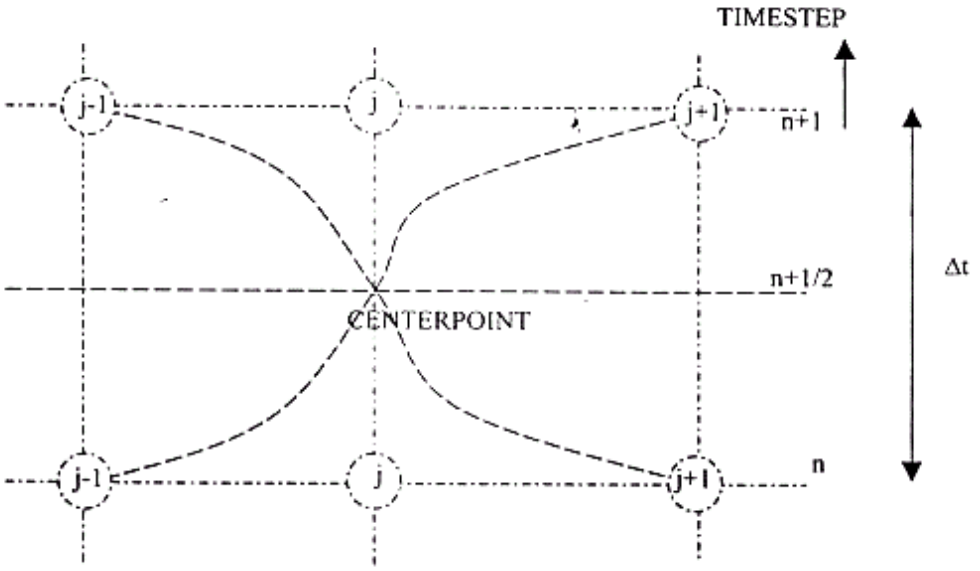

Figure 4.4: Centered 6-points Abbott Scheme

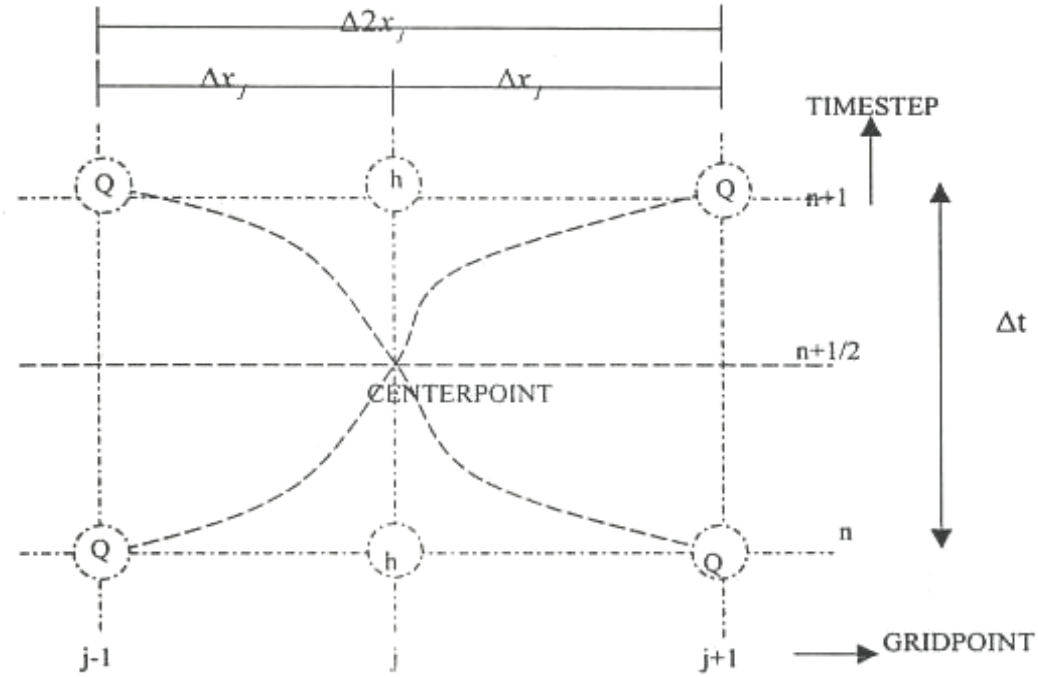

Figure 4.5: Centering of Continuity Equation in 6-point Abbott Scheme

The derivatives in Equation (4.14) are expressed at the time level, n+1/2, as follows:

$$\frac{\partial Q}{\partial x} \approx \frac{\frac{\left(Q_{j+1}^{n+1} + Q_{j+1}^{n}\right)}{2} - \frac{\left(Q_{j-1}^{n+1} + Q_{j-1}^{n}\right)}{2}}{\Delta 2x_j} \tag{4.15}$$

$$\frac{\partial h}{\partial t} \approx \frac{h_j^{n+1} - h_j^n}{\Delta t} \tag{4.16}$$

b_s in Equation (4.14) is approximated by:

$$b_s = \frac{A_{0j} + A_{0j+1}}{\Delta 2x_j} \tag{4.17}$$

where:

A_{0j} is the surface area between grid point j-1 and j
A_{0j+1} is the surface area between grid point j and j+1
$\Delta 2x_j$ is the distance between point j-1 and j+1

Substituting for the derivatives in Equation (4.14) gives a formulation of the following form:

$$\alpha_j Q_{j-1}^{n+1} + \beta_j h_j^{n+1} + \gamma_j Q_{j+1}^{n+1} = \delta_j \tag{4.18}$$

where α, β and γ are functions of b and δ, moreover, depend on Q and h at time level n and Q on time level n+ ½.

Momentum Equation

The momentum equation is centered at Q-points as illustrated in Figure 4.6.

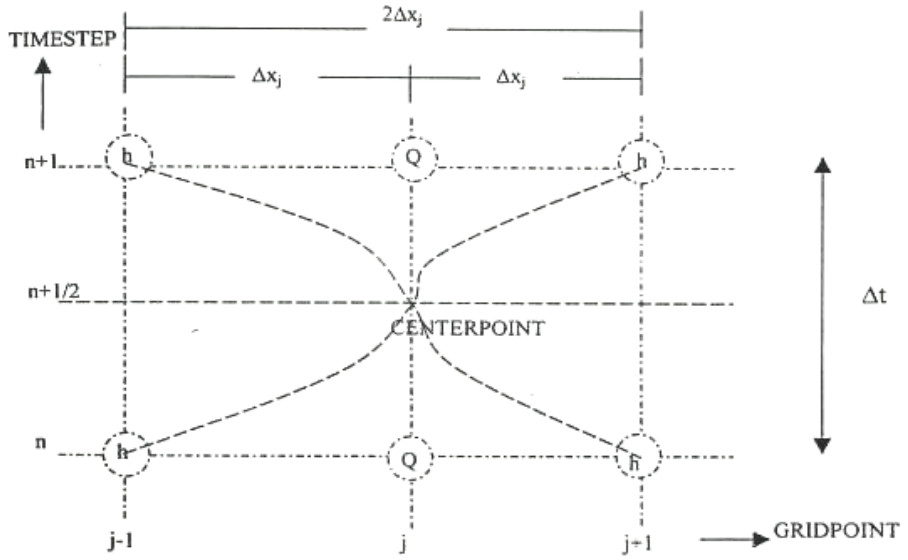

Figure 4.6: Centering of Momentum Equation in 6-point Abbott Scheme

The derivatives of Equation (4.12) the Saint Venant Equations are expressed in the following way:

$$\frac{\partial Q}{\partial t} \approx \frac{Q_j^{n+1} - Q_j^n}{\Delta t} \tag{4.19}$$

$$\frac{\partial}{\partial x}\left(\alpha \frac{Q^2}{A}\right) \approx \frac{\left(\alpha \frac{Q^2}{A}\right)_{j+1}^{n+\frac{1}{2}} - \left(\alpha \frac{Q^2}{A}\right)_{j-1}^{n+\frac{1}{2}}}{\Delta 2x_j} \tag{4.20}$$

$$\frac{\partial h}{\partial x} \approx \frac{\frac{\left(h_{j+1}^{n+1} + h_{j+1}^n\right)}{2} - \frac{\left(h_{j-1}^{n+1} + h_{j-1}^n\right)}{2}}{\Delta 2x_j} \tag{4.21}$$

For the quadratic term in (4.20), a special formulation is used to ensure the correct sign for this term when the flow direction is changing during the time step:

$$Q^2 \approx f Q_j^{n+1} Q_j^n - (f-1) Q_j^n Q_j^n \tag{4.22}$$

where f can be specified by the user (THETA coefficient in Menu G.5.5 of the user manual of MIKE 11) and by default is set to 1.0. With all the derivatives substituted, the momentum equation can be written in the following form:

$$\alpha_j h_{j-1}^{n+1} + \beta_j Q_j^{n+1} + \gamma_j h_{j+1}^{n+1} = \delta_j \tag{4.23}$$

where

$$\alpha_j = f(A)$$
$$\beta_j = f(Q_j^n, \Delta t, \Delta x, C, A, R)$$
$$\gamma_j = f(A)$$
$$\delta_j = f\left(A, \Delta x, \Delta t, \alpha, q, \nu, \phi, h_{j-1}^n, Q_{j-1}^{n+\frac{1}{2}}, Q_j^n, h_{j+1}^n, Q_{j+1}^{n+\frac{1}{2}}\right)$$

To obtain a fully centered description of A_{j+1}, these terms should be valid at time level n+1/2, which can only be fulfilled by using iteration. For the season, the equations are solved by default two times at every time step, the first iteration starting from the results of the previous time step, and the second iteration using the centered values from this calculation. The number of iterations can be changed by using the NR-ITER coefficient.

4.2 Data collection and data analysis for HD Model

The selection of stream flow stations are considered for preparing data to calibrate and validate by MIKE11-HD, presented in Table 4.1 and Figure 4.7 The criteria for selecting stream flow station are defined below:

- The selected stream flow station should have continuously long term period continuous record and settle down on the main river that will be easier for warning in the downstream on time,
- The location of stream flow station that are on the main river, Managawa.

Model data requirement
- Catchment delineation
- River and flood plain topography
- Hydrometric data for boundary conditions
- Hydrometric data for calibration and validation

Table 4.1: List of stream flow station and recording year in the upstream of Managawa River Basin

Stream flow station	*Location*		*Type of data*	*Hourly data available*
	Latitude	*Longitude*		
Managawa dam	35°54'12"	136°32'26"	Water Level (H)	1981-2004
Outflow from Sasougawa dam	35°50'38"	136°32'57"	Discharge (Q)	1981-2004
Outflow from Kumokawa dam	35°50'51"	136°27'26"	Discharge (Q)	1981-2004
Nagashima	35°52'41"	136°30'27"	Water Level (H)	1981-2004

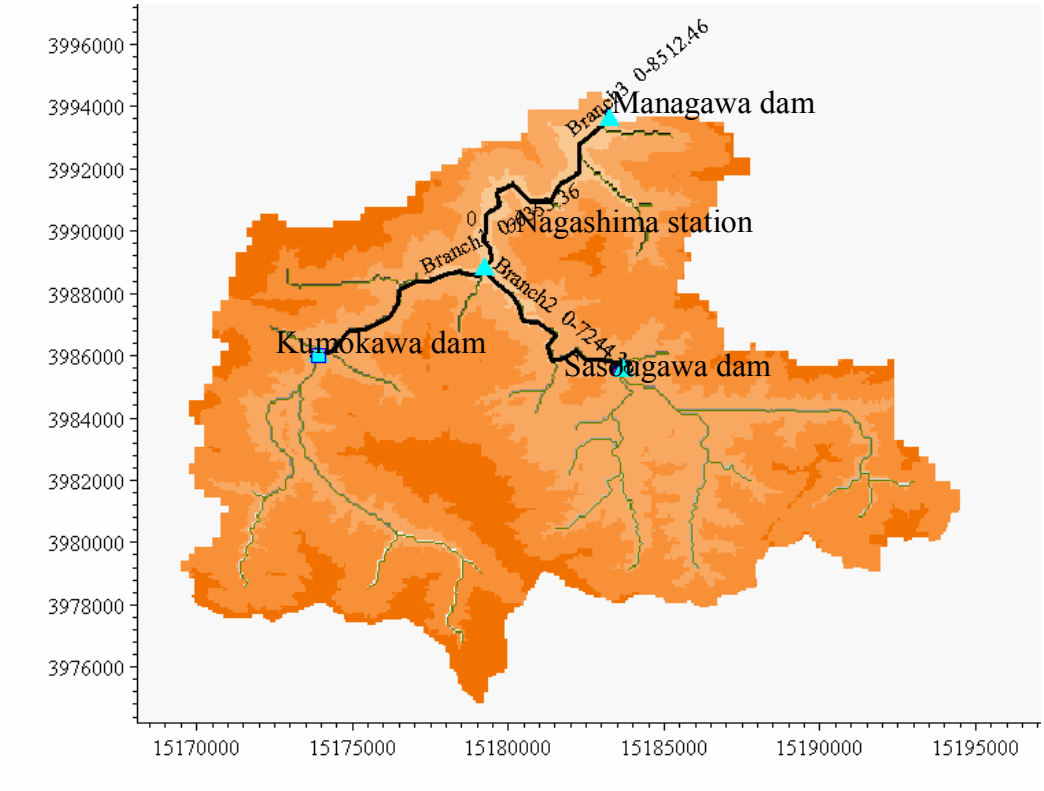

Figure 4.7 Selected stream flow stations in the upstream of Managawa dam, UTM coordinate

4.2.1 Topography and River Cross Section

Topography map is generated using Geographic Information System (GIS) as the digital elevation map; grid size is 50 x 50 meters. River cross sections based on year 2002 and 2004 in Managawa river basin are transformed into digital files for 44 sections, starting from Kumokawa dam to junction (Nagashima) called Branch 1, Sasougawa dam to junction called Branch 2 and junction to downstream stream flow station (Managawa dam) called Branch 3, as shown in Figure 4.8. The samples of cross section; the beginning and ending of each branch, are shown in Figure 4.9. Length of Branch 1, 2 and 3 are 6.4, 7.2 and 8.5 km. sequence.

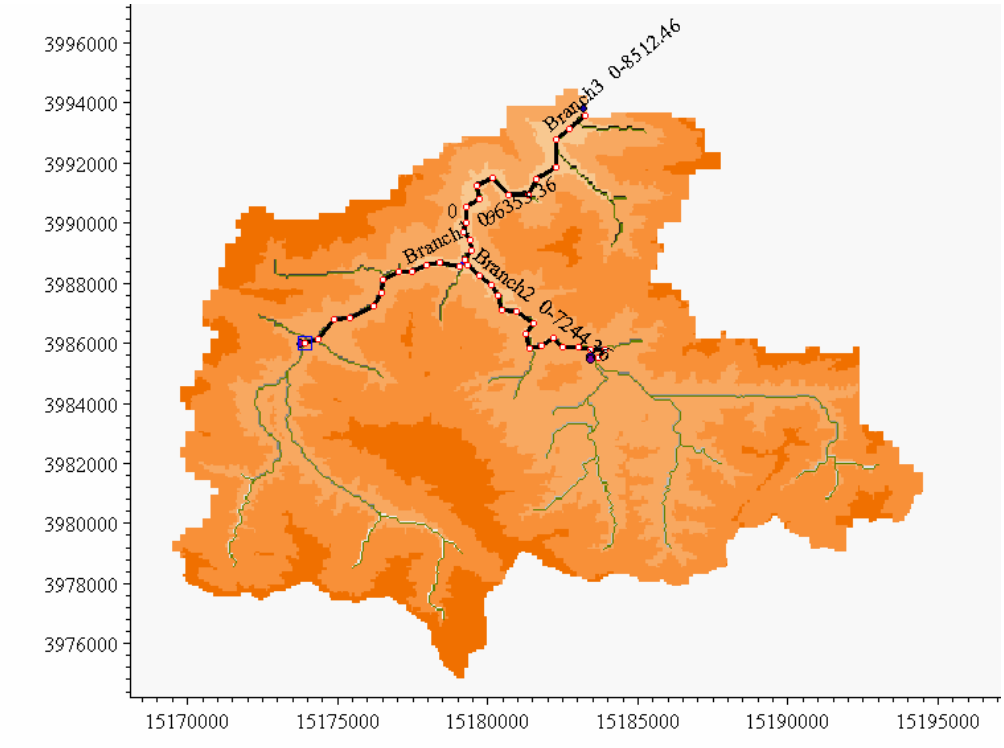

Figure 4.8: Locations of river cross sections in Managawa river basin, UTM coordinate

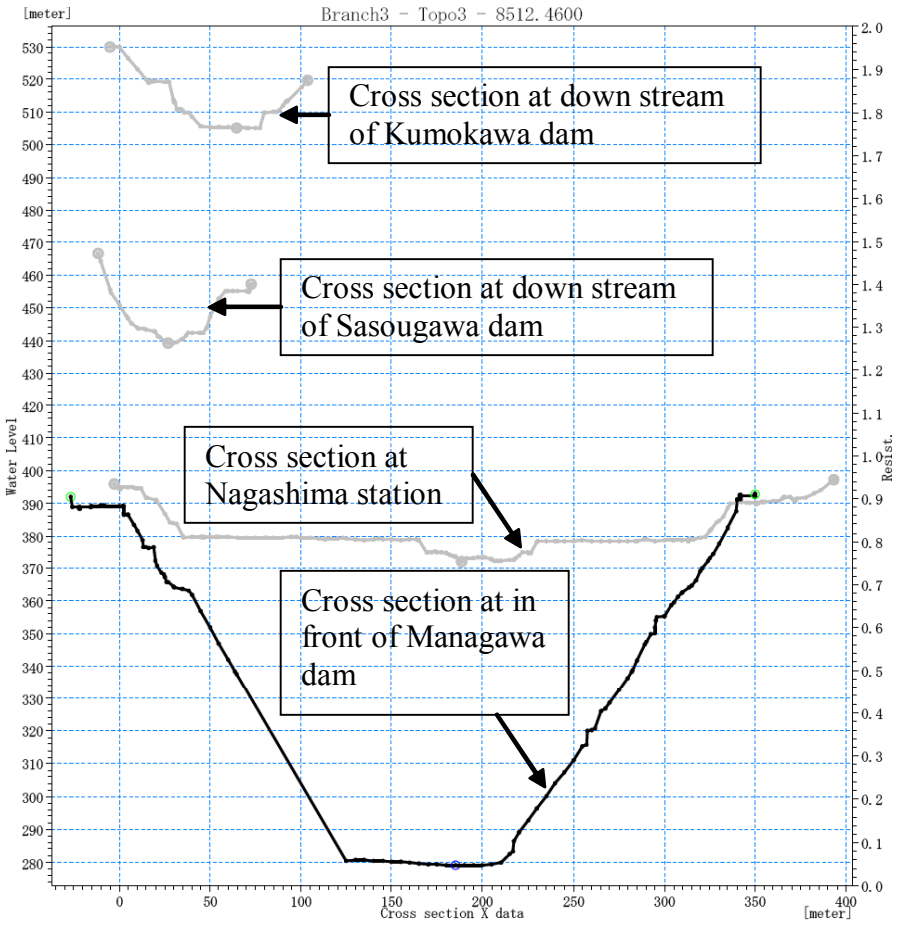

Figure 4.9: Cross sections of beginning and ending of each branch

This river cross section data are provided by NEWJEC Company. Details of these, cross sections are put in below Table 4.2.

Table 4.2: Location of each cross section

Branch	***Cross section no.***	***Length (km)***
Branch 1	1	0.00
Branch 1	2	0.46
Branch 1	3	1.29
Branch 1	4	1.81
Branch 1	5	2.68
Branch 1	6	3.22
Branch 1	7	3.66
Branch 1	8	4.27
Branch 1	9	5.22
Branch 1	10	5.70
Branch 1	11	6.35
Branch 2	12	0.00
Branch 2	13	0.38
Branch 2	14	0.89
Branch 2	15	1.30
Branch 2	16	1.83
Branch 2	17	2.24
Branch 2	18	2.74
Branch 2	19	3.15
Branch 2	20	3.67
Branch 2	21	4.12
Branch 2	22	4.83
Branch 2	23	5.32
Branch 2	24	5.78
Branch 2	25	6.25
Branch 2	26	6.71
Branch 2	27	7.24
Branch 3	28	0.00
Branch 3	29	0.38
Branch 3	30	0.74
Branch 3	31	1.07
Branch 3	32	1.40
Branch 3	33	1.93
Branch 3	34	2.49
Branch 3	35	2.94
Branch 3	36	3.53
Branch 3	37	4.28
Branch 3	38	4.97
Branch 3	39	5.56
Branch 3	40	6.31
Branch 3	41	7.24
Branch 3	42	7.80
Branch 3	43	8.51
Branch 3	44	4.69

4.3 Results Analysis

4.3.1 Calibration and validation

For hydrodynamic model, the data range that I used to adjust model's parameter is during heavy rainfall year. Considering the historical rainfall data in Figure 4.10 I applied data in year 1995 and 2004 for adjusting model's parameter, calibrate the model. For verification, we applied data in year 1998, 2002 and 2003 for checking the efficiency of model.

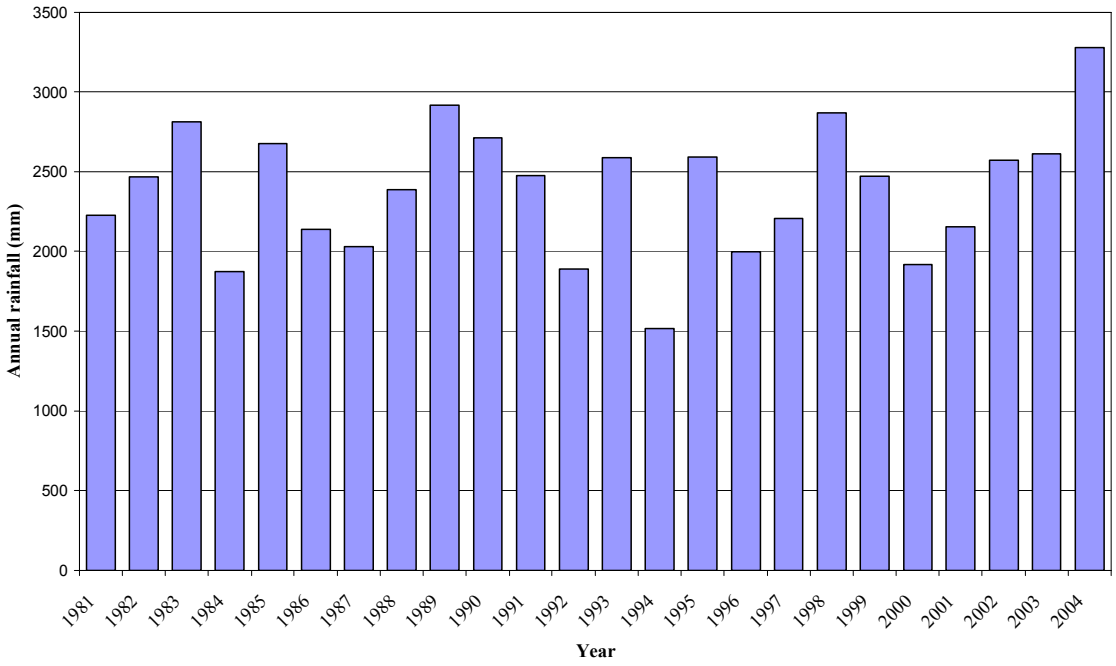

Figure 4.10: Annual rainfall at Managawa river basin from 1981 - 2004

Adjusting hydrodynamic model's parameter

The most important factor in hydrodynamic model is roughness coefficient, the roughness of bed material followed Ven Te Chow (1973), Open Channel Hydraulics. It was defined by the type of bed material in which Manning's roughness coefficient of soil is between 0.025 - 0.033 $s/m^{1/3}$ or Manning's M is about 30 – 40 $m^{1/3}/s$, soft rock is between 0.025 – 0.040 $s/m^{1/3}$ or Manning's M is about 25 – 40 $m^{1/3}/s$ and hard rock is between 0.035 – 0.050 $s/m^{1/3}$ or Manning's M is about 20 – 40 $m^{1/3}/s$.

The river bed in this river basin is soil and rock therefore I used trial and error technique to get the appropriate river roughness parameter as shown in Table 4.3. This study assumes that along the branch is same roughness value.

Table 4.3: Roughness coefficient of bed material

River name	Manning's M ($m^{1/3}/s$)
Branch 1	30
Branch 2	30
Branch 3	15

4.3.2 Efficiency of Hydrodynamic model

The performances of this model express by the efficiency index (EI) and plotting curve comparison between simulated and observed water level data at Nagashima station.

From the efficiency of the model, the calibration efficiency is about 94 %, the verification efficiency is about 88% as shown in Table 4.4. The peak time of simulated hydrograph is same with observed one, the trend of simulated curve is quite match with observed one as shown in Figure 4.11 – 4.13. The results are very satisfactory for calibration and verification in term of efficiency index and shape of hydrograph. The shapes of simulated hydrograph match well with the observed hydrograph and the statistical performances are tabulated.

Table 4.4: Statistical performance index during flood period of HD Model calibration and verification

Error Estimation	***Calibration***	***Verification***
	2004 & 1995	***1998,2002&2003***
Efficiency Index (%)	94	88

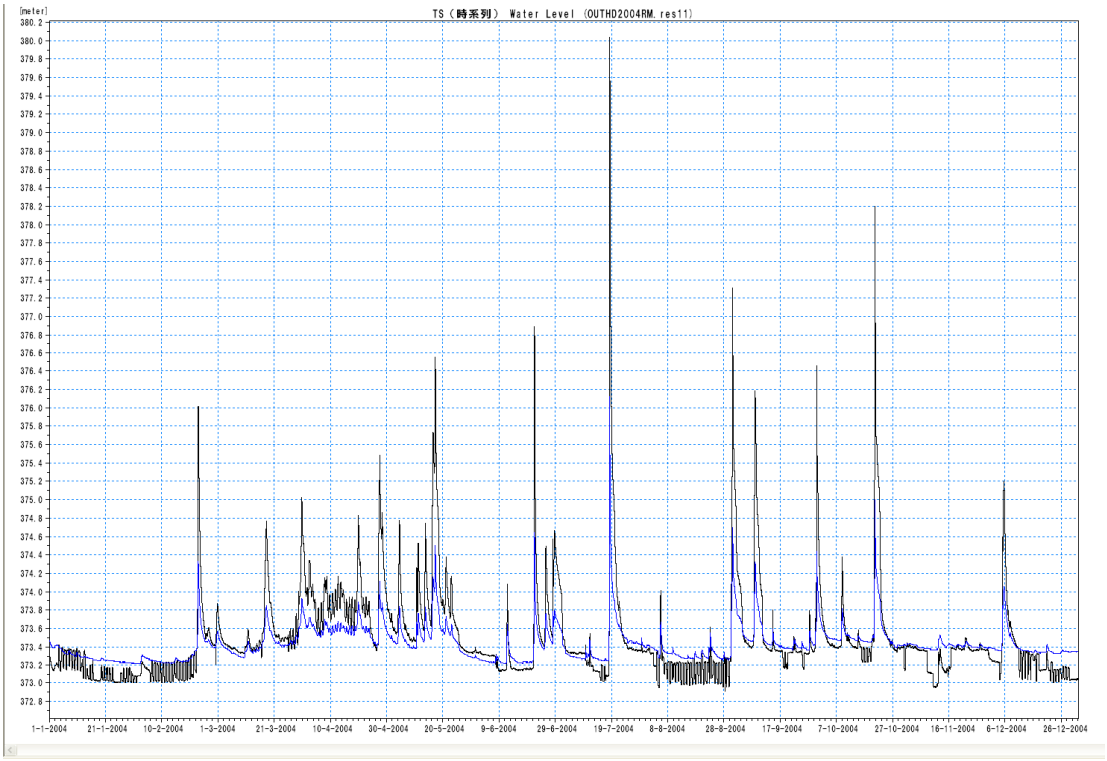

Figure 4.11: Comparison between observe and computed water level at Nagashima station, 2004

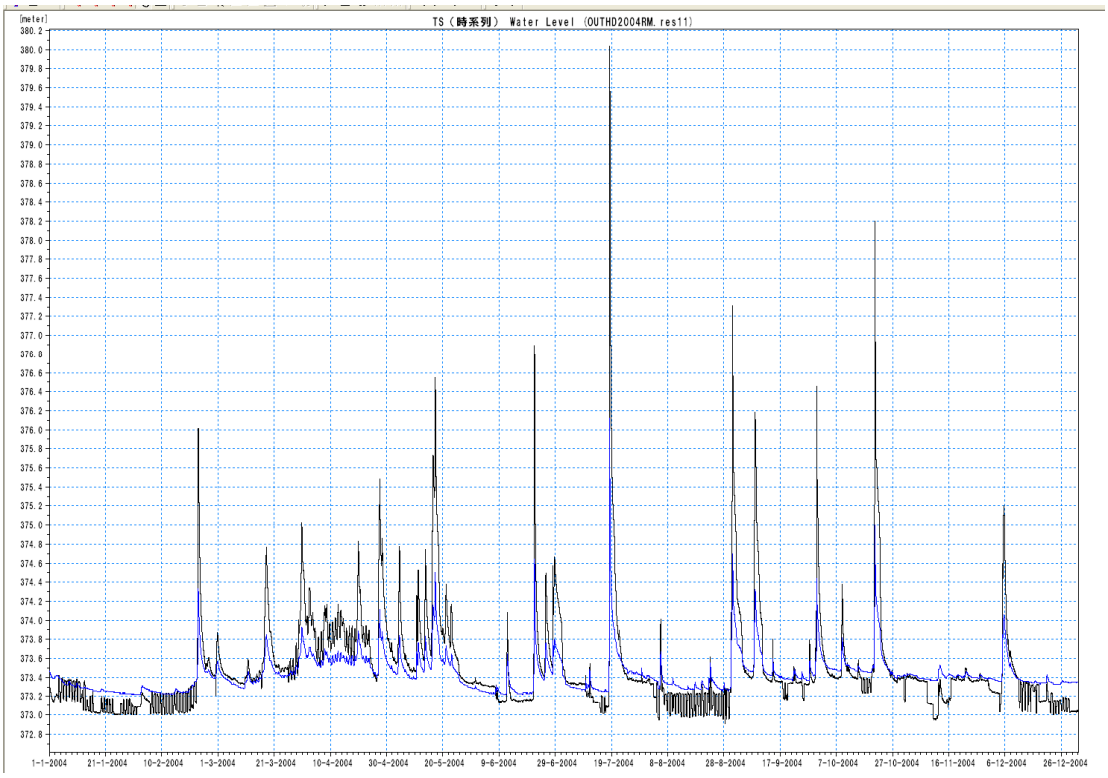

Figure 4.12: Comparison between observe and computed water level at Nagashima station, 2002

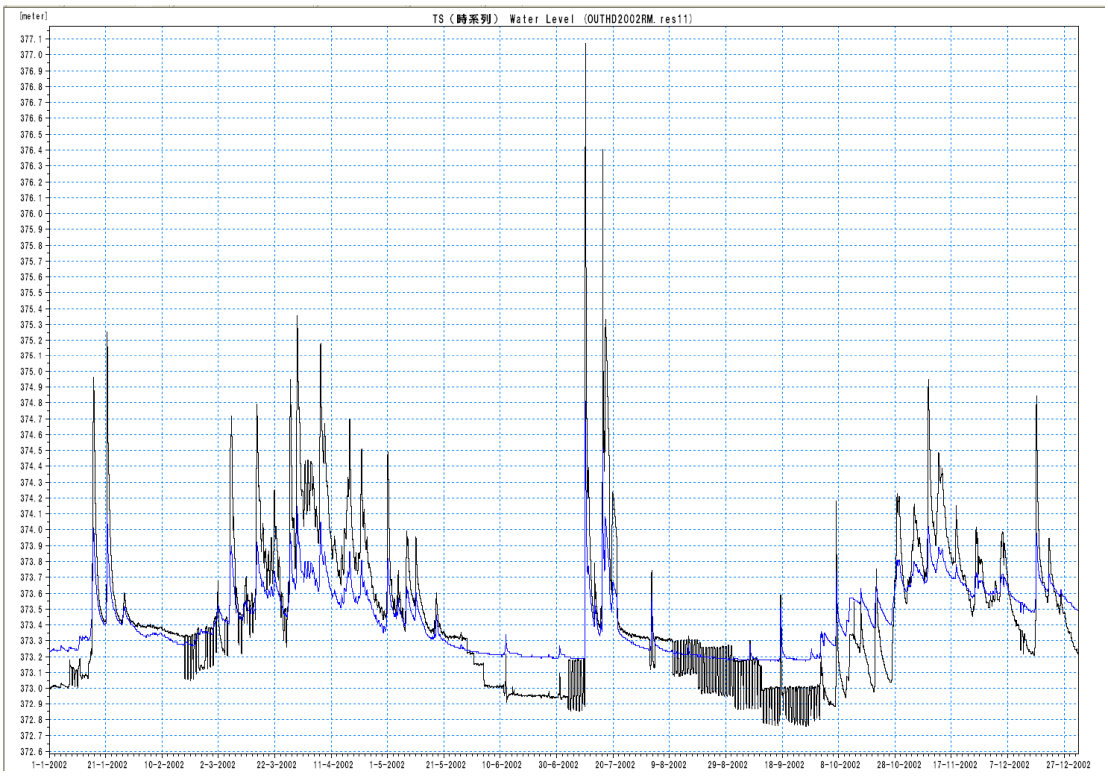

Figure 4.13: Comparison between observe and computed water level at Nagashima station, 1998

4.4 Conclusions

The flow characteristics as velocity, water discharge, water depth, etc in the Managawa river were presented by hydrodynamic model. The hydrodynamic model in this study is 1D model; MIKE 11. This study applied the heavy rainfall years to calibrate and verify the model to adjust hydraulic parameters which the main parameter for this model is bed resistant or Manning's n. -The performance of the model is quite high as shown by efficiency index and plotting curve. This hydrodynamic model will also be used with the integrated sedimentation model in the next chapter.

CHAPTER 5
Integrated Sedimentation Model

Sediment system in watershed is not only sediment yield but also including sediment transportation along the rivers. In this study, the Geographic Information System (GIS) combined with sediment yield model can be enhancing the evaluation of soil erosion estimation. Surface erosion on Managawa river basin is computed with the Modified Universal Soil Loss Equation (MUSLE) and it is verified to reflect the hydrological processes which are able to estimate soil losses. In the sediment transport routing module, total load equation is applied to carry sediment from soil surface erosion to deposit in Managawa dam. According to annual accumulation sediment volume data in Managawa reservoir during 1981 – 2003, the establish model and simulation results are satisfy. The efficiency of the Modified Universal Equation with sediment routing in rivers is higher than the simple Modified Universal Equation

The main objective of this part is computing annual depositing sediment volume in Managawa dam by using soil erosion model and sediment transportation model. Erosion on sub-basin caused by rainfall and surface runoff is computed with Modified Universal Soil Loss Equation (MUSLE), which time interval is day continuously from 1983 to 2004. After outlets of each sub-basin, sediment will be transported by main channel. This part shows the results of these combined systems.

5.1 Sediment Yield Model

5.1.1 Model description

The Soil and Water Assessment Tool (SWAT) is a long term distributed parameter model, designed to predict the impact of land management practice in a watershed (Arnold et al., 1998). In this study, the SWAT ArcView interface (DiLuzio et al., 2001) was used to write SWAT input files from GIS data layers. SWAT model calculates soil erosion caused by rainfall-runoff process using MUSLE. The model is a modified form of the USLE. The difference between the two approaches that in MUSLE rainfall energy factor is replaced with a runoff factor which represents energy used in detaching and transporting sediment. SWAT model requires a Digital Elevation Model (DEM) from which it determines the drainage network and divides the basin into sub-basins defined by grid cells, spatially related one to another, that each has geographic position in the watershed defined by surface topography.

This study applies SWAT model only to find out the soil erosion of each sub-basin at each outlet point. The MUSLE is used in this study which is given as Equation (5.1). From MUSLE, the shortest time interval of output is daily and this study need daily sediment yield data to input in sediment transport model.

$$Y = 11.8(Q_s q_p A_{area})^{0.56} K \cdot C \cdot P \cdot LS \cdot CFRG \quad (5.1)$$

Where Y is the sediment yield on a given day (ton)
Q_s is the surface runoff (mm)
q_p is the peak runoff rate (m^3/s)
A_{area} is area (km^2)
K is the USLE soil erodibility factor
C is the USLE cover and management factor
P is the USLE support practice factor
LS is the USLE topographic factor
$CFRG$ is the coarse fragment factor

SWAT estimates the surface runoff (Q_s) with the SCS curve number method and the peak runoff rate is calculated with the rational method:

$$q_p = \frac{c \cdot i \cdot A_{area}}{3.6} \quad (5.2)$$

Where q_p is the peak runoff rate (m^3/s)
A_{area} is area (km^2)
c is the runoff coefficient
i is the rainfall intensity (mm/hr)
3.6 is a unit conversion factor

5.1.2 MUSLE analysis

In this part, there are 8 sub-basins which sub-basin no.1, 2 and 3 are on the dam area so those sub-basins will directly supply sediment into dam. The soil erosion of those areas from MUSLE will be directly sum up to the total sediment volume as shown in Figure 5.1 and Figure 5.2 and the sub-basin No.9 is not supplying sediment to Managawa Dam.

Figure 5.1: Sub-basins in this study

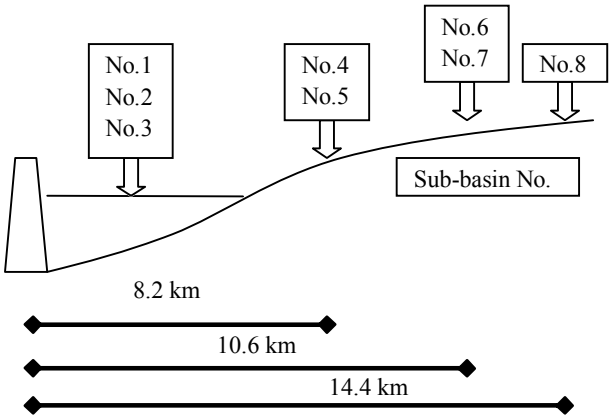

Figure 5.2 Location that sediment yield of each sub-basin from MUSLE supplied to the main river system

5.2 Sediment Transport Model

The sediment transport computations are made in parallel with the hydrodynamic computations. The sediment transport equations are solved in time and space as an implicit function of the corresponding values of the hydraulic parameters (i.e. discharge, water levels, etc.). The bottom topography is updated so that changes due to sediment transport will be included in the next hydrodynamic computations. Results are in form of sediment transport rates, bed level changes, resistance number and dune dimensions. The non-cohesive sediment transport module is equipped with five different models for the calculation of sediment transport rate and alluvial roughness. These are the Engelund and Hansen model, the Ackers and White model, and the Smart and Jaeggi model for the calculation of the total load, and the Engelund and Fredsoe and van Rijn models for the calculation of bed load and suspended load separately. All these models can be run using a single representative grain size or using number of grain sizes representing grain size fractions in graded material. Provision is also made for specifying the geometric standard division of the grain size distribution to enable the mean diameter of the suspended bed material to be computed. All above are available in both modes; explicit and morphological.

The morphological model updates the bed level due to erosion or deposition using the continuity equation for sediment transport. The model updates the level of the entire cross section or only a part of a part of it and leaving the bottom level of the remaining part of cross section unchanged.

Total load model

- Acker and White (1973) presented a semi-empirical sediment transport model. The model is partly based on dimensional analysis but physical arguments have been used to derive the form of the function that was tested.

- Engelund and Hansen (1967) presented a sediment transport formula derived from considerations of the work done by the flow on the sediment being transported. Although the formula was derived for a dune covered bed, it was found also to be applicable to the upper regime.
- Smart and Jaeggi (1983) presented a sediment transport formula which calculates the transport of coarse sediments in steep channels/rivers. The transport formula is based on the original Meyer-Peter-Mueller equation, which was derived from laboratory experiments with non-uniform sediments of various densities and flume-slopes ranging from 0.04 – 2 %.

Updating of bottom level

Various assumptions regarding the change in bathymetry of cross section during erosion and deposition can be made. Such considerations are necessary when the results from the morphological model are interpreted, as the model is only one dimensional.

Boundary condition

A sediment transport boundary condition can be applied as an external boundary or as sediment inflow. Sediment transport boundary can be applied with both positive and negative values imposing either sediment addition or abstraction (e.g. dredging).

In this study, sediment boundary condition set as sediment supply is the sediment yield from soil loss equation. This study can apply the sediment supply mode to be a boundary as sediment movement occurred from only hydrodynamic effect. For sediment supply, choosing this option, no time series file and item shall be defined and the sediment transport at the boundary locations will be calculated automatically based on the hydrodynamic conditions at the actual time. The sediment supply boundary condition could be used if e.g. measurements are not available for the sediment transport at the inflow boundary point purely based on the hydrodynamic conditions at the given time.

5.3 Integrated Sedimentation Model

In this study, the computing an annual sediment volume depositing in dam by mathematical model is necessary to input the models; soil erosion model, hydraulic model and sediment transport model, with hydrology data, hydrodynamic data, sediment data, geographic data and topographic data.

5.3.1 Data collection and data analysis

Hourly rainfall data
Hourly rainfall data from 1981-2004 were collected by 8 rain gauges located on Managawa river basin and the results from plotting double mass curve of each rainfall stations are reliable. Distribution of rainfall could be affected by topographical data such as elevation and so on, the Thiessen method was used to estimate rainfall within the entire catchment as mentioned in Chapter 3.

Hourly water flow and water level

Discharge and water level data are available in hourly to input as boundary condition in hydraulic model which outflows from Kumokawa Dam and Sasougawa Dam are the upper boundaries and water level at Managawa Dam is the lower boundary.

Topographic data

Geographic Information System (GIS) data used for finding out parameters in soil erosion model are Digital Elevation Model (DEM) 50m x 50m, land use and soil type. For land use information, there are available in 1976, 1987, 1991 and 1997 however the most of land use of the study area is forest and it does not so much change by time as shown in Figure 5.3.

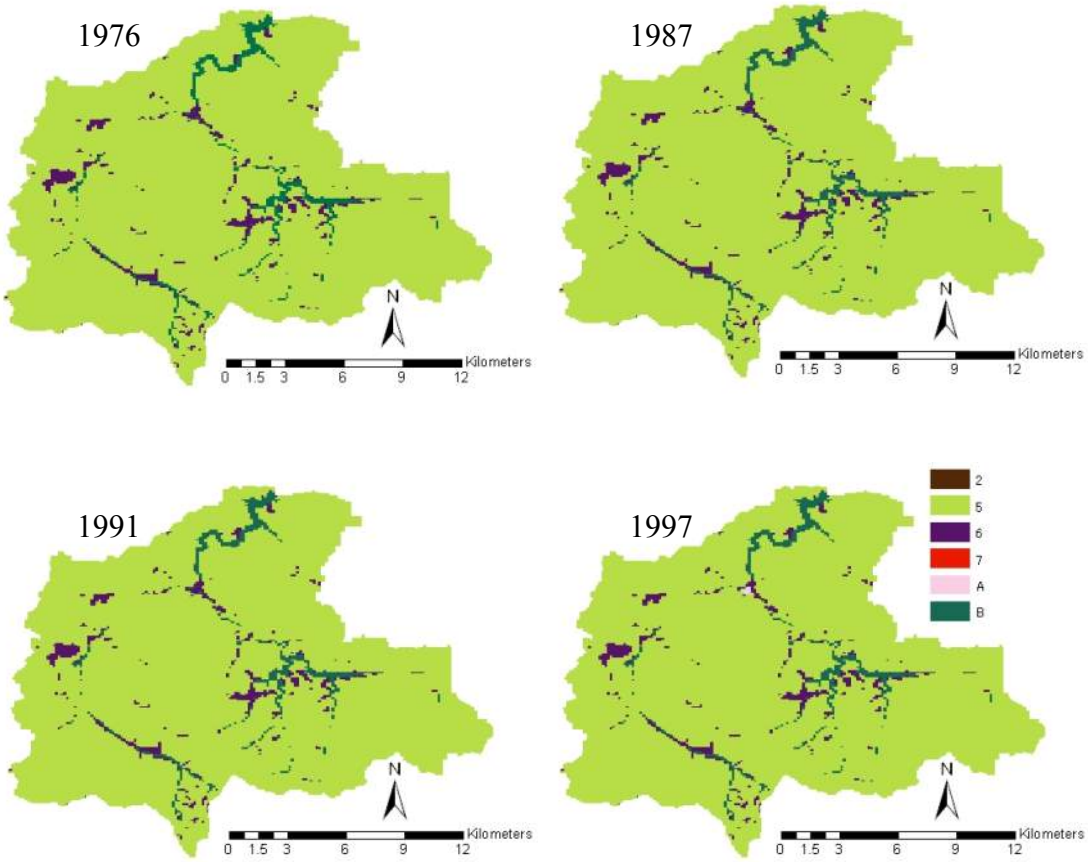

Figure 5.3: Land use in 1976, 1987, 1991 and 1997
2 = Agricultures, 5= Forest, 6=Waste Land, 7=Building,
A= Small Building, B=Water Body

Calculating soil erosion, Modified Universal Soil Loss Equation (MUSLE), in this study apply with the Soil and Water Assessment Tool (SWAT) that the watershed modeling framework is delineated starting from the digital description of the landscape as Digital Elevation Map (DEM), land use and soil data sets using ArcView interface, Spatial Analyst, with geomorphologic assessment procedures to obtain soil erosion from each sub-basin. Managawa river basin was divided into 9 sub-basins which one sub-basin on upper Sasougawa Dam is neglected because that dam will capture all sediment from upper part. After that the calculated daily sediment supply from each sub-basin will be taken to input as lateral sediment inflow to Managawa River model which hydrodynamic (HD) and sediment transport (ST) models are calculated by MIKE 11 developed by DHI Water and Environment. Flow chart of this study is shown in Figure 5.4.

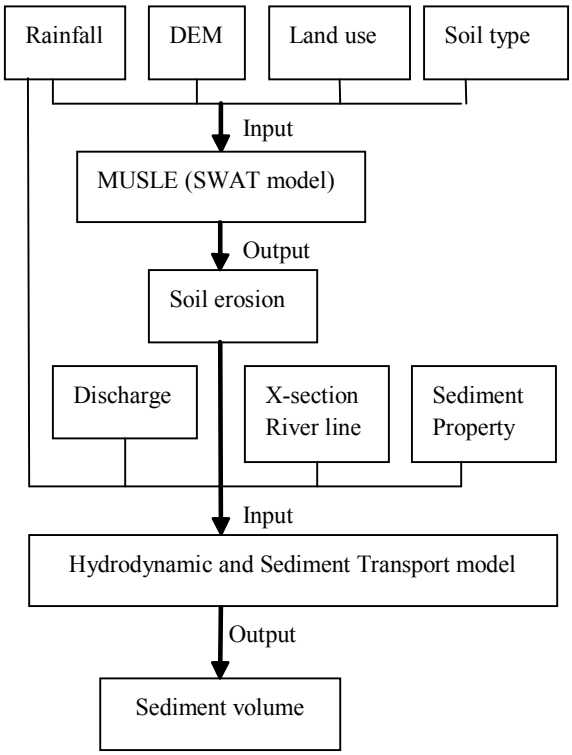

Figure 5.4: Scope of this part study

The sediment transport computations are made in parallel with the hydrodynamic computations. The sediment transport equations are solved in time and space as an implicit function of the corresponding values of the hydraulic parameters. In this study, total load model Acker and White (1973) presented a semi-empirical sediment transport mode is used for computation.

a) Boundary conditions, calibration and verification for Hydrodynamic model

As mention in Chapter 4, outflows from Kumokawa Dam and Sasougawa Dam are set to upstream hydrodynamic boundaries and water level at Managawa Dam is set to down stream boundary as shown in Figure 5.5.

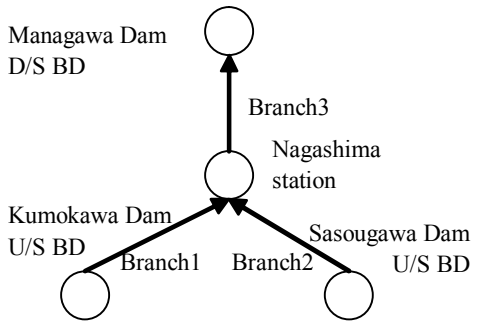

Figure 5.5: Hydrodynamic boundary condition diagram

To calibrate Hydrodynamic model by changing roughness coefficient which this study select year 1995 and 2004 for calibration and year 1998, 2002 and 2003 are for verification. The efficiency index (EI) for calibration is 94 % and for verification is 88% while roughness coefficients, Manning M, are 30, 30 and 15 for branch 1, 2 and 3 in sequence.

b) Sensitivity analysis of sediment transport model

Daily sediment yield from MUSLE computation will be supplied to the main river system at outlet points of each sub-basin. Acker and White equation need to input grain size diameter (D50). The distributed grain size diagram of 4 sediment samplings in Managawa Dam in 1998 is shown in Figure 5.6**.** Sample 1, 2 and 3 were taken near dam body and sample 4 was taken around upstream delta deposits. Based on these data, the sediment transportation model will apply the approximate value for D50 as 0.005 m in this study.

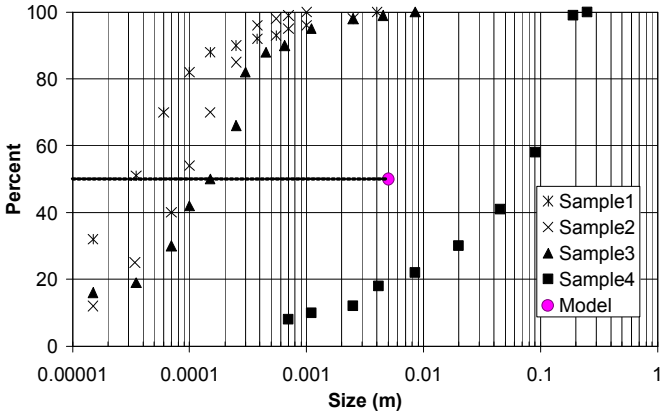

Figure 5.6: Sediment distribution curve of 4 samplings in Managawa Dam, 1998

For reference, sensitivity analysis of grain size diameter is shown in Figure 5.7**.** When grain size becomes finer, sediment accumulation volume becomes larger.

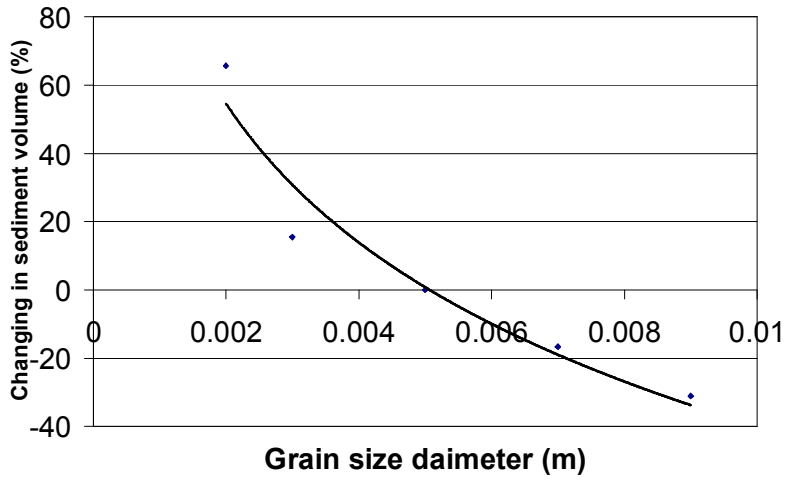

Figure 5.7: Sensitivity analysis of grain size diameter effect to accumulation sediment volume in 1995

5.4 Results Analysis

5.4.1 Topographic results

This study has generated a watershed to 8 sub-basins as shown in Figure 5.1 excluding Sasougawa dam basin. From 50m x 50m grid, I can obtain topographic information as area, average slope and average elevation in Table 5.1.

Table 5.1: Topographic information of each sub-basin

Sub basin	*Area (km2)*	*Slope (%)*	*Elevation (m)*	*Manning's n*
1	9.39	0.44	546	0.035
2	12.76	0.52	363	0.035
3	11.54	0.52	546	0.035
4	9.84	0.45	704	0.035
5	27.35	0.45	557	0.035
6	8.01	0.49	1089	0.035
7	17.64	0.42	705	0.035
8	53.81	0.44	629	0.035

5.4.2 Soil surface erosion results

Average annual sediment yields (t/ha) for each sub-basin during 1981 to 2004 were computed by MUSLE with SWAT model as shown in Table 5.2**.**

Table 5.2: Annual average soil surface erosion from MUSLE

Sub-basin	***Average Erosion (t/ha/year)***
1	9.66
2	12.04
3	12.08
4	9.86
5	10.39
6	10.94
7	9.26
8	10.58

Sub-basin No. 2 and 3 show high erosion rate because these slopes are so steep. The average sediment yield from the whole watershed calculated from Equation (5.3) is about 60,161 m^3/year.

$$S_y = \frac{\sum Y_a \cdot Area \cdot 100}{\sigma} \tag{5.3}$$

Where S_y is the average sediment yield (m^3)
Y_a is the sediment yield (t/ha)
$Area$ is sub-basin area (km^2)
σ is soil density about 2.65 t/m^3.

5.4.3 Sediment volume in dam

The volume of sediment depositing in the large dams are measured every year in Japan. Sediment volume data of Managawa Dam is also available from starting operation until recently year but some data was disappear because of technical error as shown in Table 5.3.

After sediment yield from each sub-basin was computed by MUSLE, those data were used to input in total load transport model, Acker and White (1973). And then sediment will be routed along the river and deposited in the dam reservoir. Computed results are shown with observed ones in Table 5.3. Observed data in 2004 was extremely large mainly because of the Fukui heavy rainfall in July 18, 2004.

Table 5.3: Observed and computed sediment volume, 1981-2004, in Managawa Dam

Year	*Observed Volume (m^3)*	*Computed Volume (m^3)*
1981	-	42,304
1982	-	75,108
1983	78,664	77,730
1984	15,768	66,523
1985	166,907	53,337
1986	16,726	73,660
1987	23,477	75,525
1988	59,272	54,324
1989	79,652	93,670
1990	353,591	106,494
1991	-	58,157
1992	-	41,525
1993	175,980	66,901
1994	-	52,652
1995	106,271	60,281
1996	-	52,339
1997	4,812	42,950
1998	249,132	121,724
1999	41,822	66,315
2000	-	50,654
2001	101,227	81,551
2002	237,574	83,042
2003	36,322	63,617
2004	1,078,341	145,913

(-) data is not available

5.5 Discussion and conclusions

5.5.1 Discussion

The computed sediment volumes in this study show large differences with the observed data because the observed data have some errors in some year. Therefore, total accumulated sediment volumes were compared between them. Observed and computed total sediment volumes until year 2003 were 1,747,197 m^3 and 1,560,381 m^3 respectively, which error is about 10%. In some year, the accumulative data are not much difference as shown in Figure 5.8. Therefore, the sediment yield and sediment transport model in this study can be used to estimate the sediment accumulation volume in Managawa Dam.

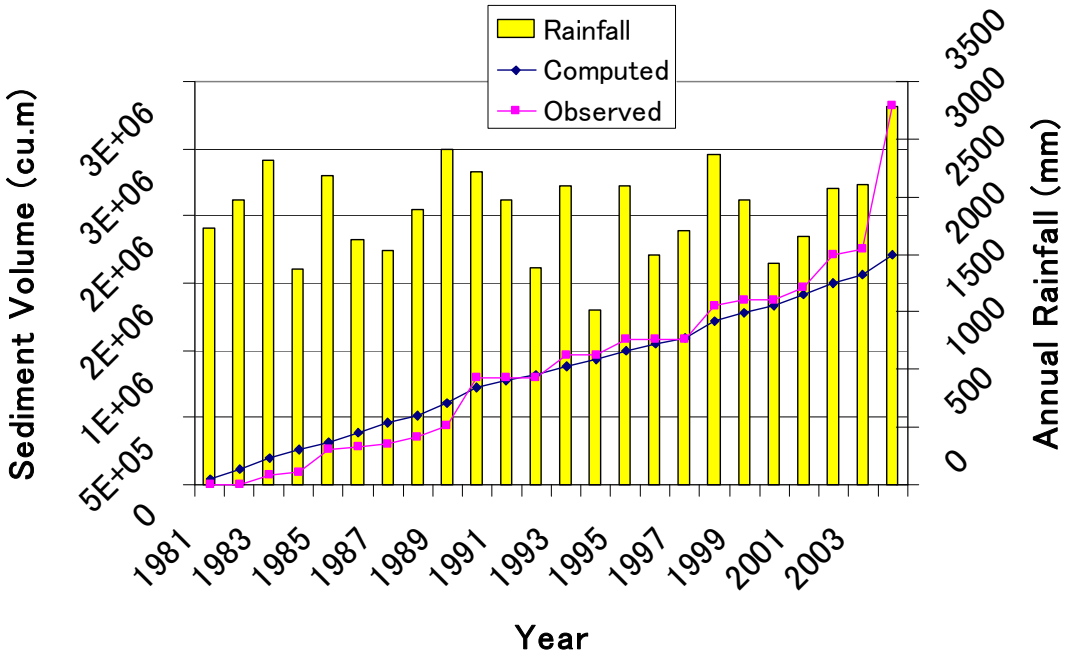

Figure 5.8: Annual rainfall, observed and computed accumulation sediment volume

In order to determine efficiencies of the MUSLE model, a logarithmic form of Nash-Sutchliffe model is adopted, which is given by:

$$Z_{\ln} = 1 - \frac{\sum_{e=1}^{n} (\ln(A_{eo}) - \ln(A_{ep}))^2}{\sum_{e=1}^{n} (\ln(A_{eo}) - A_{\ln m})^2} \qquad (5.4)$$

Where A_{eo} is the observed soil loss for event e

A_{ep} is the predicted soil loss

$A_{\ln m}$ is the mean value of $\ln(A_{eo})$ for all the events selected.

The Nash-Sutchliffe efficiency for this combined MUSLE and sediment transport model is about 0.30 where a model efficiency of 1.0 represents a perfect fit of the model to observed values. Negative values indicate that use of the average is a better predictor than the model (Nash-Sutchliffe, 1970). The Nash-Sutchliffe efficiency for the simple MUSLE is -0.84 and then the present model of MUSLE with the river routing system is increasing the efficiency.

In order to improve the model, the relationship among annual rainfall, annual discharge, and observed and computed sediment volumes are analyzed. The annual runoff flowed into Managawa Dam has good correlation with annual rainfall as plotted in Figure 5.9. The annual sediment volume in dam is not only depended on the soil surface properties and rainfall but depended on discharge also. Figure 5.10 and Figure 5.11 show that the

computed sediment volume from the model has moderately correlation with annual discharge but the observed one is varying more widely. R-square of computed sediment volume and annual discharge is 0.34, whereas the one of observed sediment volume and annual discharge is 0.16. Correlation may be dropped by the large rainfall events and other modifications are needed to compute sediment yield and transport process in such high flood periods. However, this study shows that this MUSLE with sediment transport model can be used to estimate reservoir sedimentation volumes and its tendency if basic characteristics of each catchment such as topographical, geological, meteorological conditions may change.

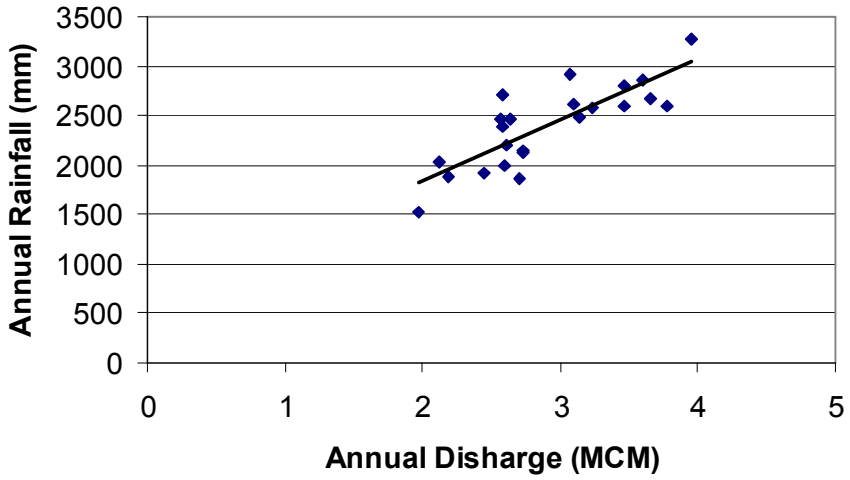

Figure 5.9: Relationship between Annual Discharge and Annual Rainfall, 1981-2004

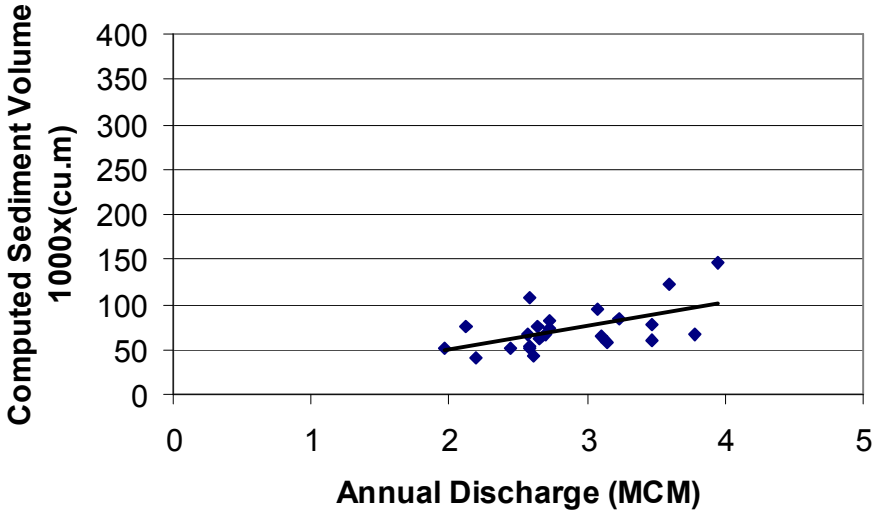

Figure 5.10: Relationship between Annual Discharge and Computed Sediment Volume

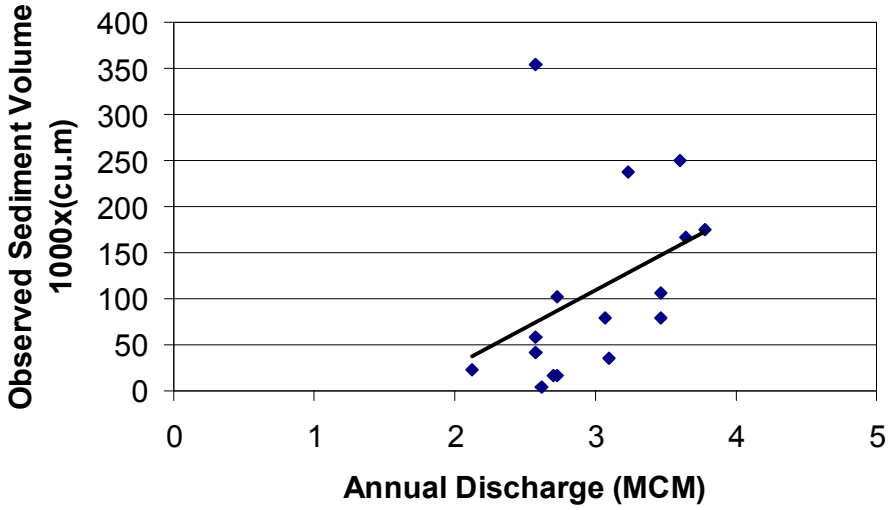

Figure 5.11: Relationship between Annual Discharge and Observed Sediment Volume

5.5.2 Conclusions

This study is an attempt to estimate the yearly volume of sediment deposition in Managawa Dam using the Modified Universal Soil Loss Equation (MUSLE) with sediment transport model. The MUSLE was developed for simulating the impact of land management practices on eco-hydrologic system (Arnold et al., 1995). The results of annual sediment accumulating volume for this study area show large differences with the observed data but total volumes almost coincided very well. In order to improve the model, other modifications may be needed to compute sediment yield and transport process in high flood periods. However, this model can be used to estimate reservoir sedimentation volumes and its tendency if catchment's conditions may change. The sediment yield in this study was mainly from rainfall effect and it did not include the freezing, throwing and chemical effect.

CHAPTER 6
Sediment Prediction Model

Artificial neural network (ANN) is used to estimate the hourly suspended sediment concentration at Okumotani station, the upstream of Managawa dam, Japan. This artificial neural network (ANN) was calibrated and validated by using recently suspended sediment data from December 2006 to January 2008. Choosing an appropriate neural network structure and providing field data to that network for training purpose are address by using a constructive back propagation algorithm. Without the previous step of suspended sediment data as input the outputs from network were fairly good agreement with observed data. However, it is demonstrated that the artificial neural network (ANN) is capable of modeling the hourly suspended sediment concentration with good accuracy when appropriate variables; rainfall, discharge, rainfall in two hours, their previous time step on suspended sediment concentration and the absolute of discharge changing are used as inputs of network.

Suspended sediment in river is an important parameter for reservoir management and it is an index for the status of soil erosion and ecological environment of a catchment. Mathematical models are widely used in studying soil erosion and sediment transportation which many empirical models and physical models have been developed to model the suspended sediment flux of a catchment. Some sediment yield model as Modified Universal Soil Loss Equation (MUSLE) was applied to Managawa river basin same as the study area of this research. That Modified Universal Soil Loss Equation (MUSLE) empirically relates soil erosion to rainfall erosivity, soil erodibility, topographic factor, plant cover and erosion control practices and the results from this model are the daily sediment yield from watershed (Chutachindakate and Sumi, 2007). Artificial neural network (ANN) is a type of empirical model. It is derived from the researches on the nature of the human brain (Muller et al., 1995). Hydrologic applications of artificial neural network (ANN) include the modeling of daily rainfall-runoff-sediment yield process, snow-rainfall process, assessment of stream's ecological and hydrological responses to climate change, rainfall-runoff forecasting, ground water quality prediction and ground water remediation. Artificial neural network (ANN) can be applied to predict the monthly, weekly and daily suspended sediment in the catchment by relating it to average rainfall, temperature, rainfall intensity and water discharge (Yun-Mei Zhu, 2007). Because of its ability to simulate nonlinear complex system without any priori assumption about the processes involved, artificial neural network (ANN) provides a promising alternative for the conventional empirical and physical models in sediment modeling. This study is an attempt to predict an hourly suspended sediment concentration on the river by using back propagation artificial neural network with hydrologic and hydrodynamical data as inputs of network. This artificial neural network was applied to simulate an hourly suspended sediment concentration from December 2006 to January 2008 in the Okumotani river, the upstream of Mangawa reservoir, Fukui prefecture, Japan. The performances of neural network were compared with that of multiple linear regression (MLR) models and sediment rating curve (SRC) model

6.1 Artificial Neural Network (ANN) model

Artificial Neural Networks (ANNs) are being used increasingly to predict and forecast water resources variables. Based on the consideration of the hydrological process (*Dooge, 1974*) divides hydrological models into three categories-physically based distributed model, lumped conceptual models and black box models. Neural Network models which inherently involves mapping of input and output vectors can be considered as a black box model. Such black box models can be considered of little significance in enhancing the understanding of hydrological and hydraulic processes, nevertheless in operational hydrology their usefulness can be paramount. The excessive requirement of field data in the case of physically based distributed models and the large number of parameters and subsequent difficulty in calibration in the case of lumped conceptual models render such models less suitable in operation flood forecasting use. This is reason why simple black box or storage based models found to be used extensively as flood forecast models. Several algorithms of neural networks model exist.

However, back propagation which belongs to supervised learning algorithm that performs a gradient descent search in weights space using generalized delta rule is often reported in applications (*Minn and Halls, 1986*). Back Propagation (BP) networks were developed by *Rumelhart and McClelland* (1986 and 1988) for learning associations between input and output patterns using more than a single layer perception, which overcomes some limitations of a single-layer perception (no layer hidden). A three layer feed forward neural network model is shown in Figure 6.1. Any BP network is based on supervised learning technique that compares the actual output from output units to the target or specified output and then readjust the weights backward in the network. The same input is presented to the network in the next iteration, so the actual output will be closer to the target output.

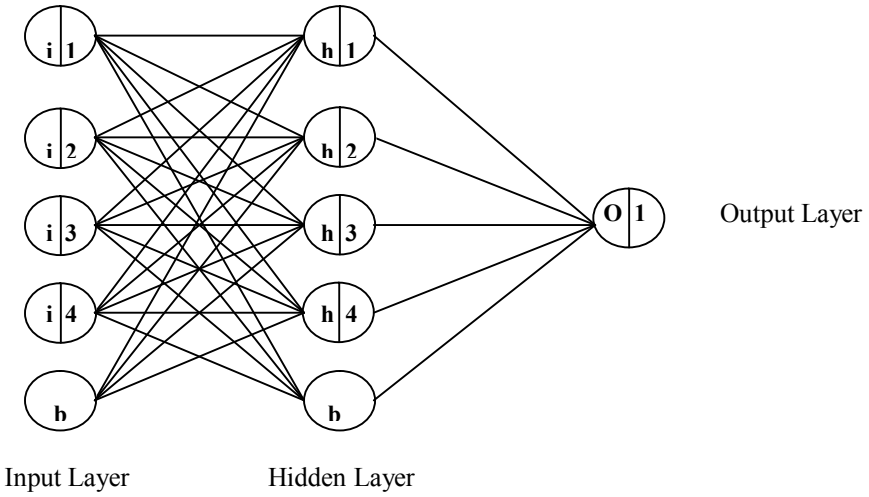

Figure 6.1: Typical Three Layers Neural Network Architecture

6.1.1 ANNs Procedures

ANNs uses the standard back propagation training algorithm as following;

- Data pre-processing; normalize data, initialize the weight factors and biases
- Forward Pass
- Backward Pass
- Data post-processing

Weights and statistic resulted from training iterations are saved periodically. Corresponding to each network, a set of weights and biases is found. Using those weights and biases, statistics are evaluated.
After getting the best network from the training phase, the parameters, which determined from the training process, are kept. The testing process starts with the data and the parameters, obtained from the training process for testing.

6.1.2 Numerical method of ANNs

Modeling with Neural Networks
The training and testing phases in a neural network are similar to the calibration and verification of the Rainfall-Runoff Model. In the neural network architecture, the output node represents the water level or discharges to be forecasted. The hidden nodes, which are the internal part of the system, enable to learn the non-linear relationship between the output and input. The parameters on which the forecast value depends with some function represent the input nodes.

The training process is made using different number of input units, different number of hidden units, different cycles learning rate and momentum factor are tried during the training process. Weights and statistic resulted from training iterations are saved periodically. Corresponding to each network, a set of weights and biases is found. Using those weights and biases, statistics are evaluated. Among these networks, the network, which has the smallest value of total sum of the square error (TSSE), is selected to be the best network.

After getting the best network from the training phase, the parameters, which determined from the training process, are kept. The testing process starts with the data and the parameters, obtained from the training process for testing.

Selection of Number of Input Units and Hidden Layers and Nodes
The parameters on which the forecast value depends with some function represent the input nodes which are based on the extreme rainfall events and historical record information including real time rainfall information.

- The first stage is the determination of number of input units and hidden layers and nodes that is called the neural network architecture which depend on the available data and the numbers of inputs was decided as to keep minimum with the effective number of inputs to have better results. The Architecture generally used consists of a set

of input units, hidden units, output units and connection between them.

- The second stage in NN modeling is the determination of hidden layers and nodes. These are no constraints about the number of hidden layers. Most of the researchers generally used to 0 to 2 hidden layers with various numbers of units. To make the problem easy and avoid complexity, architecture with three layers is used, i.e. input layer, hidden layer and output layer as shown in Figure 6.1. The small number of hidden nodes may not be able to train the network and a very large number of hidden nodes only pose difficulty to the training but may also weaken the effective learning strength of the networks. Therefore the determination on of the hidden layers and nodes is made by the trial and error process depending on the condition of the problem.

Data Pre-Processing and Data Post-Processing

The both processing are calculated by based on the same algorithm of neural network, back propagation which belongs to supervised learning algorithm that performs a gradient descent search in weights space using generalized delta rule is often reported in applications (*Minn and Halls, 1986*). Back Propagation (BP) networks were developed by *Rumelhart and McClelland (1986 and 1988)* for learning associations between input and output patterns using more than a single layer perception, which overcomes some limitations of a single layer perception (no layer hidden) Any BP network is based on supervised learning technique that compares the actual output from output units to the target or specified output and then readjust the weights backward in the network. The same input is presented to the network in the next iteration, so the actual output will be closer to the target output. On this procedures will be selected logistics activation function whose output lied in the interval [0,1] that the interval [0.05,0.95] will be chosen instead of interval [0,1]

In this procedure can be described the functional of parameters as following;

- Initials Weights and Biases: The initial weights were selected randomly between two limits (-3 and 3).
- Stopping Criteria
- Learning parameter (η) and Momentum rate (α): There is no specific rule for the selection of the values of these parameters. These parameters are adjusted by trial and error process. Normally, the range of learning parameter is from 0.01 to 1.0 and the momentum rate is also between 0 and 1.

Data Pre-Processing

BP networks use logistics activation function whose output lies in the interval [0,1]. The interval [0.05, 0.95] is chosen instead of interval [0,1] simply because of the logistics function is asymptotic, so it never reaches the value of 0 or 1.

The following formula is used to transform the data before presenting to the network.

$$y'_t = \frac{[0.9(y_t - a)]}{(b - a)} + 0.05 \qquad (6.1)$$

Data Post-Processing

$$y_t = \frac{\left[(b - a)(y'_t - a)\right]}{0.9} + a \qquad (6.2)$$

After the best network is found, the outputs from the network should be transformed back into the original value by using the following formula:
Where y_t is actual value
a is minimum value
b is maximum value
y't is transformed value

Initial Weights and Biases
The initial weight values should be small, randomly generated positive and negative quantities. For cells with many inputs, the initial weights should be smaller so that weighted sums (nets) are not too far from 0. Otherwise, if these sums are too large (positive of negative) it will make the output of weighted sums too close to 0 so that learning will be slowed. The initial weights were selected randomly between two limits (-3 and 3).

Stopping Criteria
The stopping rule indicates the convergence of the back propagation algorithm. It was based on the target error. The target error of 0.05 is set for all patterns. If the target error is equal to or less than 0.05, the back propagation algorithm converges. If a network stops training an acceptable solution, a change in the number of hidden units of in the learning parameter will often fix the problem or start over with a different set of initial weights.

Sometimes the network converges to a local minimum or no converges at all. To avoid possible infinite loops, the maximum numbers of approaches were set.

Learning Parameter and Momentum Rate
η is a constant which represents learning rate. The larger the learning rate, the changes in the weight increases, thus the faster desired weight found. But if η is too big, it causes an oscillation. The problem is to choose the maximum *n* without leading to oscillate. To do this *Rumelhart et.al. (1986)* describes a method for improving the training time of the back propagation algorithm, while enhancing the stability of the process. Called momentum, the method involves adding a term to the weight adjustment that is proportional to the amount of previous weight change. The momentum term

- Gives a momentum of weight change. Therefore, if learning rate is small, momentum helps in moving faster and even jumping local minima to reach the best minima.
- Helps to avoid the oscillation if the learning rate is high and allowing effective weight steps to be bigger.

There is no specific rule for the selection of the values of these parameters. These parameters are adjusted by trial and error process. Normally, the range of learning parameter is from 0.01 to 1.0 and the momentum rate is also between 0 and 1.

6.1.3 Training and Testing with Standard Back Propagation Algorithm

The ANNs procedures consist of two phases; training and testing which are similar to the calibration and verification. The training process is made using different number of input units, different number of hidden units, different cycles.

Standard Back Propagation Algorithm

In Figure 6.2, showing the flowchart of calculation process in back propagation neural network and Figure 6.3 shows the flowchart of back propagation training and testing process.

Let $W_{ji,m}(n)$ = weight of the effect received by j^{th} unit in layer m caused by i^{th} unit in layer (m-1) at n^{th} iteration.

$O_{j,m}$ = output of the j^{th} element in layer m (m=1,2,…,L)

I_i = i^{th} element of the input

t_j = j^{th} element of the desired output (target)

n_m = number of units in the m^{th} layer

In the forward pass, *Rumelhart et al. (1986b*) introduced a set of non-linear activation functions called Semi-linear function is a function in which the output of a unit is a non-decreasing and differentiable to the net total output.

$$O_{j,m} = f(N_{j,m}) \tag{6.3}$$

$$\textit{where } N_{j,m} = \sum_{i=1}^{n_{m-1}} W_{ji,m} O_{i,m-1} + \theta_{j,m} \tag{6.4}$$

$O_{i,m-1} = I_{i,m}$ input unit

$\theta_{j,m}$ = a bias

One of the basic requirements of BP training is that the activation function be continuous and differentiable. The sigmoid logistic non-linear function which fulfills the above requirement and which has a simple derivative making the implementation of algorithm easier *(Minns and Hall,1995*) is often used. The sigmoid function has the value ranging between 0 and 1. The characteristics of logistic function as shown in Figure 6.3 can be graphically illustrated as below.

$$O_{j,m} = f(N_{j,m}) = \frac{1}{1+e^{-N_{j,m}}} \tag{6.5}$$

is used as semi-linear function because it is non-decreasing function and has simple derivative:

$$f'(N_{j,m}) = O_{j,m}(1 - O_{j,m}) \tag{6.6}$$

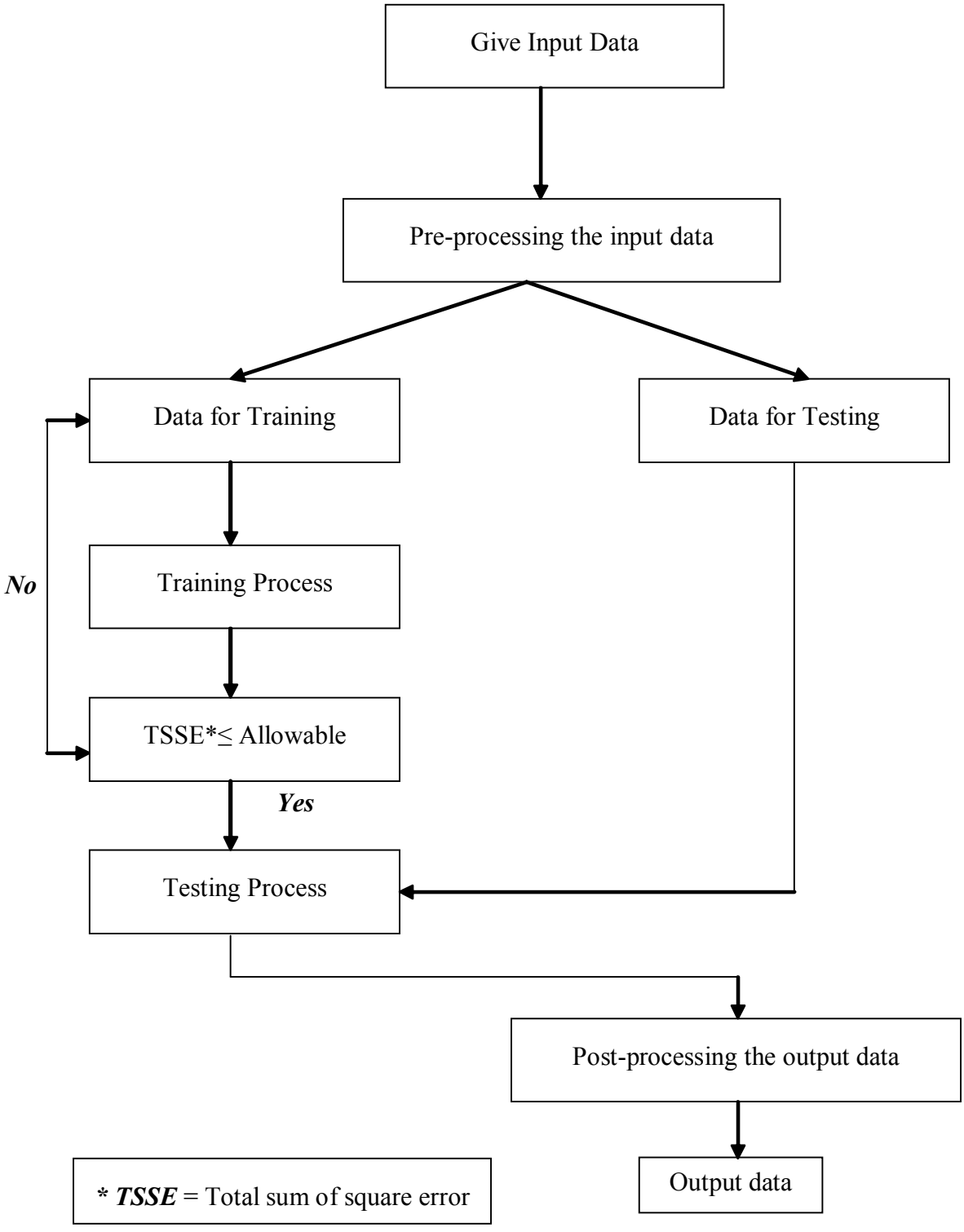

Figure 6.2: Flowchart of Calculation Process in Back Propagation Neural Network Model

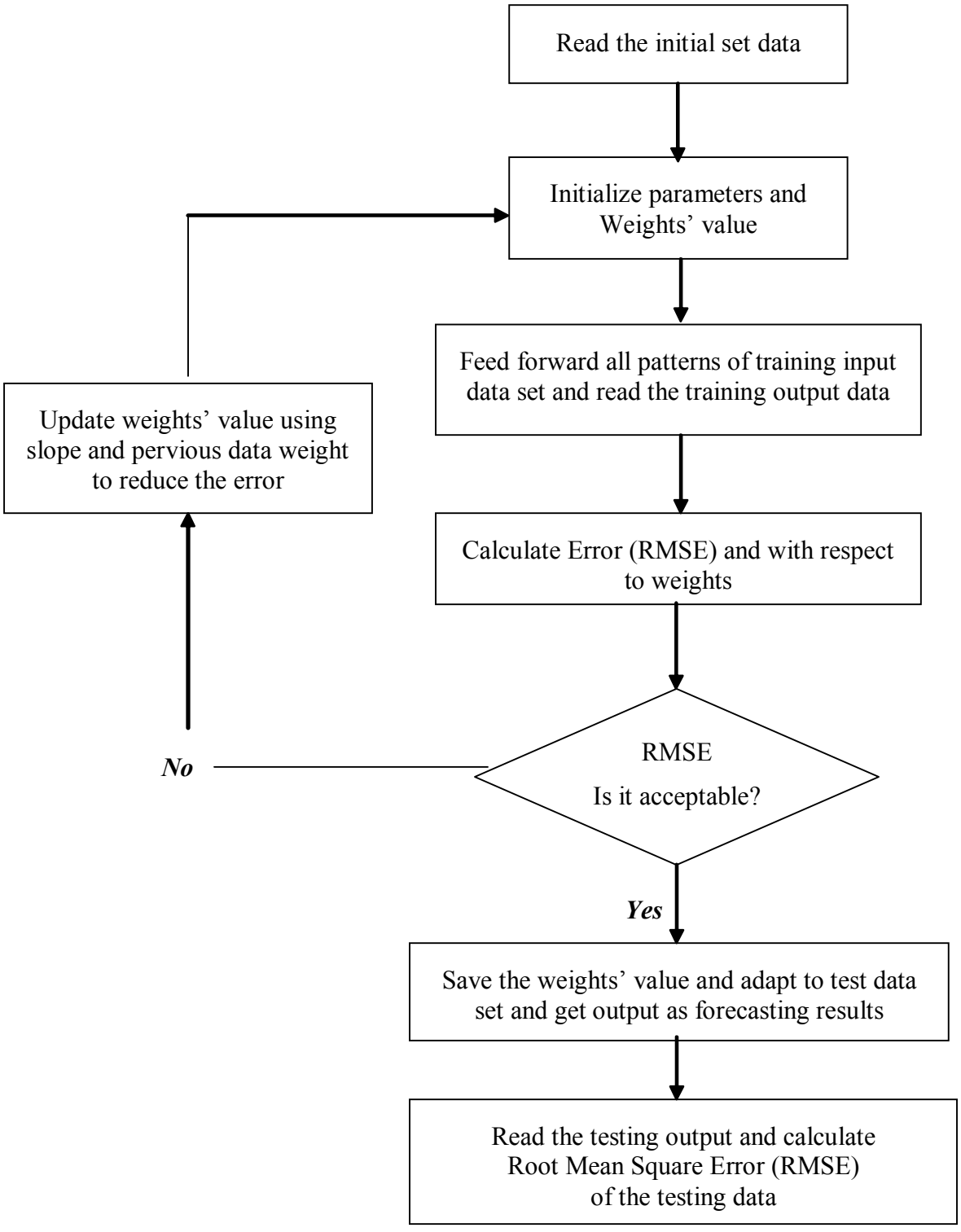

Figure 6.3: Flowchart of Back Propagation Training and Testing Process

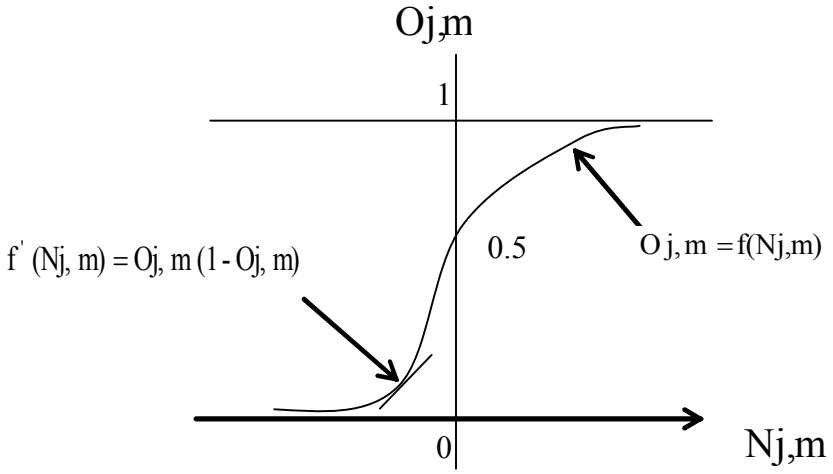

Figure 6.4: Sigmoid Logistics Activation Function with Its Derivative

After passing the last layer, the actual output of the network is compared with the desired output. The objective is to minimize the overall network E for all input pattern n in the training set. Error of pattern p is computed as follows:

$$E_p = \frac{1}{2}\sum_{j=1}^{n_1}(t_j - O_{j,1})^2 \tag{6.7}$$

Where as total error is:

$$E = \sum_p E_p \tag{6.8}$$

Back propagation method tries to minimize the error by adjusting its weights

$$\frac{\partial E_p}{\partial W_{ji,m}} = \frac{\partial E_p}{\partial N_{j,m}} . \frac{\partial N_{j,m}}{\partial W_{ji,m}} \tag{6.9}$$

In the above equation, the first factor is defined as " delta", δ

$$\frac{\partial E_p}{\partial W_{ji,m}} = -\delta_{j;m}\, O_{i,m-1} \tag{6.10}$$

Where

$$\delta_{j,m} = \frac{\partial E_p}{\partial N_{j,m}} \tag{6.11}$$

For units in the output layer:

$$\delta_{j,m} = -\frac{\partial E_p}{\partial O_{j,m}} . \frac{\partial O_{j,m}}{\partial N_{j,m}} \tag{6.12}$$

$$\delta_{j,m} = (t_j - O_{j,m}) . f'(N_{j,m}) \tag{6.13}$$

For units in the hidden layers:
Unlike for the output nodes, the desired outputs of the hidden nodes are unknown.

$$\delta_{j,m} = -\frac{\partial E_p}{\partial O_{j,m}} . \frac{\partial O_{j,m}}{\partial N_{j,m}} \tag{6.14}$$

$$\delta_{j,m} = \left[\sum_{k=1}^{n_{m+1}} W_{kj,m+1} \delta_{k,m+1} \right] . f'(N_{j,m}) \quad (6.15)$$

$$\delta_{j,m} = \left[- \sum_{k=1}^{n_{m+1}} \frac{\partial E_p}{\partial N_{k,m+1}} . \frac{\partial N_{k,m+1}}{\partial O_{j,m}} \right] . \frac{\partial O_{j,m}}{\partial N_{j,m}} \quad (6.16)$$

So the weight changes are:

$$\Delta W_{ji,m}(n+1) = \eta . \delta_{j,m} . O_{i,m-1} \quad (6.17)$$

$$\text{Where } \delta_{j,m} = \begin{cases} f'(N_{j,m}).(t_j - O_{j,m}) & (6.17a) \\ f'(N_{j,m}) . \sum_{k=1}^{n_{m+1}} W_{kj,m+1} \delta_{k,m+1} & (6.17b) \end{cases}$$

In Equation 6.17a, m is for out layer, meanwhile in Equation 6.17b, m is for hidden layer. In Equation 6.17, η is a constant which represents learning rate. Learning is a process by which the free parameters of a neural network are adapted through a continuing process of simulation by the environment in which the network is embedded (*Mendel and McClaren.*, 1970). A prescribed set of well-defined rules for the solution of a learning problem is called algorithm. The larger η, the larger the changes the weight, thus the faster desired weight found. However, if η is too big, it causes an oscillation. The problem is to choose the maximum η without leading to oscillation. To do this, *Rumelhart et al*.(1986) proposed an additional term called momentum, which they believed, would increase learning rate without leading to oscillation. With the additional of momentum term, weights are modified according to the following equations:

$$W_{ji,m}(n+1) = W_{ji,m}(n) + \Delta W_{ji,m}(n+1) \quad (6.18)$$

Where,

$$\Delta W_{ji,m}(n+1) = \eta . \delta_{j,m} . O_{i,m-1} + \alpha . \Delta W_{ji,m}(n) \quad (6.19)$$

With α being a constant which determines the effect of the pass weight changes on the current direction of the movement.

The Standard Back Propagation Training Algorithm

Figure6.5 shows the Artificial Neural with Activation Function

1) Initialize all weights and bias factors to small random values.

Forward Pass:

2) Present input vector (I_1, I_2…Ino) and specify the desired output (t_1, t_2….t_{n1})

3) For layer m = 1,2,….,l:

a. Compute $N_{j,m} = \sum_{i=1}^{n_{m-1}} W_{ji,m} . O_{i,m-1} + \theta_{j,m}$ (6.20)

with $O_{i,0} = I_i$ (6.21)

b. Compute the output of the j th unit in layer m

$$O_{j,m} = \frac{1}{1+e^{-N_{j,m}}}; j=1,2,...,n_m \quad (6.22)$$

4) Compute the final output ($O_{1,1},O_{2,1},\ldots,O_{n1,1}$) with the desired output ($t_1,t_2,...,t_{n1}$). If the difference is acceptable, the process is terminated and the system has learned. Otherwise, continue to the next step. When the number of epochs is reached while the difference is not acceptable, the convergence is not attained. One should try with a new set of initial values, or even modify the structure of the network.

Backward Pass:

For layer m = l, l-1, l-2,…, l)

a. For j=1,2,…, n_m; compute:

$$O_{j,m}(1-O_{j,m})(t_j - O_{j,m}); m: \text{output layer} \quad (6.23)$$

$$\delta_{j,m} \begin{cases} \\ O_{j,m}(1-O_{j,m})\sum_{k=l}^{n_{m+l}} W_{kj,m+l}\delta_{k,m+l}; m: \text{hidden layer} \end{cases} \quad (6.24)$$

b. Compute the weight increments:

$$\Delta W_{ji,m}(n+1) = \eta\delta_{j,m}O_{i,m-1} + \alpha.\Delta W_{ji,m}(n) \quad (6.25)$$

c. Compute the new values of the weights:

$$W_{ji,m}(n+1) = W_{ji,m}(n) + \Delta W_{ji,m}(n+1) \quad (6.26)$$

5) Go to step 2.

Where,

$\delta_{j,m}$ = the value of δ for neuron j in layer m
t_j = target value of neuron j in output layer
$O_{j,m}$ = output of neuron j in layer m
$N_{j,m}$ = Net of neuron j in layer m
$\theta_{j,m}$ = bias value for neuron j in layer m
η = learning parameter
α = momentum constant
$W_{ji,m}(n)$ = weight value between node j in layer m and node i at n iteration
$W_{ji,m}(n+1)$ = weight value between node j in layer m and node i at n+1 iteration
$\Delta W_{ji,m}(n)$ = weight change between node j in layer m and node I at n iteration.
$\Delta W_{ji,m}(n+1)$ = weight change between node j in layer m and node I at n+1 iteration
$O_{j,m-1}$ = Ii,m
n = iteration number (starting from 1)

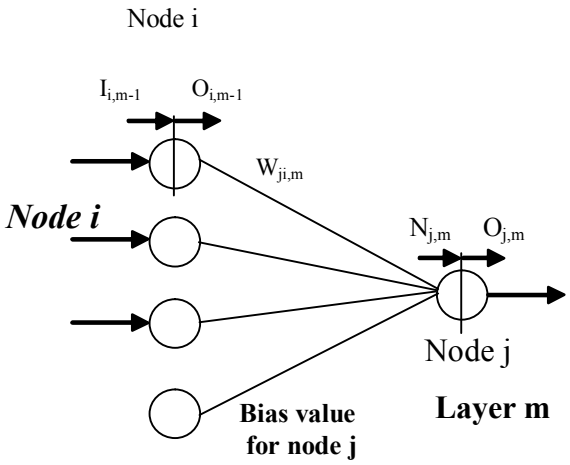

Figure 6.5: Artificial Neural with Activation Function

6.2 Multiple Linear Regression (MLR) model

Multiple linear regression (MLR) models were employed to simulate the relationship between the proper input variables and the hourly suspended sediment concentration. The proper input variables will be defied from the input variables of good performance neural networks. The multiple linear regression (MLR) model is denoted as Equation 6.27.

$$SS_i = b_0 + b_1 x_{i1} + b_2 x_{i2} + \ldots + b_j x_{ij} \tag{6.27}$$

Where SS_i is suspended sediment concentration for the i-th pattern
x_{ij} is the j-th independent variable for the i-th pattern
b_0 is the regression intercept
b_j is the coefficient of the j-th independent variable

6.3 Sediment Rating Curve (SRC) model

A rating curve consists of a graph or equation, relating suspended sediment concentration to water discharge, which can be used to estimate sediment loads from the water discharge record. The sediment rating curve generally represents a functional relationship of the form as Equation 6.28 and it worked on hourly scale.

$$SS = aQ^c \tag{6.28}$$

Where SS is suspended sediment concentration
Q is water discharge
a and c are coefficients

Values of a and c for a particular stream are determined from data by a linear regression between (log SS) and (log Q).

6.4 Data measurement and location

Sediment yield and turbidity are the serious problems for reservoir management therefore the monitoring of sediment flow into this reservoir is necessary. The serious area of sediment erosion of Managawa river basin is monitored by the suspended sediment gauge, Compact-HTW by JFE Alec Co., Ltd. As shown in Figure 6.6, settled on Okumotani river as shown in Figure 6.7 which is an upstream branch of Managawa river. Okumotani catchment is about 8.01 km^2, the average land slope is about 0.49.

Figure 6.6: Turbidity measuring equipment: Compact-HTW JFE-Alec Electron Co.Ltd

- Compact-HTW

Compact-HTW is the turbidity meter with measurement range between 0-70,000 ppm. Ten data of the interval of one second are recorded and averaged in every 10 minutes. In this study, I applied the average hourly data for testing and training the numerical model.

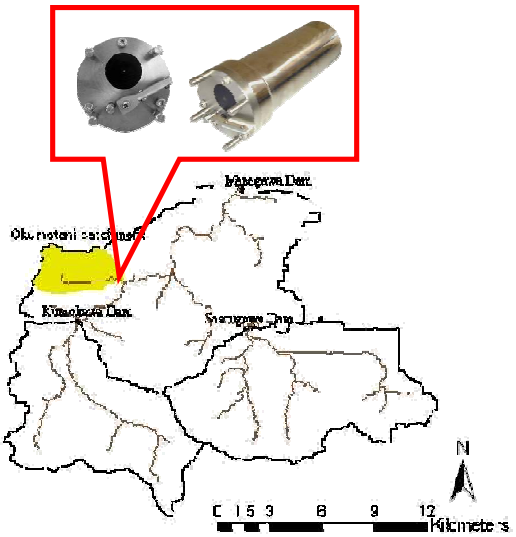

Figure 6.7: Suspended Sediment Gauge located at Okumotani catchment

- Okumotani station

The turbidity meter is installed at Okumotani power station to record the suspended sediment concentration. Figure 6.8 shows the intake at Okumotani power station; Compact-HTW's location. Figure 6.9 shows the weir at Okumotani power station.

Figure 6.8: Intake at the Okumotani power station

Figure 6.9: Weir at Okumotani station

6.5 Results analysis

Although suspended sediment concentration at Okumotani station has been measured once twenty minutes since December 2006, this study applies an hourly suspended sediment concentration data for training and testing the network. The climate inputs were selected based on physical relationships and correlations between the input and output variables. Rainfall is the direct driving force of sediment yield and transportation. Temperature can influence the sediment generation and transportation through several indirect ways as through its influence on the evapotranspiration, runoff and reduce decomposition rate.

In the beginning of this study, climate variables as hourly rainfall (R), temperature (T), wind (W), solar (SL) and snow (SN) were considered as inputs. Neural networks were established with these inputs and it was found that rainfall (R) and temperature (T) were closely related with suspended sediment concentration, while adding wind (W), solar (SL) and snow (SN) as inputs did not improve the performance of the networks. Thus wind (W), solar (SL) and snow (SN) were not used for analysis. About the hydrodynamics data as inputs of network, hourly water discharge (Q) and suspended sediment concentration (SS) data have been measured and available on this study area. To improve the network the prospective processed variables will be added as inputs that

in this study rainfall in two hours (A) and the absolute of discharge changing (D) are considered as inputs of network. The rainfall in two hours (A) is accumulated rainfall with rainfall in previous time step ($R_t + R_{t-1}$) and the absolute of discharge changing (D) in this study is the absolute value of different of discharge in this time step and previous two time step then divided by two or $|Q_t-Q_{t-2}|/2$.

The climate, hydrologic and hydrodynamic data from December 2006 to January 2008 were used in this study as calibration and validation steps. Because of the limitation of data, this study applied with the heavy rainfall events to evaluate the network which the sediment yield is serious during heavy rainfall events. For the calibration step, the heavy rainfall events in February 2007, June 2007 and December 2007 were considered and the heavy rainfall events during December 2006, March 2007 and May 2007 were used as verifying the network. Therefore only data in 6 months were used for this modeling.

The correlation coefficients between climatic, hydrologic and hydrodynamic variables; rainfall (R), temperature (T), water discharge (Q), rainfall in two hours (A) and the absolute of discharge changing (D), and suspended sediment concentration (SS) are given in Table 6.1. It can be seen that the suspended sediment concentration has relative higher linear correlations with rainfall (R), rainfall in two hours (A), discharge (Q) and the absolute of discharge changing (D). Temperature (T) has fair good relationship with suspended sediment.

Table 6.1: Correlation coefficients between input variables and suspended sediment

Time	***R***	***T***	***Q***	***A***	***D***	***SS***
t	0.594	0.219	0.436	0.633	0.486	1.000
t-1	0.583	0.226	0.354	-	-	0.640
t-2	0.450	0.235	0.280	-	-	0.464

The original input and output data consist of different parameters with different physical meaning and units and thus their ranges are highly variable. To ensure that each variable is treated equally in a model, raw data are usually rescaled to a certain interval. The inputs were normalized to [-3, 3] and outputs were normalized to [0, 1].

6.5.1 Artificial neural network (ANN)

The efficiency index (EI) and root mean square error (RMSE) values of 22 networks during calibration and verification periods are given in Table 6.2. The performance of network is depended on inputs and network structure. The network in case of discharge (Q) and temperature (T) are inputs, show relatively poor performance as case 1 which the error is about 50% in verification step. From linear correlation efficiency, rainfall (R) has good relationship with suspended sediment (SS), therefore it is necessary to add rainfall as input variable that the efficiency of case 4 is higher than case 1. The below discussion is first focusing on the values for verification period because the generalization ability of the networks is interest for application. Adding discharge (Q) as input variable is

improving the performance of network which the efficiency index (EI) during verification period of case 3 and case 4 are 0.387 and 0.545 respectively. And also when compare the efficiency of case 3, rainfall (R) and temperature (T) are inputs, and case 6, rainfall (R) and discharge (Q) are inputs, found that the efficiency of case 3 is lower than case 6. To improve the network which rainfall (R) and discharge (Q) are inputs, it should add rainfall in two hours (A) to one of input then the efficiency will rise to 68 % as shown by case 9. Therefore the network which rainfall (R), rainfall in two hours (A) and discharge (Q) are inputs is good for forecasting suspended sediment concentration as network case 9. Adding rainfall in two hours (A) into input of network makes the efficiency of network increasing that it was confirmed by the results of network case 14 and case 11 which each network error are about 33.96 % and 36.32 % respectively. If rainfall (R) is not one of input of network as case of discharge (Q) and previous time step suspended sediment (SS) are inputs, the performance is fare good as shown in case 16. When the absolute of discharge changing (D) is added to network as case 17, the efficiency is a bit improving from case 16.

Table 6.2: Performances of neural networks

Input	***Case No.***	***Time Step***	***Network***	***Calibration***		***Verification***	
				EI	***RMSE %***	***EI***	***RMSE %***
T,Q	1	t	2,8,1	0.431	45.01	0.182	50.09
R,T	2	t	2,6,1	0.509	43.96	0.409	44.18
	3	t,t-1	4,16,1	0.733	32.39	0.387	43.35
R,T,Q	4	t	3,3,1	0.590	40.17	0.545	37.33
R,Q	5	t	2,4,1	0.708	33.91	0.509	38.79
	6	t,t-1	4,8,1	0.591	40.09	0.554	36.97
	7	t,t-1,t-2	6,12,1	0.859	23.48	0.449	41.12
R,A,Q	8	t	3,3,1	0.655	36.87	0.392	43.19
	9	t,t-1	5,3,1	0.648	37.21	0.676	31.51
	10	t,t-1,t-2	7,5,1	0.730	32.60	0.611	34.52
R,SS	11	t	2,4,1	0.663	36.43	0.570	36.32
	12	t,t-1	4,20,1	0.835	25.43	0.562	36.62
R,A,SS	13	t	3,20,1	0.830	25.80	0.568	36.37
	14	t,t-1	5,5,1	0.709	33.84	0.624	33.96
Q,SS	15	t	2,2,1	0.512	43.83	0.497	39.26
	16	t,t-1	4,4,1	0.579	40.70	0.503	39.05
Q,D,SS	17	t	3,3,1	0.572	41.04	0.541	37.53
	18	t,t-1	5,5,1	0.607	39.33	0.328	45.38
R,Q,SS	19	t	3,12,1	0.892	20.58	0.553	37.02
	20	t,t-1	6,6,1	0.789	28.78	0.376	43.75
R,Q,D,SS	21	t	4,16,1	0.868	22.78	0.487	39.65
	22	t,t-1	7,18,1	0.796	28.27	0.544	37.37

For SS at time t, it means SS_{t-1} and for SS at time step t-1, it means SS_{t-2}

However adding the absolute of discharge changing (D) when rainfall (R) is one of input, the efficiency does not improve as shown in case 19 and 22. Because the rainfall (R) is more effect to suspended sediment concentration than the absolute of discharge changing (D).

6.5.2 Multiple linear regression (MLR) and sediment rating curve (SRC)

The multiple linear regression (MLR) models are necessary to define the proper variables which should relate with suspended sediment therefore this study applied the set of proper variables in regression model same as inputs of neural network models. Because the efficiency of the neural networks during verification period is not clearly different, the efficiency of calibration period is considered to select the proper variables for multiple linear regression (MLR) models. Thus there are three cases; case 13, case 19 and case 21, were considered to apply with multiple linear regression (MLR) models as in Equation 6.27. The units of each variable are followed; rainfall (mm/hr), discharge (m^3/s), rainfall in two hours (mm/2hrs), the absolute of discharge changing (no unit) and suspended sediment (ppm).

Multiple linear regression (MLR) model No.23; rainfall, rainfall in two hours and suspended sediment are variables, is shown in Equation 6.29. Multiple linear regression (MLR) model No.24; rainfall, discharge and suspended sediment are variables, is shown in Equation 6.30 and multiple linear regression (MLR) model No.25; rainfall, discharge, the absolute of discharge changing and suspended sediment are variables, is shown in Equation 6.31.

$$SS_t = 16.28R_t - 1.29A_t + 0.52SS_{t-1} + 0.93 \quad (6.29)$$

$$SS_t = 14.54R_t + 0.61Q_t + 0.42SS_{t-1} - 6.73 \quad (6.30)$$

$$SS_t = 14.10R_t + 0.52Q_t + 1.66D_t + 0.40SS_{t-1} - 6.76 \quad (6.31)$$

Where SS is suspended sediment concentration,
R is rainfall
A is rainfall in two hours
Q is discharge
D is the absolute of discharge changing

The sediment rating curve (SRC) or power relation (PR) model is designed to study the direct relationship between water discharge and sediment flow as Equation 6.28. The sediment rating curve (SRC) model was calibrated by the same data as neural network model and the relationship is shown in Equation 6.32.

$$SS = 0.4853Q^{1.1377} \quad (6.32)$$

Where SS is suspended sediment concentration
Q is discharge

6.6 Discussion and conclusions

6.6.1 Discussion

When the performances of all neural networks in this study are considered both calibration and verification periods, it found that the best three networks are case 13, 19 and 21. The efficiency as shown in Table 6.3 of these neural networks is about 75% when all data; both calibration and verification periods, are considered and the root mean square error is about 30%. The graphs of comparison between observed and computed suspended sediment of each case are shown in Figure 6.10. The computed time to peak of all three neural networks is almost equal to the observed one but some computed peak value of network case 19 is more over than the observed data. For network case 13, it is most closed to the observed one. The network case 13 is the best for hourly suspended sediment prediction on Okumotani catchment. However all three neural networks are good acceptable for hourly suspended sediment prediction.

Table 6.3: Performances of neural networks, multiple linear regression and sediment rating curve models

Model	*Input*	*Case No.*	*All data*	
			EI	*RMSE %*
ANN	R,A, SS_{t-1}	13	0.754	30.88
	R,Q, SS_{t-1}	19	0.782	29.08
	R,Q,D, SS_{t-1}	21	0.746	31.43
MLR	R,A, SS_{t-1}	23	0.638	37.47
	R,Q, SS_{t-1}	24	0.654	36.26
	R,Q,D, SS_{t-1}	25	0.657	36.48
SRC	Q	26	0.118	55.52

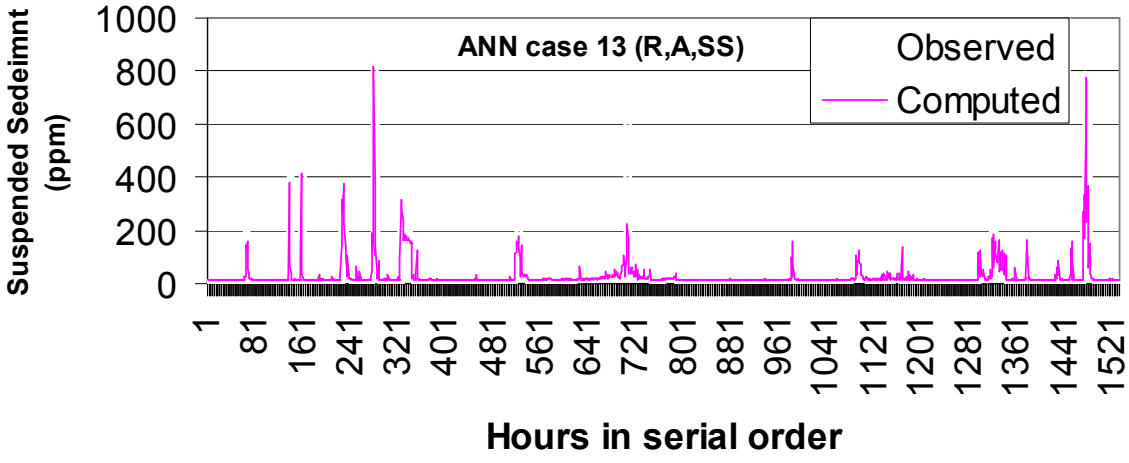

Figure 6.10: Comparisons between the observed and computed suspended sediment concentration of each model; case 13, 19, 21, 25 and 26 respectively

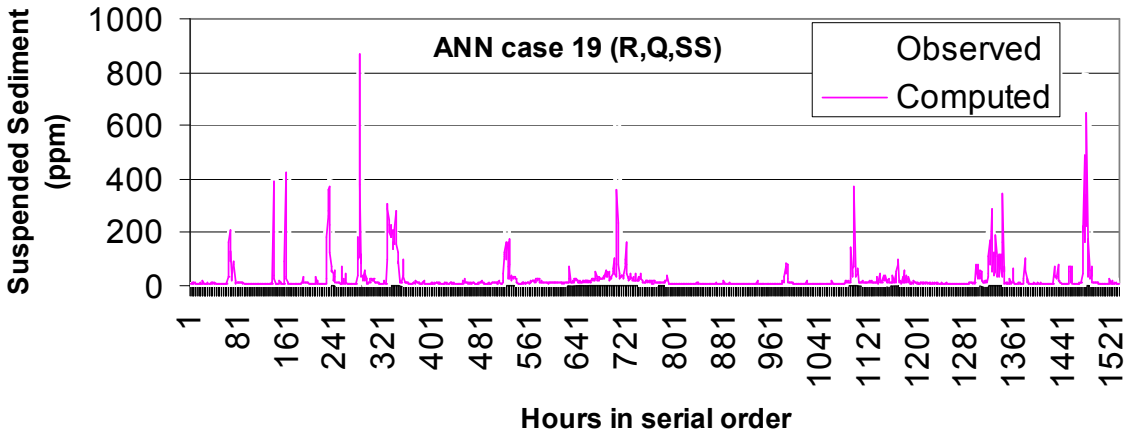

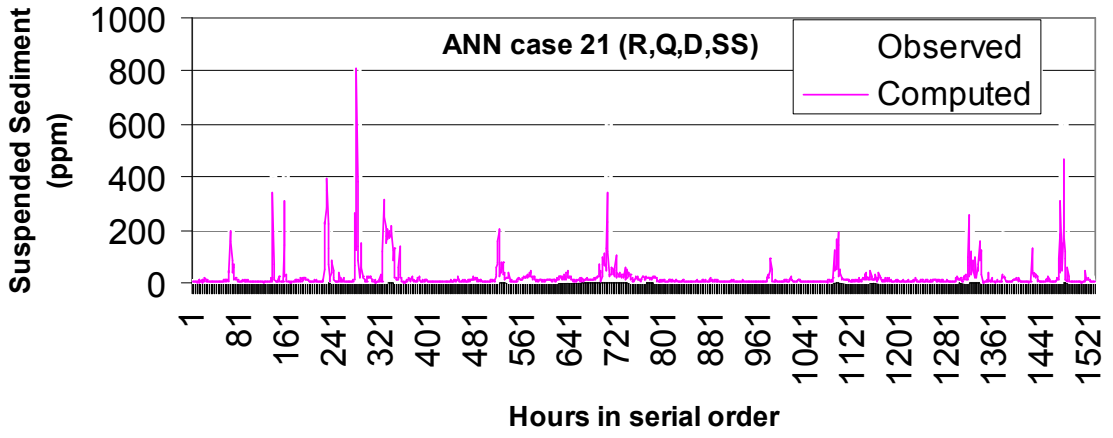

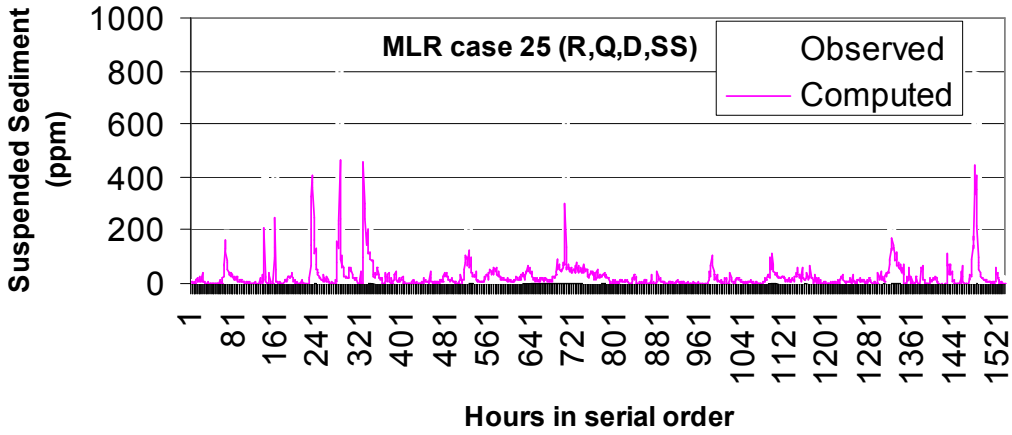

Figure 6.10: Comparisons between the observed and computed suspended sediment concentration of each model; case 13, 19, 21, 25 and 26 respectively (Continued)

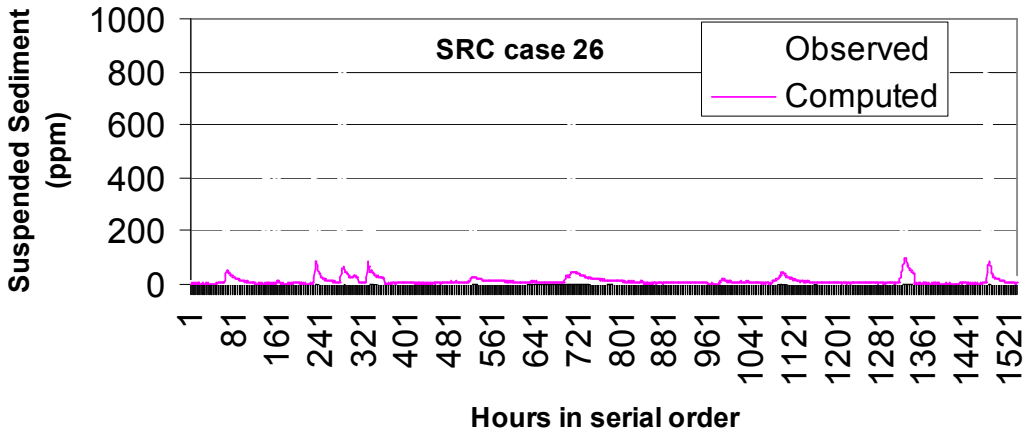

Figure 6.10: Comparisons between the observed and computed suspended sediment concentration of each model; case 13, 19, 21, 25 and 26 respectively (Continued)

The multiple linear regression models in this study are also good performance but its efficiency is a bit less than the neural network models about 10% as shown in Table 6.3. The multiple linear regression model case 25 has the highest efficiency among three regression model. Although the computed peak value of the multiple linear regression model is always less than the observed data but computed time to peak is fit with observed one, the regression models can be used for hourly suspended sediment prediction.

For the sediment rating curve model, the performance is poor because the sediment yield and transport process in this study area are hardly depended on rainfall as shown by correlation coefficient and the coefficient of rainfall variable in multiple linear regression equations. Therefore sediment rating curve model is not suitable for hourly suspended sediment prediction.

6.6.2 Conclusions

This study is an attempt to predict hourly suspended sediment concentration at Okumotani station, the upstream of Managawa reservoir, by using the application of the artificial neural network (ANN), the multiple linear regression (MLR) and the sediment rating curve (SRC).

The neural networks were train and test by the recently data at Okumotani catchment that the appropriate variables were rainfall, water discharge, rainfall in two hours, the absolute of discharge changing and previous time step of suspended sediment concentration. It is demonstrated that the artificial neural network (ANN) is capable of modeling the hourly suspended sediment concentration with good accuracy when the appropriate variables were inputs of neural network. Rainfall and it's accumulated with previous time step are the important factors to relate with suspended sediment prediction model. Only rainfall and discharge data are used for inputs of neural network, it makes the accuracy of network is quite good and to improve this network the rainfall in two hours should be

added to input of network. These models can be used for real time prediction when the previous time step of suspended sediment data is known and the previous time step of suspended sediment concentration makes the efficiency of network increase.

Artificial neural network (ANN) can generate a better fit to the observed suspended sediment concentration than the multiple linear regression (MLR) model. However this study found that the multiple linear regression models can be used to predict hourly suspended sediment when appropriate variables were parameters of models. The sediment rating curve (SRC) model approach gives worse estimates of suspended sediment concentration than the neural network and multiple linear regression models.

In order to improve and confirm these hourly suspended sediment concentration prediction models for upstream of Managawa dam, the seasonal effect, climate changing and land surface changing should be considered as one of parameters of models and the duration of training and testing the model should be extended because the limited of data this study was used only one year data for training and testing models.

CHAPTER 7
Effects of Climate Change on Water Resources and Sediment Yield

Based on hydrology, temperature and rainfall data from last 30 years, the climate change on water resources in Managawa river basin were investigated. The historical trends of meteorological variables, such as temperature at Ono station located near study area and rainfall at Managawa station, Fukui prefecture were detected using both parametric and nonparametric statistical test. The trends of these metrological variables were then employed to generate sediment yield in the future climate conditions using Modified Universal Soil Loss equation (MUSLE).

7.1 Climate Change Information

Atmospheric carbon dioxide levels have recorded continue increases since the 1950s, a phenomenon that may significantly after global and local climate characteristics, such as temperature and usable water resource. The most obvious effect is climate change, which has resulted in the increase of global temperature and modified precipitation patterns. One of the most significant consequences of climate change may be the alternative of the regional hydrological cycles and subsequent changes in water resources and stream flow regimes. The effects of changes in temperature and precipitation on hydrology have been investigated by many hydrologists that the global warming has clearly been increasing during recent decades and the trend may worsen in the future. If the current trend does not change, the impact of global warming on future climatic conditions will become a major concern. It is very important for water resource managers to know and prepare to deal with the effects of climate change on hydrologic cycles and stream flow regimes. Estimates of global warming are generally based on the application of general circulation models (GCMs), which attempt to predict the impact of increased atmospheric CO_2 concentrations on weather variables. Since information on the local or regional impacts of climate change on hydrological processes and water resources over different areas in the world is of great interest, assessing the impact of climate change has received extensive attention.

This part investigates the impact of climate change on water resources and sediment yield in Managawa river basin. The purpose of this part was to reveal the association between climate change and the variability of hydrological process response elucidate the effects of climate change on hydrological processes, water resources and sediment yield process. Long term historical data on meteorological variables was gathered first, including mean daily temperature and daily rainfall, to determine the presence and degree of any increasing or decreasing tendencies. A weather generating model was then constructed to extrapolate future climate conditions based on the long term historical tendencies of these meteorological variables. Finally, the generated future climatic conditions were inputted into the sediment yield model; MUSLE, to investigate changes in sediment yield on the study area.

7.2 Data collection and processing

The important information for climate change consideration in this study are temperature and rainfall. The daily temperature data of this study area is not available at Managawa dam office therefore the nearest meteorological station as called Ono station located in Fukui prefecture was selected for representative of Managawa watershed area. The temperature and other climate data are available and can be downloaded via web site of Japan Meteorological Agency.

For rainfall data as the information in Chapter 3, there are 8 rain gauge stations located on Managawa watershed as named Akio, Sasougawa dam, Nukumi, Heikedaira, Nagajima, Managawa dam, Kumanoko and Kumogawa dam. The hourly rainfall data are provided from Managawa dam office. Table 7.1 presents and lists the locations of the gauge stations used herein, in which the meteorological station maintained long term records of daily temperature from 1977 to 2008 and daily rainfall from 1965 to 2008 depended on each station. However in this study the data length from 1981 to 2008 was used to detect trends in temperature and rainfall because Managawa dam started to operation from 1981 so this study is considered after Managawa dam operation started and the method of mean areal precipitation computation in this study is by Thiessen method see in Chapter 3. The rainfall records were checked for consistency using double mass tests which they passed.

Table 7.1: The gauge stations used in this study and their record length

Station Name	*Lat. (N)*	*Long. (E)*	*Data*	*Record length*
Managawa dam	35º54'12"	136º32'26"	Rainfall	1967-2008
Nakajima	35º52'41"	136º30'27"	Rainfall	1967-2008
Kumokawa dam	35º50'51"	136º27'26"	Rainfall	1973-2008
Heikedaira	35º49'56"	136º29'16"	Rainfall	1978-2008
Kumanoko	35º49'38"	136º26'19"	Rainfall	1967-2008
Nekumi	35º47'59"	136º28'53"	Rainfall	1977-2008
Sasougawa dam	35º50'38"	136º32'57"	Rainfall	1965-2008
Akiu	35º50'03"	136º35'43"	Rainfall	1976-2008
Ono	35º58'18"	136º29'48"	Temperature	1977-2008

Figure 7.1 shows the maximum, minimum and average monthly weighting rainfall at Managawa river basin. On average, 70% of total annual rainfall falls between April and October in the high flow period or the wet season, while November to March of the next year is the low flow period with about 30% of annual rainfall. Average yearly rainfall is 2,340 mm/year for the period 1981 – 2008 with an annual minimum of 1,515 mm in 1994 and an annual maximum of 3,280 mm in 2004. The maximum, minimum and average monthly temperatures at Ono station are shown in Figure 7.2. The trend of monthly mean temperature is increasing from January to August then decreasing to December.

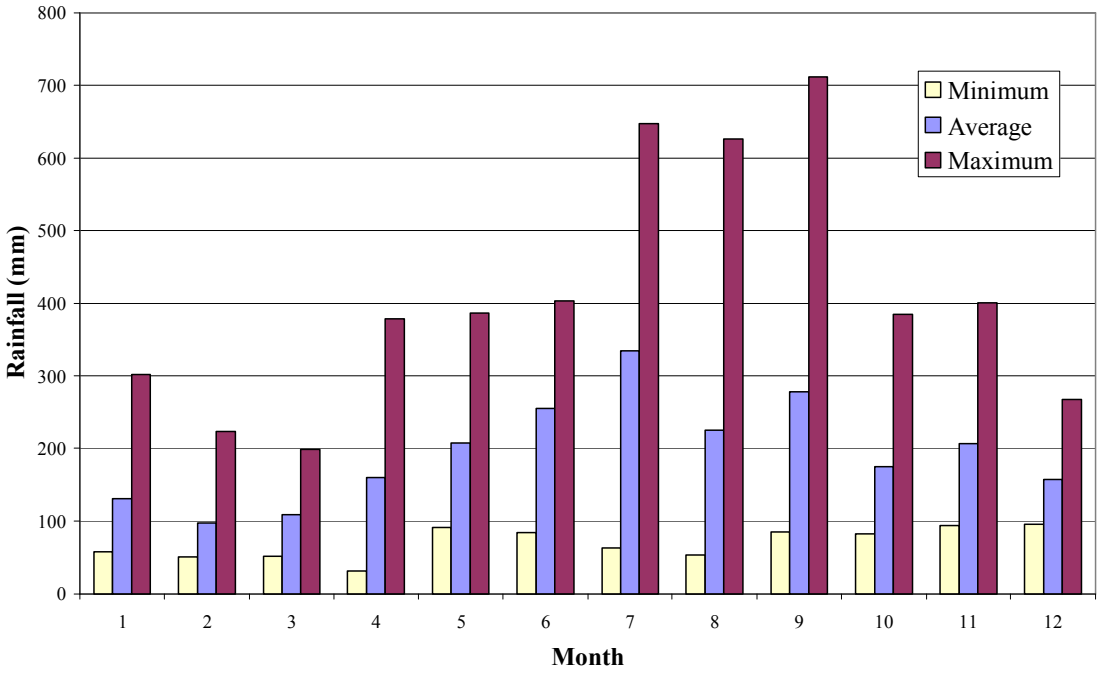

Figure 7.1: Maximum, minimum and average monthly rainfall at Managawa river basin; 1981-2008

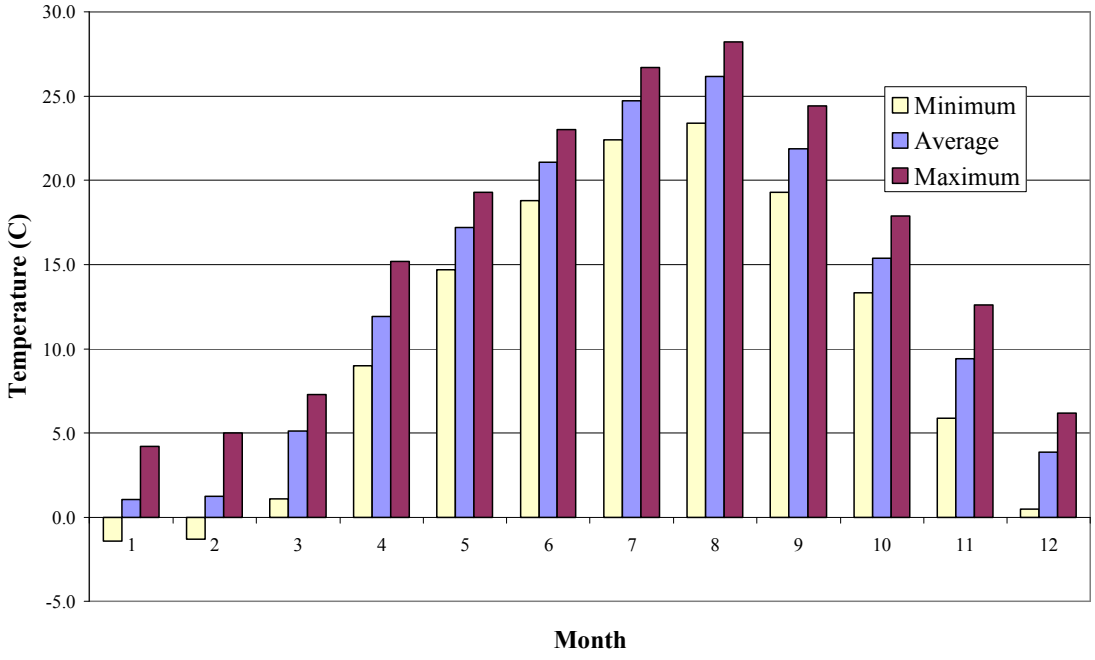

Figure 7.2: Maximum, minimum and average monthly temperature at Ono station; 1981-2008

7.3 Analysis of long term trends in meteorological variables

Meteorological variables such as temperature and precipitation are found to be highly sensitive in predictions of the effect of climate change on water resources. Consequently, investigating the historical trends of such variables would help to reveal the effects of climate change on water resources. The trend of a time series can be tested using a non-parametric statistical test, Mann-Kendall method (Kendall, 1975), which investigates whether the time series exhibits a significantly increasing or decreasing trend.

Both parametric and non-parametric tests may be employed for trend detection. However, in terms of the power of the test, i.e., the ability to distinguish between null hypothesis H_0 and alternative hypothesis H_1 (the Mann-Kendall test for monotonic trends and the Mann-Whitney test for step changes) perform well. In this study a non-parametric test was employed to detect possible trends in hydrological processed and climate change.

7.3.1 Mann-Kendall method

The Mann-Kendall method, suggested by the World Meteorological Organization (1988), is a common method of testing the trend of a time series. The test statistic is given as follows. In the Mann-Kendall test, the null hypothesis H_0 states that the data $(X_1,X_2,\ldots,X_n)$ are a sample of n independent and identically distributed random variables. The alternative hypothesis H_1 of a two sided test is that the distribution of X_k and X_j are not identical for all k and j. The Kendall's statistic S is:

$$S = \sum_{i=1}^{n-1} \sum_{k=i+1}^{n} \mathrm{sgn}(x_k - x_i) \tag{7.1}$$

Let time series x_i be ranked from i=1,2,…,n-1, and let x_k be ranked from k=i+1,…,n. Each data point x_i is used as a reference point and is compared with all other data points x_j such that:

$$\mathrm{sgn}(\theta) = \begin{cases} 1, & \theta > 0 \\ 0, & \theta = 0 \\ -1, & \theta < 0 \end{cases} \tag{7.2}$$

If the data set is identically and independently distributed, then the mean of S is zero and the variance of S is:

$$\mathrm{var}(S) = \frac{\left(n(n-1)(2n+5) - \sum t(t-1)(2t+5)\right)}{18} \tag{7.3}$$

Where, n is the length of data set, t is the extent of any given time, and $\sum$ denotes the summation over all times. Then the test statistic (Z_c) is given as:

$$Z_c = \begin{cases} \dfrac{S-1}{\sqrt{\mathrm{var}(S)}}, & S > 0 \\ 0, & S = 0 \\ \dfrac{S+1}{\sqrt{\mathrm{var}(S)}}, & S < 0 \end{cases} \tag{7.4}$$

The magnitude of the trend is given as:

$$\beta = Median(\frac{x_i - x_j}{i - j}), \forall_j < i \tag{7.5}$$

In which $1<j<i<n$. A positive value of β indicates an upward trend and a negative value of β indicates a downward trend.

The Mann-Kendall test may then be stated simply as follows: null hypothesis H_0: $\beta=0$ (β is the slope trend); significance level: p; test statistics: Z_c; rejected H_0: $|Z_c| > Z_{1-\alpha/2}$, in which $\pm Z_{1-\alpha/2}$ are the standard normal deviates, and α is the significance level for the test.

7.3.2 Mann-Whitney test for step trend

Given a data vector $X=(x_1,x_2,\ldots,x_n)$, we partition X such that $Y=(x_1,x_2,\ldots,x_{n1})$ and $Z=X=(x_{n1+1},x_{n1+2},\ldots,x_{n1+n2})$. The Mann-Whitney test statistic is given as:

$$Z_c = \frac{\sum_{t=1}^{n1} r(x_t) - n_1(n_1+n_2+1)/2}{\sqrt{n_1 n_2 (n_1+n_2+1)/12}} \tag{7.6}$$

In which $r(x_t)$ is the rank of the observations. The null hypothesis H_0 is accepted if $-Z_{1-\alpha/2} \le Z_c \le Z_{1-\alpha/2}$, where $\pm Z_{1-\alpha/2}$ are $1-\alpha/2$ quintiles' of the standard normal distribution corresponding to the given significance level α for test.

7.3.3 Trend of temperature and rainfall times series

There are two main ways that climate change affects water resources: natural transition and anthropogenic disturbance. The nature transition is a process in which climate factors change the elements of the hydrological cycle and regional natural conditions, subsequently affecting the quality and temporal spatial distribution of water resources. The statistical for temperature and rainfall time series is given in Table 7.2.

Table 7.2: Statistics for the annual temperature and precipitation time series

Statistics	*Mean*	*Standard Deviation*	*Coefficient of Variation*	*Coefficient of Skewness*	*Maximum Value*	*Minimum Value*	*Range*
Temperature (C)	13.2	0.64	0.049	-0.080	14.5	12	2.5
Rainfall (mm)	2337	408	0.174	0.127	3280	1515	1764

Figure 7.3 and Figure 7.4 show the plot of the mean annual temperature and rainfall respectively. For visualization purposes, the 10 year moving average (MA) is also given in the graph.

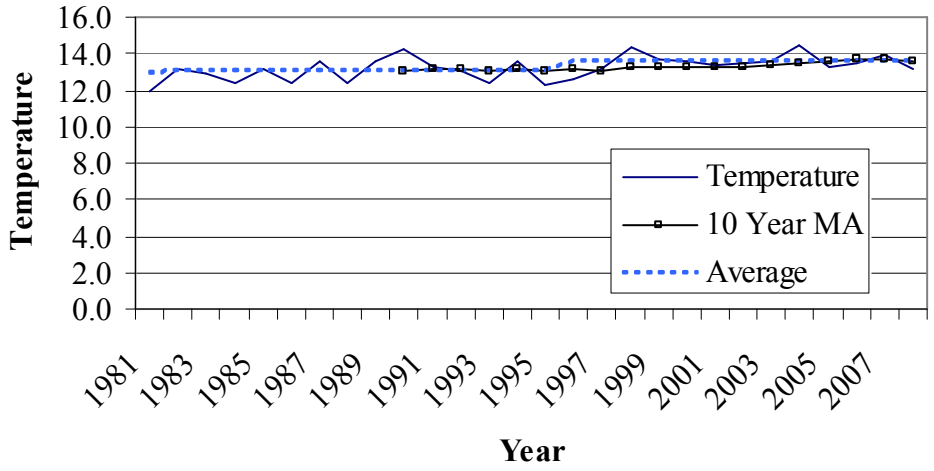

Figure 7.3: Annual average temperature, 10 year moving average and average temperature before and after 1995 (possible step trend)

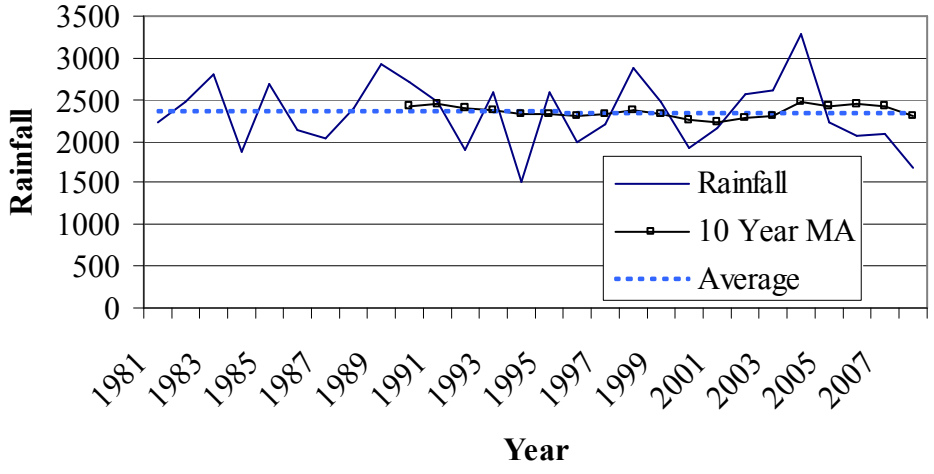

Figure 7.4: Annual average rainfall, 10 year moving average and average rainfall

1) The test on step trends

From literature study on trend and step changes in Japanese precipitation, it presents the results of t-test and Mann-Whitney test on precipitation during 1897-1999 that both parametric and nonparametric approaches give the same results: significant step changes in 1924 and 1941 (Xu, Takeuchi and Ishidaira, 2003). Therefore the step changes did occur in annual national precipitation over Japan around 1924 and 1941.

In this study for both temperature and precipitation data, the possible partition point is identified by visual observation. In this visual identification, two principles were used. One is that large difference between the mean values of the two subdivided time series should exist; the other is that any one of the two subdivided series has to have enough length of record. The temperature data set is clearly visual identification at 1995 as shown in Figure 7.3 and followed that point; it was applied to precipitation data set too as shown in Figure 7.4. The temperature and rainfall time series are divided into two subseries as shown in Table 7.3.

Table 7.3: Partitions of the temperature and rainfall time series

Data	*Time Series*	*Length of record*	*Mean Value*	*Standard Deviation*	*Coefficient of Variation*
Temperature	1981-1995	15	13.0	0.63	0.05
	1996-2008	13	13.6	0.50	0.04
Rainfall	1981-1995	15	2353	398.4	0.16
	1996-2008	13	2318	433.4	0.18

The t-test results on the assessment of step changes for temperature and rainfall time series data are presented in Table 7.4. Table 7.5 presents the Mann-Whitney test results. Obviously, both parametric and non parametric approaches give the same results: significant step change in 1995 for temperature time series data but rainfall time series from 1981 to 2008 is not clearly the step change that also confirmed by the annual report of Japan Ministry of Land, Infrastructure and Transport, 2008. Thus, although the climate background needs to be further investigated, the analysis in this study shows that step change did occur in annual temperature on this study area around 1995 as shown in Figure 7.3.

Table 7.4: t-test results of step trend for temperature and rainfall time series

Data	*Series*		*Test*	
	n_1	n_2	T_c	H_0
Temperature	15	13	2.304	R
Rainfall	15	13	-0.210	A

R: reject H_0; A: accept H_0

Table 7.5: Mann-Whitney test results of step trend for temperature and rainfall time series

Data	*Series*		*Test*	
	n_1	n_2	T_c	H_0
Temperature	15	13	-2.441	R
Rainfall	15	13	0.437	A

R: reject H_0; A: accept H_0

2) The test on monotonic trend

The results of Mann-Kendall test on monotonic trend for both temperature and rainfall time series are summarized in Table 7.6. In this table, β is the Mann-Kendall slope β_1 is the linear slope obtained from linear regression test.

Table 7.6: Monotonic trend test for temperature and rainfall time series

Data	*Mann-Kendall test*			
	β	β_1	Z_0	H_0
Temperature	0.033	0.039	2.45	R
Rainfall	-8.170	-5.189	-0.53	A

R: reject H_0; A: accept H_0

The results from rainfall time series suggest that the null hypothesis H_0, i.e. there is no monotonic trend in the precipitation time series, could not be rejected. In other words, the long-term monotonic trend in annual precipitation is weak over time and statistically insignificant. Although the average annual precipitation on Managawa river basin decreased by 52 mm per decade or 2.2% per decade, the Mann-Kendall test results show that this decrease is statistically insignificant. Thus it is still too early to conclude about any systematic nationwide monotonic trend in rainfall over this study area.

For temperature time series, the results shows that the null hypothesis H_0, i.e. there is monotonic trend in the temperature time series. It means that long-term monotonic trend in annual temperature is statistically significant. Although the average annual temperature on Managawa river basin increased by 0.4 ºC per decade or 2.9% per decade, the Mann-Kendall test results show that this increase is statistically significant. Thus it should be concluded that the temperature over this study area will be increase by statistical test.

3) Seasonal consideration

According to seasonal consideration; dry season and wet season, the dry season is start from November to April of next year and the wet season is from May to October. The results of Mann-Kendall test on monotonic trend for rainfall time series during both dry season and wet season are summarized in Table 7.7.

Table 7.7: Monotonic trend test for rainfall time series during dry season and wet season

Data	***Mann-Kendall test***			
	β	β_1	Z_0	H_0
Dry Season	3.585	4.576	1.17	A
Wet Season	-11.225	-9.765	-1.17	A

R: reject H_0; A: accept H_0

The results from rainfall time series during both dry season and wet season suggest that the null hypothesis H_0, i.e. there is no monotonic trend in the precipitation time series, could not be rejected. Although the average annual precipitation during dry season on Managawa river basin increased by 46 mm per decade and during wet season decreased by 98 mm per decade, anyway the Mann-Kendall test results show that the increase and decrease are statistically insignificant. Thus it is still too early to conclude about any systematic nationwide monotonic trend in rainfall over this study area.

7.4 Weather generating model

Weather generating records were selected to reflect possible variations in daily temperatures and precipitation heights. The generation algorithms were based on procedures developed by Pickering et al. (1988) and Selker and Haith (1990). Daily temperatures were calculated by first order autoregressive equation presented in Pickering et al. (1988). For generating daily precipitation heights, daily precipitation height on wet days was then determined by sampling from Weibull distribution. The temperature and precipitation generating models are detailed further below.

7.4.1 Temperature generating model

A first order autoregressive model was utilized to generate daily temperature sequences, with the following form:

$$t_k = \mu_T + \rho_{1T}(t_{k-1} - \mu_T) + \sqrt{1-\rho_{1T}^2}\,\sigma_T \upsilon_k \qquad (7.7)$$

Where t_k denotes the temperature on day k

μ_T represents the mean temperature for a period (1 month)

σ_T is the standard deviation of temperature during that period

ρ_{1T} denotes the lag-one autocorrelation coefficient of temperature during that period

υ_k represents the random standard normal variation

Given the parameters, μ_T , σ_T and ρ_{1T} , a daily temperature sequence can be generated using this model.

To generate the daily temperature sequence of future climatic conditions, three parameters of future climate conditions must be determined, namely, $\mu_{T_{ij}}$, $\sigma_{T_{ij}}$ and $\rho_{1T_{ij}}$, where $\mu_{T_{ij}}$ denotes the mean temperature for month *j* in year *i*, $\sigma_{T_{ij}}$ represents the standard deviation of the temperature for month *j* in year *i*, and $\rho_{1T_{ij}}$ is the lag-one autocorrelation coefficient of the temperature for month *j* in year *i*.

Herein, the trends of mean monthly temperature and mean monthly precipitation were determined using not only the Mann-Kendall test but also linear regression analysis. The test results revealed that in most months the series could pass the F-test, and thus the series clearly contain linear components, series vibration can be simulated by using the stochastic component. A linear regression equation (linear component) combined with a first-order autoregressive model (stochastic component) was developed to calculate the future value of $\mu_{T_{ij}}$, as follows:

$$\mu_{T_{ij}} = S_{T_j} \times (i - y_0) + \overline{\mu}'_{T_j} + \rho'_{T_j} . \frac{\sigma'_{T_j}}{\sigma'_{T_{j-1}}} . (\mu_{T_{i,j-1}} - \overline{\mu}'_{T_j}) + \sqrt{1 - \rho'^2_{T_j}} \sigma'_{T_j} \upsilon_{ij} \qquad (7.8)$$

Where S_{T_j} denotes the coefficient of the linear regression equation relating mean temperature in month *j* to time (year)

$\overline{\mu}'_{T_j}$ represents the mean value of mean temperature in month *j*

ρ'_{T_j} denotes the autocorrelation coefficient of mean temperature values between months *j* and *j-1*

y_0 represents the initial year of generation

υ_{ij} is the random standard normal variation

The former four parameters are calculated using the data during the current climatic period.

Since the mean values and standard deviations of temperature for all months were found to correlate strongly, this study attempted to establish the relationship between historical mean temperatures, μ_T, and standard deviations, σ_T, for all months by a linear regression equation, as follows:

$$\sigma_T = -0.0153 \times \mu_T + 1.4818 \qquad (7.9)$$

Correlation coefficient = 0.474

After obtaining the mean monthly temperature for future climatic conditions, the standard deviation of monthly temperature for future climatic conditions can be obtained by substituting the mean temperature into the above regression equation. The lag-one autocorrelation coefficient of temperature for future climatic conditions for month *j* in year *i*, $\rho_{1T_{ij}}$, was considered herein to be the same as that current climatic conditions.

Table 7.8 lists the lag-one autocorrelation coefficients of temperature for all months, calculated using the data during the current climatic period.

Table 7.8: The lag-one autocorrelation coefficient of temperature for each month

Month	***Jan***	***Feb***	***Mar***	***Apr***	***May***	***Jun***	***Jul***	***Aug***	***Sep***	***Oct***	***Nov***	***Dec***
Value	0.50	0.51	0.67	0.69	0.56	0.62	0.67	0.66	0.74	0.71	0.66	0.64

To validate the above temperature generating model, parameters, $\mu_{T_{ij}}$, $\sigma_{T_{ij}}$ and $\rho_{1T_{ij}}$ from Equation 7.9 were obtained for each month by using historical daily temperature records during the period from 1981 to 2008 at Ono station and sets of daily temperature sequences with the same period were generated to determine whether the first two statistical moments of daily temperature for each month could be preserved. Figure 7.5 compares the mean temperature generated for each month with observed values, and reveals that the temperature generating model achieves good validation results. These good validation results also implicitly justify the assumptions of the temperature generating model, such as the form of Equation 7.7 and the probabilistic distribution of daily temperature values.

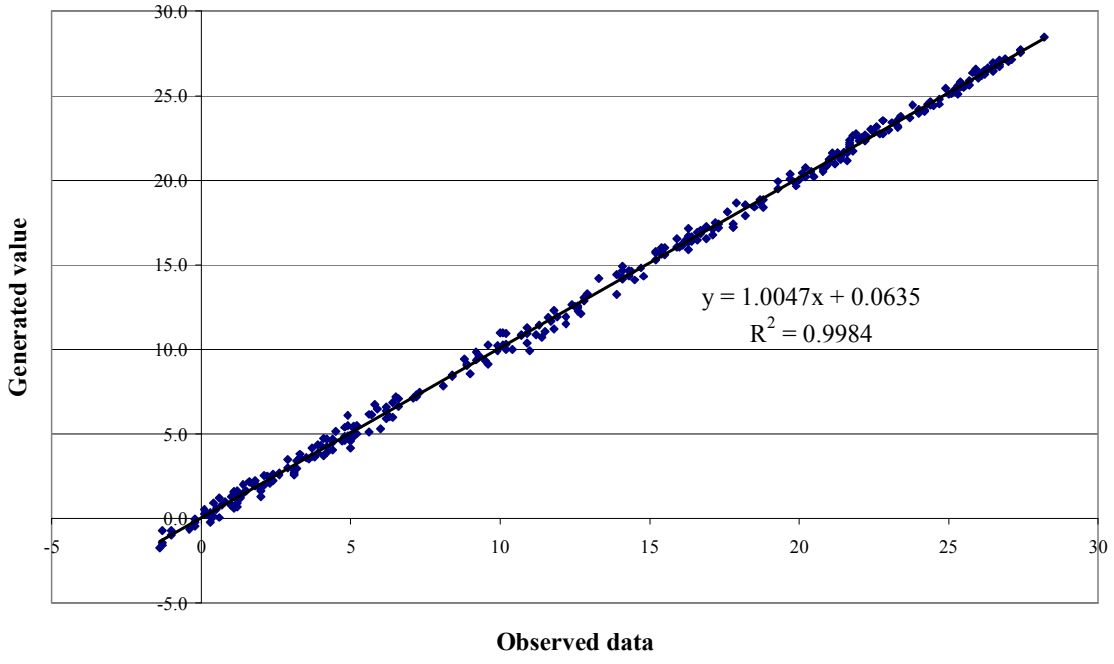

Figure 7.5: Validation results of the temperature generating model

7.4.2 Precipitation generating model

For generating daily precipitation height, the probabilistic distribution of precipitation height on wet day produces the overall probability distribution for precipitation height. Though various probabilistic distributions have been considered for wet day precipitation height (Pickering et al., 1988; Selker and Haith, 1990), the two more commonly used

distributions, that is the exponential distribution and Weibull distribution, were adopted herein to test their suitability to the study area, and the Weibull distribution was found to be superior to the exponential distribution. The Weibull distribution takes the following form:

$$p_t = \alpha \exp\{-\frac{1}{\beta}.\ln[\ln(1-u_t)]\} \tag{7.10}$$

Where p_t denotes the precipitation height on day t

u_t represents the random variable between 0 and 1,

α and β are the parameters of the Weibull distribution, which can be estimated using the mean precipitation height, μ_p, and the standard deviation of precipitation, σ_p.

To generate the daily precipitation height sequences of future climatic conditions, the values of the parameters must be predicted. Herein, the mean precipitation height for month j in year i for future climatic conditions, $\mu_{p_{ij}}$, is determined by an equation similar in form to Equation 7.8, where temperature is modified by precipitation.

To obtain the standard deviation of precipitation height for month j in year i, $\sigma_{p_{ij}}$ for the future climatic conditions, the historical mean values, μ_p, were related to the standard deviations of precipitation height, σ_p, for all months, revealing a high correlation coefficient, as follows:

$$\sigma_p = 0.9815 \times \mu_p - 0.0234 \tag{7.11}$$

Correlation coefficient = 0.71

The standard deviation of precipitation height for future climatic conditions can be calculated by substituting the generated mean precipitation height of future climatic conditions into this equation.

To validate the precipitation generating model, parameters, μ_p and σ_p were obtained for each month from daily areal precipitation height records, as estimated from the precipitation records of the eight rain gauges using Thiessen weights during the period from 1981 to 2008. Sets of daily precipitation height sequences with the same period were generated to determine whether the values of μ_p and σ_p generated in each month could be preserved as well as the observed values. Figure 7.6 compares the generated values of mean precipitation for all months with observed one, revealing that the precipitation generating model has good validation results. These good validation results also implicitly justify the assumptions of the precipitation height generating model, such as the form of the probabilistic distribution of daily precipitation heights.

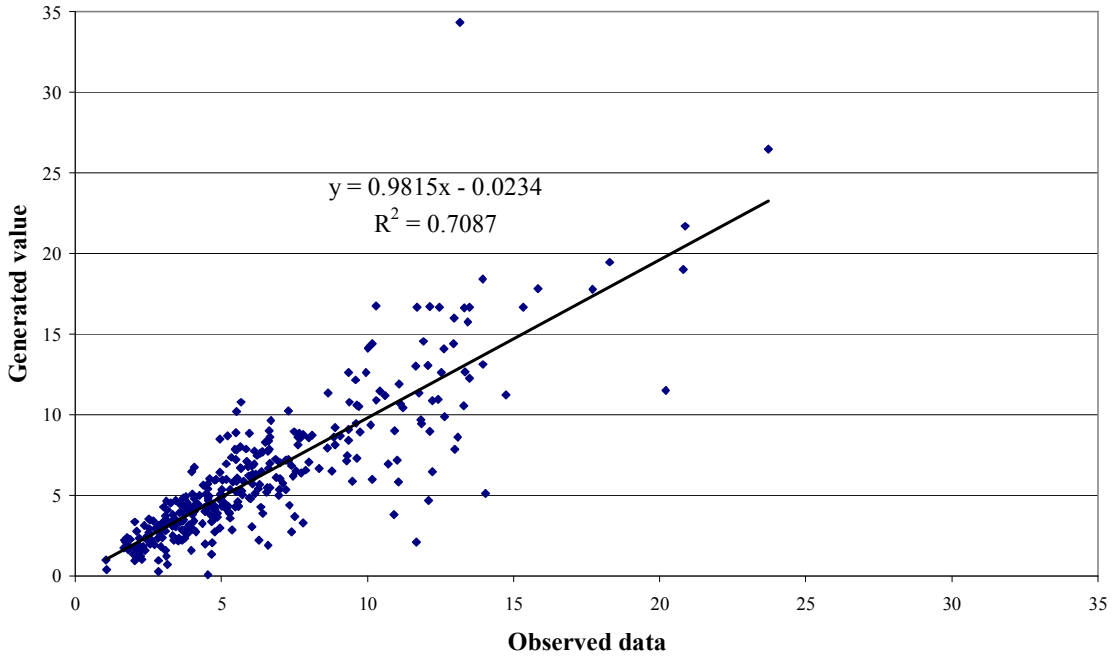

Figure 7.6: Validation results of precipitation generating model

7.5 Impact of global warming on water resources

By using the weather generating model, sets of future weather sequences (for 2009-2060) are generated including daily temperature and precipitation height sequences.

7.5.1 Effects to hydrology

The daily temperature series are extrapolated in future by using Equation 7.7. The monthly statistical parameters are shown in Table 7.9. The temperature trend is increasing for all months. Figure 7.7 represents the generated mean temperature for 2009 – 2060. Trend is increasing and slope of trend line is about 0.0412 which it means that the temperature on this study area is increasing 0.0412 ºC every year or 0.4 ºC per decade. This result is supported by monotonic trend test as shown in the previous information in this Chapter.

Table 7.9: Monthly statistical parameters for temperature (1981-2008)

Month	***Jan***	***Feb***	***Mar***	***Apr***	***May***	***Jun***	***Jul***	***Aug***	***Sep***	***Oct***	***Nov***	***Dec***
Mean	1.06	1.23	5.10	11.91	17.21	21.07	24.70	26.14	21.87	15.40	9.43	3.86
Slope	0.030	0.052	0.047	0.016	0.037	0.041	0.030	0.002	0.079	0.078	0.035	0.031
SD	2.33	2.40	3.18	3.71	2.80	2.14	2.07	1.93	2.83	3.04	3.29	2.84

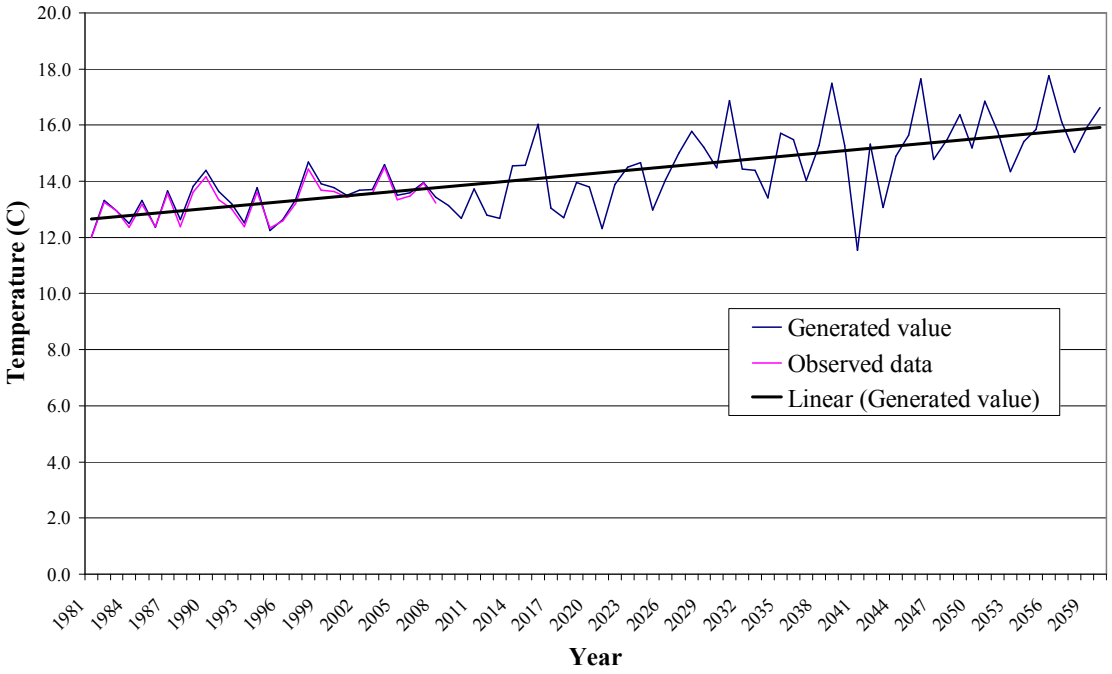

Figure 7.7: Generated mean temperature for the future year

The daily rainfall series are extrapolated in future by using Equation 7.7 where temperature is modified by precipitation. The monthly statistical parameters are shown in Table 7.10. The rainfall trend is decreasing for overall. Considering each month found that rainfall during April to September is decreasing and during October to March of next year is increasing. Then it can be concluded that the trend of rainfall in each month during wet season is decreasing and the trend of rainfall in each month during dry season is increasing. Figure 7.8 represents the generated annual rainfall for 2009 – 2060. Trend is decreasing and slope of trend line is about 3.787 which it means that the rainfall on this study area is decreasing 3.787 mm every year or 38 mm per decade. This decreasing rate is less than the monotonic trend test; 52 mm per decade, as shown in the previous information in this Chapter.

Table 7.10: Monthly statistical parameters for rainfall (1981-2008)

Month	***Jan***	***Feb***	***Mar***	***April***	***May***	***Jun***	***Jul***	***Aug***	***Sep***	***Oct***	***Nov***	***Dec***
Mean	4.23	3.44	3.51	5.32	6.70	8.52	10.79	7.28	9.26	5.66	6.89	5.07
Slope	0.024	0.002	0.034	-0.085	-0.030	-0.068	-0.055	-0.006	-0.091	0.036	0.011	0.041
SD	5.04	4.57	5.45	9.37	12.49	16.74	20.53	15.65	17.85	11.32	10.38	6.34

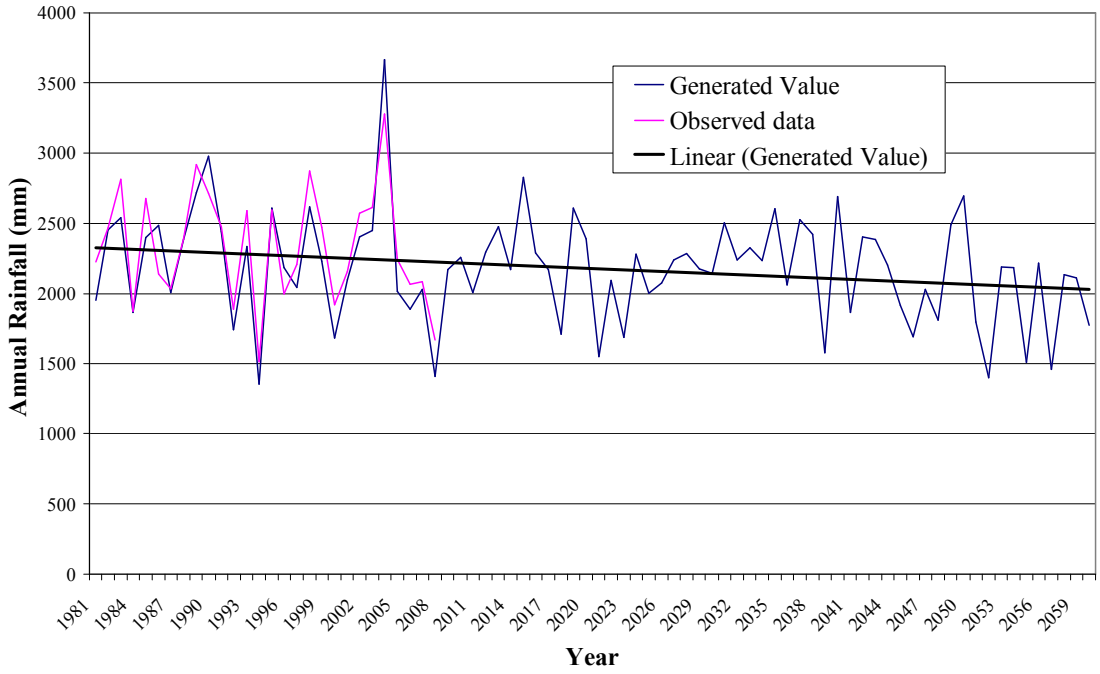

Figure 7.8: Generated annual precipitation height for the future year

-Recommendation for applying the extrapolated data to rainfall runoff model

In Chapter 3 Rainfall Runoff model, the NAM model was calibrated and validated with historical data and the efficiency is acceptable therefore to find out the extrapolated runoff in this watershed area it is necessary to input the extrapolated rainfall data into the rainfall runoff model. The extrapolated rainfall can be generated by Equation 7.7 where temperature is modified by precipitation and the detail is mention above. The trend of monthly discharge should be reduced because of the decrease in precipitation.

7.5.2 Effects to sediment yield

In Chapter 5 Integrated sedimentation model, the sediment yield and sediment transport model were applied in the integrated sedimentation model. This part will show the results only from the sediment yield model because there are some limitations of sediment transport model.

- Assumption and inputs of MUSLE model

This part also applies SWAT model only to find out the soil erosion of each sub-basin at each outlet point and there are 9 sub-basins as shown in Figure 5.1. The MUSLE is used in this study which is given as Equation 5.1. From MUSLE, the shortest time interval of output is daily and it was used to find an annual sediment yield on each sub-basin. The efficiency of soil erosion model in this study as explained in Chapter 5 that the efficiency of MUSLE model applied on this study area is fare acceptable.

Input information to MUSLE model by extrapolated data is followed items:

1) Extrapolated rainfall
2) Extrapolated temperature
3) Land use (assume that there is no changing from 1997 as shown in Figure 5.3)
4) Digital elevation map (DEM)
5) Soil type

- Soil surface erosion results

Average annual sediment yields (t/ha) for each sub-basin in decade were computed by MUSLE with SWAT model as shown in Table 7.11**.** Sub-basins of Managawa river basin are shown in Figure 5.1.

Table 7.11: Annual average soil surface erosion from MUSLE of each decade (t/ha/year)

Sub-basin	***2011-2020***	***2021-2030***	***2031-2040***	***2041-2050***
1	6.22	5.91	5.48	4.16
2	7.88	6.93	6.93	5.29
3	8.86	6.91	6.92	5.27
4	6.36	5.59	5.61	4.26
5	6.88	6.04	6.04	4.63
6	7.08	6.23	6.24	4.74
7	6.06	5.33	5.33	4.07
8	7.08	6.22	6.21	4.77
Average sediment yield (m^3/year)	40,078	35,004	34,849	26,650

Sub-basin No. 2 and 3 show high erosion rate because these slopes are so steep. The average sediment yields from the whole watershed calculated from Equation (5.3) are given in the last row of upper table. The trend of annual soil surface erosion should be reduced because of the decrease in precipitation however it should be remind that the decreasing trend of precipitation is not significant at the 5% level of significance.

7.6 Discussion and conclusions

This study investigated the impact of climate change on water resources and sediment yield in Managawa river basin, Japan. The weather station at Ono station was selected for representative of temperature over this study area and 8 rain gauge stations located on the study area were used to calculated weighted rainfall of this area.

The study area seems to have become warmer in the last few decades. The results obtained by using both parametric and nonparametric techniques show that the increasing tendency of temperature has a 5% level of significance, and the temperature increased by almost 1 ºC over the past 30 years. Temperature was found herein to follow a clear and

steady trend every month. The average annual temperature exhibited an increasing trend with a magnitude 0.4 ºC per decade.

Several hypothesis test techniques to identify the long term trends in time series have been used in this study. Application of the Mann-Kendall and Mann-Whitney test for rainfall time series on Managawa river basin showed no step change and no monotonic trend in Managawa precipitation. Thus the downward changes in the observed century-long precipitation are within the range of normal fluctuations and could not be definitively ascribed to monotonic trend. The average annual precipitation exhibited a decreasing trend with a magnitude 52 mm per decade. The mean values of precipitation height exhibit increasing trends during October to March of next year (low flow period), while monthly precipitation height exhibit decreasing trend during high flow period.

The research results through the t-test and Mann-Whitney test show that temperature contradicts the null hypothesis but there is no step change in rainfall time series information. A step change occurred in temperature time series around 1995. To find out whether this step change, further studies with the combination of climatologically analysis is required. The physical mechanism producing this kind of jump change needs further investigation.

Finally, the generated weather series; temperature and precipitation height, for future climatic conditions were inputted into the soil loss equation to investigate the change in sediment sources and extrapolated rainfall can be inputted to rainfall runoff model to investigate the change in runoff for future climate change condition. It shows that sediment yield rate is reducing by each decade because of decreasing trend of an annual rainfall.

The trend of increasing temperature noted herein may not be entirely caused by global warming, despite accurately reflecting local climate change. Though the increasing temperature trend may be a combination of the results of global warming and urbanization, distinguishing between the effects of global warming and urbanization in local area is difficult. Therefore this work merely assumes the increasing temperature to indicate local climate change, leaving the possible of a connection with global warming to be investigated by a future study.

CHAPTER 8
Summary, Conclusion and Recommendation

In this research study, the sedimentation and sediment management were done and investigated by several mathematical models that the study area is Managawa river basin or the upstream of Managawa dam located in Fukui prefecture, Japan. There are mainly three topics considered for sedimentation and sediment management which are integrated sedimentation, real time suspended sediment prediction and climate change effects to water resources and sediment yield.

Rainfall and evaporation data were inputted into rainfall runoff model; NAM model, to convert rainfall to surface flow and to get the flow volume on watershed then hydrodynamic model was used for routing the flow in river that the results of hydrodynamic model are flow characteristics; discharge, flow velocity, flow depth, etc.

In point view of integrated sedimentation, rainfall will scour soil surface and soil will be transported by surface flow to drop into river. The soil loss equation was used to be a tool for investigating sediment yield on study area. The soil loss equation or Modified Soil Loss Equation (MUSLE) was developed in this study. The sedimentation in this study as shown in term of sediment depositing volume in reservoir is calculated by sediment yield model with sediment transport model.

To monitoring the sediment flow into reservoir, the suspended sediment gauge was installed at the upstream of reservoir. Hourly suspended sediment prediction is done by applying Artificial Neural Network (ANN). The neural network are used the back propagation (BP) algorithm for hourly suspended sediment concentration forecasting. The results of network were compared with Multiple Linear Regression (MLR) and Sediment Rating Curve (SRC). It can be applied for real time suspended sediment concentration forecasting by using the weather information as inputs.

Climate change was considered for one part of this study. Mainly weather data used for water resources management are rainfall and temperature. First the trends of climatic time series both rainfall and temperature were investigated as step trend and monotonic trend. Then the weather generating models were generated then produced the daily temperature and daily precipitation in the future year. The outputs; extrapolated rainfall and extrapolated temperature, from weather generating models were inputted to rainfall runoff model and sediment yield model therefore the sediment yield were investigated in the future year.

This study is mainly considering in sedimentation and it's characteristics on reservoir watershed. According to the results presented in the previous chapters, the following research techniques can be summarized.

8.1 Summary

- Integrated sedimentation

1. Hourly rainfall data were obtained from Managawa dam office at 8 rain gauges located on the study area. The reliability of rainfall data was performed by double mass curve technique then rainfall were be weighted by Thiessen polygon to be the representative of rainfall at Managawa river basin. The considered duration was from 1981 to 2004.

2. The weighted rainfall is input of NAM model that would transform rainfall to runoff with specific parameters in this region.

3. There are two dams located at the upstream of Managawa dam which are Sasougawa dam and Kumokawa dam. The outflows from both dams are the upstream boundary conditions of hydrodynamic model and down stream boundary condition is water level at Managawa dam. For checking the efficiency of 1D hydrodynamic model, the calculated discharge and water depth at Nagajima station are used to compare with the observed value.

4. The calibration and verification steps for rainfall runoff model and hydrodynamic model are the applicability of flood or heavy rainfall years.

5. The one of objective of this research is to compute sediment depositing volume in reservoir that it is the sediment processing on the upstream of reservoir.

6. The integrated sedimentation model in this study consists of soil erosion model and sediment transport model. Modified Soil Loss Equation (MUSLE) was the tool for generating daily soil surface yield volume. The efficiency of soil erosion model is rare acceptable to be the representative of sediment depositing in reservoir therefore in this study try to improve by basic knowledge that the sedimentation should not be only sediment yield but also include sediment transport part. So the watershed had to be divided in to many sub-basins; there are 9 sub-basins in this study, then sediment yield of each sub-basin was generated. Then the sediment would be carried by river flow which the tools were sediment transport model (ST model); total load Acker and White, and hydrodynamic model. The sediment would be deposited in reservoir.

7. The results of sediment yield with sediment transport model called integrated sedimentation were calculated from 1981 to 2004.

- Real time suspended sediment concentration prediction

1. Suspended sediment gauge was installed at intake of Okutani power station, the upstream of Managawa dam where it is the serious area of sediment erosion. Ten

minute turbidity data was recorded by suspended sediment gauge. This study used average hourly data for modeling.

2. The duration of this part of research was from December 2006 to January 2008 which the meteorological data could be down loaded from web site of Japan Meteorological Agency because the turbidity gauge has been installed from November 2006.

3. Real time suspended sediment concentration forecasting in this study was used Artificial Neural Network (ANN) with back propagation technique as the tool for generating suspended sediment concentration then compared the results with other models; Multiple Linear Regression (MLR) and Sediment Rating Curve (SRC).

4. The correlation among data; suspended sediment concentration and meteorological data, for suspended sediment concentration forecasting are very important for model although high correlation value between suspended sediment concentration and other inputs may not imply for getting the better simulation results. Not only the correlation defined above is being considered as in the first priority, but the other inputs that have good correlation with suspended sediment concentration, are also important for model simulation. In this study, the inputs getting high correlation with suspended sediment concentration are rainfall data, discharge and the previous step of suspended sediment concentration data.

5. The accuracy of model is measured by Efficiency Index (EI), Root Mean Square Error (RMSE) and visual inspection on the shape of hydrograph with peak error and volume error.

6. About network pattern, hidden nodes were assigned by trial and error technique, the input nodes were equal to number of inputs and the output node was a suspended sediment concentration node.

7. This part of the study also tried to complicate the inputs data that there was using only rainfall information, rainfall's products and the previous step of suspended sediment concentration data. Rainfall's products mean rainfall intensity and computed discharge which it is transformed from rainfall runoff model.

- Climate change effects to water resources and sediment yield

1. The significant climatic information in this study was temperature time series and rainfall time series. The daily mean temperature data from 1981 to 2008 at Ono station, Fukui prefecture can be down loaded from web site of Japan Meteorological Agency. The hourly rainfall data from 1981 to 2008 were obtained by Managawa dam office that the reliability of data and weighted data were explained same as in rainfall runoff section.

2. The historical data as temperature and rainfall time series were detected by using both parametric and nonparametric statistical tests.

3. Trends of both temperature and rainfall time series were investigated and shown by step trend test and monotonic trend test which the statistical methods used in this study were Mann-Kendall test, Mann-Whitney test and t-test.

4. Temperature trend was considered in the term of average temperature of each year. For rainfall, rainfall trend was not considered only in the term of annual rainfall but also the amount of rainfall during high flow season and low flow season were investigated.

5. Weather generating models were based on procedure of the first order autoregressive model utilized to generate daily temperature sequences and precipitation height in the future year.

6. In this study, the statistical parameters of weather generating models were calculated from historical data from 1981 to 2008 then extrapolating daily temperature and rainfall were generated to 2060. The validation results of both monthly temperature and monthly rainfall were expressed by R-square or simple correlation between generated value and observed data.

7. To investigate the effects of climate change on water resources and sediment yield in this study area, the extrapolated temperature time series and the extrapolated rainfall time series calculated from weather generating models should be assigned as inputs in rainfall runoff model and sediment yield model.

8.2 Conclusion

- Integrated sedimentation

1. The efficiency of the computed sediment depositing volume in reservoir is expressed by Nash-Sutchliffee index. The efficiency of simple MUSLE is poor but the combined MUSLE with sediment transport model produced acceptable efficiency.

2. The results of annual sediment accumulating volume for this study area show large differences with the observed data but total volumes almost coincided very well. The accumulated sediment depositing volumes were compared between observed and computed total sediment volumes until year 2003 that the error is about 10%.

3. This study shows that this MUSLE with sediment transport model can be used to estimate reservoir sedimentation volumes and its tendency if basic characteristics of each catchment such as topographical, geological, meteorological conditions may change.

- Real time suspended sediment concentration prediction

1. The neural networks were trained and tested by the recently data at Okumotani catchment that the appropriate variables were rainfall, water discharge, rainfall in two hours, the absolute of discharge changing and previous time step of suspended sediment concentration. It is demonstrated that the artificial neural network (ANN) is capable of modeling the hourly suspended sediment concentration with good accuracy when the appropriate variables were inputs of neural network.

2. Only rainfall and discharge data are used for inputs of neural network, it makes the accuracy of network is quite good and to improve this network the rainfall in two hours should be added as input of network.

3. These models can be used for real time suspended sediment concentration forecasting when the previous time step of suspended sediment data is known and available which the previous time step of suspended sediment concentration makes the efficiency of network increase.

4. Artificial neural network (ANN) can generate a better fit to the observed suspended sediment concentration than the multiple linear regression (MLR). However this study found that the multiple linear regression models can be used to predict the hourly suspended sediment. The sediment rating curve (SRC) model produced the outputs which were not match with observed suspended sediment concentration data.

5. Rainfall and its products; the computed discharge from rainfall runoff model and rainfall intensity, with the previous step of suspended sediment concentration were applied as inputs to neural network that the efficiency of this real time suspended sediment concentration forecasting model was acceptable.

- Climate change effects to water resources and sediment yield

1. The study area seems to have become warmer in the last few decades. Temperature was found herein to follow a clear and steady trend every month. The average annual temperature exhibited an increasing trend with a magnitude 0.4 ºC per decade.

2. Application of the Mann-Kendall and Mann-Whitney test for rainfall time series on Managawa river basin showed no step change and no monotonic trend in Managawa precipitation. Although there is a decreasing tendency in an annual precipitation during the past century, the decreasing trend is not significant at the 5% level of significance. From monotonic trend test, the average annual precipitation exhibited a decreasing trend with a magnitude 52 mm per decade.

3. The mean monthly values of precipitation height exhibit increasing trends low flow period, while monthly precipitation height exhibit decreasing trend during high flow period.

4. The weather generating models both temperature and rainfall expressed the high efficiency for validation step. The generated weather series 2009 - 2060; temperature and precipitation height, for future climatic conditions can be inputted into the soil loss equation to investigate the change in sediment sources and extrapolated rainfall can be inputted to rainfall runoff model to investigate the change in runoff for future climate change condition.

8.3 Recommendation

- Integrated sedimentation

This integrated sedimentation model can not use for predicting in the future year because the outflows from upstream dams are the ones of input to hydrodynamic model which it is depended on each dam's operation. But sediment yield model can be used for predicting in the future year as show in Chapter 7.

In order to improve the model, other modifications may be needed to compute sediment yield and transport process in high flood periods. However, this model can be used to estimate reservoir sedimentation volumes and its tendency if catchment's conditions may change.

- Real time suspended sediment concentration prediction

This model can be used for real time suspended sediment concentration forecasting. The sediment flow does not include only suspended sediment but include bed load also. In other words, total load consists of suspended sediment and bed load. Therefore the bed load can be estimated by using the approximate 30% of suspended load by unit weight.

In order to improve and confirm these hourly suspended sediment concentration prediction models for upstream of Managawa dam, the seasonal effect, climate changing and land surface changing should be considered as one of parameters of models and the duration of training and testing the model should be extended because the limited of data this study was used only one year data for training and testing models.

- Climate change effects to water resources and sediment yield

The trend of increasing temperature noted herein may not be entirely caused by global warming, despite accurately reflecting local climate change. Though the increasing temperature trend may be a combination of the results of global warming and urbanization, distinguishing between the effects of global warming and urbanization in local area is difficult. Therefore this work merely assumes the increasing temperature to

indicate local climate change, leaving the possible of a connection with global warming to be investigated by a future study.

Japan is an island country with frequent typhoons. If all the typhoon-related precipitation data are separated from the present precipitation, the rainfall time series should be changes. Although these ideas are beyond the study represented in this study, they will be interested field of research in the on-going investigation.

References

Alan F. Hamlet and Dennis P. Lettenmaier (1999) Effects of climate change on hydrology and water resources in the Columbia river basin, Journal of the American Water Resources Association, Vol.35, No.6: 1597-1623

Avinash A, Singh R.D, Mishra SK, Bhunya PK (2005) ANN-based sediment yield models for Vamsadhara river basin, India. Water SA, Vol.31 No.1: 95-100

Brent Frakes and Zhongbo Yu (1999) An evaluation of two hydrologic models for climate change scenarios, Journal of the American Water Resources Association, Vol.35, No.6: 1351-1363

CHEN Ya-ning, LI Wei-hong, XU Chang-chun, HAO Xin-ming (2006) Effects of climate change on water resources in Tarim river basin, Northwest China, Journal of Environmental Sciences: 488-493

Chjeng-Lun Shieh and Sen-Yaun Lee (2005) Sediment yield model for a watershed: a case study of Choushui River, Taiwan, Eropean Geosciences Union, Vol.7, 05931, 2005

Chris Huntingford, John Gash and Anna Maria Giacomello (2006) Climate change and hydrology: next steps for climate models, Hydrological Processes, Wiley InterScience: 2085-2087

Cigizoglu HK, Alp M (2006) Generalized regression neural network in modeling river sediment yield. ELSEVIER Advances in Engineering Software 37: 63-68

Cigizoglu HK, Kisi O (2006) Methods to improve the neural network performance in suspended sediment estimation. Journal of Hydrology 317: 221-238

D. Mbano, J. Chinseu, C. Ngongondo, E. Sambo and M. Mul (2009) Impacts of rainfall and forest cover change on runoff in small catchments: A case study of Mulunguzi and Namadazi catchment area in Southern Malawi, J. SCI & TECHNOL.: 11-17

Eileen Chen and D. Scott Mackay (2004). Effects of distribution-based parameter aggregation on a spatially distributed agricultural non point source pollution model, Science Direct, Journal of Hydrology, Vol.295, Issue 1-4: 211-224

Emrah Dogan, Ibrahin Yuksel and Ozgur Kisi (2007) Estimation of total sediment load concentration obtained by experimental study using artificial neural networks, Environ Fluid Mech, Springer: 271-288

Fumitoshi IMAIZUMI and Roy C. SIDLE (2005). Relationship between Sediment Supply and Transport Process in Miyagawa Dam Catchment, Annuals of Disas. Prev. Res. Inst., Kyoto University, No.48C

Guoqiang WANG, Qing FU, Kuniyoshi TAKEUCHI and Hiroshi ISHIDAIRA (2007) Estimation of River Sediment Concentrations during Hydrologic Event, Annual Journal of Hydraulic Engineering, JSCE, Vol.51: 109-114

H. Thodsen, B. Hasholt and J.H. Kjarsgaard (2008) The influence of climate change on suspended sediment transport in Danish rivers, Hydrological Processes, Wiley InterScience: 764-774

Hikemet Kerem Cigizoglu (2002) Suspended sediment estimation and forecasting using artificial neural networks, Turkish J. Eng. Env. Sci.: 15-25

Hikemet Kerem Cigizoglu (2002) Suspended sediment estimation for rivers using artificial neural networks and sediment raiting curves, Turkish J. Eng. Env. Sci.: 27-36

Hikemet Kerem Cigizoglu and Murat Alp (2006) Generalized regression neural network in modeling river sediment yield, Advances in Engineering Software, Elsevier: 63-68

I. Sumathi and S. Santhana Bosu (2002). Using GIS for facilitating Sediment Yield Estimation, Asian Agricultural Information Technology and Management, October 2002: 453-455

K.F. Golson, T.D. Tsegaye, N.B. Rajbhabdari, T.H. Green and T.L. Coleman (2000) Evaluating Modified Rainfall Erosion Factors in the Universal Soil Loss Equation, IEEE Xplore: 2017-2020

Kisi O (2005) Suspended sediment estimation using neuro-fuzzy and neural network approaches. Hydrological Sciences-Journal-des Sciences Hydrologiques: 683-696

M. Sharif and D. H. Burn (2007) Improve K-Nearest neighbor weather generating model, Journal of Hydrologic Engineering, ASCE: 42-51

Mikhal A. Semennov (1997) Use of a stochastic weather generator in the develonment of climate change scenarios, Climate Change, Kluwer Academic Publisher: 397-414

Nagy HM, Watanabe K, Hirano M (2002) Prediction of sediment load concentration in rivers using artificial neural network model. Journal of hydraulic engineering: 588-595

Niklas S. Christensen, Andrew W. Wood, Nathalie Voisin, Dennis P. Lettenmaier and Richard N. Palmer (2004) The effects of climate change on the hydrology and water

resources of the Colorado river basin, Climate Change, Kluwer Academic Publisher: 337-363

Norman L. Miller (2003) California climate change, hydrologic response and flood forscasting, International Expert Meeting on Urban Flood Management, The Netherlands

Ozgur Kisi (2005) Suspended sediment estimation using neuro-fuzzy and neural network approaches, Hydrological Science-Journal-des Sciences Hydrologiques, IAHR Press: 683-696

Ozgur Kisi (2007) Constructing neural network sediment estimation models using a data-driven algorithm, Mathematics and Computers in Simulation, Elsevier: 10 pages

Pao-Shan Yu, Tao-Chang Yang and Chih-Kang Wu (2002) Impact of climate change on water resources in southern Taiwan, Journal of Hydrology, Elsevier: 161-175

Rabin Bhattarai and Dushmata Dutta (2007) Estimation of Soil Erosion and Sediment Yeild Using GIS at Catchment Scale, Water Resource Management, October 2007, Vol.21, No.10: 1573-165

Raveendra KR, Mathur BS (2008) Event-based sediment yield modeling using artificial neural network. Water Resources Management 22: 423-441

S.H. Sadeghi and T. Mizuyama (2007) Applicability of the Modified Universal Soil Loss Equation for prediction of sediment yield in Khanmiraza watershed, Iran, Hydrological Sciences-Journal-des Science Hydrologiques, IAHR Press: 1068-1074

S.H. Sadeghi (2004) Application of MUSLE in prediction of sediment yield in Iranian, Conserving Soil and Water for Society, Sharing Solutions: Paper No.998

S.L. Neitsch, J.G. Arnold, J.R. Kiniry, J.R. Williams (2005). Soil and Water Assessment Tool Theoretical Documentation, Agriculture Reserch Service and Experiment Station, Temple, Texus, Version 2005

Seyed Hamidreza Sadeghi, Takahisa Mizuyama and Babak Ghaderi Vangh (2007) Conformity of MUSLE Estimates and Erosion Plot Data for Storm-Wise Sediment Yield Estimation,Terr. Atmos. Ocean Sci, Vol.18: 117-128

Vaclav Dvorak, Josef Hladny and Ladislav Kasparek (1997) Climate change hydrology and water resources impact and adaptation for selected river basins in the Czech Republic, Climate Change, Kluwer Academic Publisher: 93-106

Van-Thanh-Van Nguyen (2005) Downscaling methods for evaluating the impacts of climate change and variability on hydrological regime at basin scale, Role of Water Sciences in Transboundary River Basin Management, Thailand : 1-8

Yun-Mei Zhu, X.X. Lu and Yue Zhou (2007) Sediment flux sensitivity to climate change: A case study in the Longchuanjian catchment of the upper Yangtza river, China, Global and Planetary Change, Elsevier: 14 pages

Z.X. Xu, K. Takeuchi and H. Ishidaira (2003) Monotonic trend and step changes in Japanese precipitation, Journal of Hydrology, Elsevier: 144-150

Zhu YM, Lu XX, Zhou Y (2007) Suspended sediment flux modeling with artificial neural network: An example of the Longchuanjiang River in the Upper Yangtze Catchment, China. Geomorphology 84:111-125

APPENDIXES

APPENDIXES

Appendix A: Integrated sedimentation

Table A-1: Depositing sediment volume in Managawa dam, Sasougawa dam and Kumokawa dam (1981-2004)

Year	Managawa dam (cu.m)	Sasougawa dam (cu.m)	Kumokawa dam (cu.m)
1981	-	33730	28700
1982	-	30975	18804
1983	78664	25217	12014
1984	15768	29773	19413
1985	166907	50324	18846
1986	16726	53326	-
1987	23477	54808	-
1988	59272	49442	-
1989	79652	66252	22731
1990	353591	44205	13193
1991	-	38286	-
1992	-	17151	11274
1993	175980	-	-
1994	-	50435	11709
1995	106271	-	9154
1996	-	476308	438
1997	4812	746063	-
1998	249132	465283	458
1999	41822	3226	26120
2000	-	204130	14091
2001	101227	32439	3772
2002	237574	120344	-
2003	36322	97841	3832
2004	1078341	72148	29083

(-) data is not available

Appendix A (Continued)

Table A-2: Annual average soil surface erosion from MUSLE (t/ha/year)

Year	Sub-basin No.								
	1	2	3	4	5	6	7	8	9
1981	8.31	10.20	10.28	8.46	8.70	9.34	7.83	8.77	9.66
1982	7.16	8.76	8.85	7.29	7.46	8.05	6.73	7.51	8.27
1983	16.78	20.91	20.99	17.14	18.05	19.02	16.09	18.37	20.34
1984	21.37	26.87	26.88	21.84	23.32	24.27	20.66	23.85	26.45
1985	3.21	4.04	4.03	3.26	3.49	3.60	3.08	3.56	3.95
1986	14.79	18.44	18.50	15.10	15.93	16.77	14.19	16.24	18.00
1987	5.20	6.53	6.53	5.31	5.66	5.89	5.02	5.79	6.43
1988	5.96	7.36	7.40	6.07	6.30	6.70	5.65	6.38	7.05
1989	1.48	1.88	1.87	1.51	1.64	1.66	1.44	1.69	1.88
1990	6.90	8.65	8.65	7.04	7.47	7.79	6.63	7.62	8.44
1991	7.43	9.42	9.39	7.60	8.23	8.47	7.25	8.48	9.44
1992	3.23	4.04	4.04	3.29	3.47	3.63	3.09	3.53	3.91
1993	3.12	3.83	3.86	3.17	3.27	3.51	2.94	3.30	3.63
1994	3.50	4.37	4.38	3.57	3.78	3.96	3.36	3.85	4.27
1995	13.63	17.24	17.21	13.95	15.04	15.52	13.27	15.47	17.22
1996	4.71	5.96	5.95	4.82	5.20	5.35	4.58	5.34	5.94
1997	21.08	25.53	25.88	21.44	21.62	23.67	19.64	21.62	23.75
1998	4.18	5.26	5.25	4.27	4.55	4.73	4.03	4.65	5.16
1999	12.30	15.02	15.18	12.52	12.80	13.84	11.55	12.89	14.20
2000	6.01	7.56	7.56	6.14	6.56	6.81	5.81	6.72	7.46
2001	9.77	12.42	12.37	10.00	10.87	11.15	9.56	11.22	12.51
2002	13.81	17.51	17.46	14.13	15.31	15.74	13.48	15.77	17.56
2003	12.21	15.22	15.26	12.45	13.11	13.80	11.69	13.33	14.74
2004	25.80	32.05	32.20	26.34	27.59	29.22	24.65	28.03	31.00
Average	9.66	12.04	12.08	9.86	10.39	10.94	9.26	10.58	11.72

Appendix A (Continued)

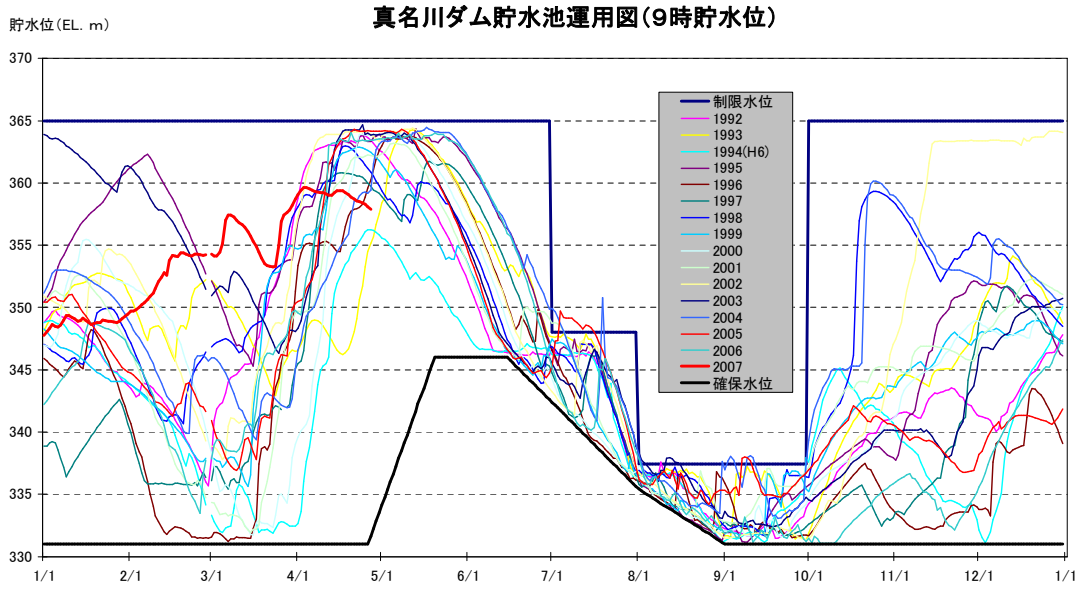

Figure A-1: Reservoir operation chart of Managawa dam, water level at 9:00am

Appendix B: Sediment prediction

Table B-1: The example of trial and error of network pattern: case 13 and 14: RASS

Time step t				Time step t-1			
train		test		train		test	
3,3,1		3,3,1		5,5,1	t-1	5,5,1	t-1
RMS Errors	0.0398593			RMS Errors	0.040558		
Iterations	28575			Iterations	40820		
Good Pats	65			Good Pats	62		
Target Err	0.01	Target Err	0.01	Target Err	0.01	Target Err	0.01
Eta	0.01	Eta	0.01	Eta	0.01	Eta	0.01
Alpha	0.5	Alpha	0.5	Alpha	0.5	Alpha	0.5
EI	0.6738823	EI	0.5295702	EI	0.709189	EI	0.624149
RMSE	35.851389	RMSE	37.995907	RMSE	33.84082	RMSE	33.96232
train		test		train		test	
3,6,1		3,6,1		5,10,1	t-1	5,10,1	t-1
RMS Errors	0.0299089			RMS Errors	0.030637		
Iterations	32785			Iterations	17090		
Good Pats	67			Good Pats	69		
Target Err	0.01	Target Err	0.01	Target Err	0.01	Target Err	0.01
Eta	0.01	Eta	0.01	Eta	0.01	Eta	0.01
Alpha	0.5	Alpha	0.5	Alpha	0.5	Alpha	0.5
EI	0.8163823	EI	0.4984119	EI	0.8107558	EI	0.4465395
RMSE	26.888318	RMSE	39.23404	RMSE	27.29565	RMSE	41.212857
train		test		train		test	
3,12,1		3,12,1		5,20,1	t-1	5,20,1	t-1
RMS Errors	0.0305076			RMS Errors			
Iterations	21270			Iterations			
Good Pats	70			Good Pats			
Target Err	0.01	Target Err	0.01	Target Err	0.01	Target Err	0.01
Eta	0.01	Eta	0.01	Eta	0.01	Eta	0.01
Alpha	0.5	Alpha	0.5	Alpha	0.5	Alpha	0.5
EI	0.8089573	EI	0.4229447	EI	0.8469008	EI	0.2918932
RMSE	27.429838	RMSE	42.082169	RMSE	24.545115	RMSE	46.616405
train		test		train		test	
3,20,1		3,20,1		5,8,1	t-1	5,8,1	t-1
RMS Errors	0.0287133			RMS Errors	0.028595		
Iterations	18450			Iterations	37235		
Good Pats	60			Good Pats	62		
Target Err	0.01	Target Err	0.01	Target Err	0.01	Target Err	0.01
Eta	0.01	Eta	0.01	Eta	0.01	Eta	0.01
Alpha	0.5	Alpha	0.5	Alpha	0.5	Alpha	0.5
EI	0.8307692	EI	0.5689155	EI	0.8322665	EI	0.3277813
RMSE	25.798604	RMSE	36.372286	RMSE	25.684458	RMSE	45.419745

Eta (η): The learning parameter

Alpha(α): The momentum parameter

Appendix B (Continued)

Correlation Coefficient

The equation of correlation coefficient is given as follows:

$$\rho_{x,y} = \frac{\mathrm{Cov}(x,y)}{\sigma_x . \sigma_y} \tag{b.1}$$

$$\mathrm{Cov}(x,y) = \frac{1}{n}\sum_{1}^{n}(x_i - \mu_x)(y_i - \mu_y) \tag{b.2}$$

$$\sigma_x^2 = \frac{1}{n}\sum_{1}^{n}(x_i - \mu_x)^2 \tag{b.3}$$

$$\sigma_y^2 = \frac{1}{n}\sum_{1}^{n}(y_i - \mu_y)^2 \tag{b.4}$$

where

x	=	Data set x
y	=	Data set y
n	=	Number of data
$\rho_{x,y}$	=	Correlation coefficient
Cov(x,y)	=	Covariance
σ^2_x , σ^2_y	=	Variance of data set x and y.
σ_x, σ_y	=	Standard deviation of data set x and y.
μ_x, μ_y	=	Mean value of data set x and set y

Table B-2: Correlation between suspended sediment concentration and weather data

Parameters	Correlation
Rainfall	0.5944
Acc. Rainfall	0.0765
Rainfall in two hours	0.6333
Temperature	0.2191
Wind speed	0.0627
Sun duration	-0.0660
Snow	-0.0605
Acc. Snow	-0.1151
Discharge	0.4364
Absolute of discharge changing	0.4856

Appendix C: Climate Change

Table C.1: Monthly temperature (1981-2008)

Month	Jan	Feb	Mar	Apr	May	Jun	Jul	Aug	Sep	Oct	Nov	Dec	Average
1981	-1.4	-0.4	3.1	10.2	15.5	20.9	26.5	25.2	20.2	14.1	7.2	2.9	12.0
1982	1.2	1.0	6.4	11.7	18.7	19.7	23.3	25.1	20.1	15.2	11.3	5.2	13.2
1983	1.4	0.2	4.9	14.5	17.8	20.2	23.2	26.7	22.1	14.3	8.1	1.9	12.9
1984	-1.3	-1.3	1.1	9.9	16.3	22.0	25.3	27.4	21.0	14.1	9.6	4.1	12.4
1985	-1.0	1.3	5.1	12.6	18.2	20.5	24.7	28.2	21.9	15.5	8.8	2.3	13.2
1986	-1.0	-1.3	3.5	12.2	16.6	20.8	23.3	26.5	21.3	13.3	8.4	5.0	12.4
1987	2.0	2.1	5.2	11.8	17.1	21.7	25.4	26.0	21.7	16.3	10.1	3.3	13.6
1988	2.4	0.1	4.2	11.2	16.2	20.9	23.1	25.9	21.7	14.1	6.5	2.2	12.4
1989	4.2	4.4	6.3	12.5	16.7	20.0	24.2	25.4	21.8	14.3	10.1	3.3	13.6
1990	1.0	5.0	6.4	11.8	16.9	22.2	25.5	27.1	22.8	15.4	10.9	4.8	14.2
1991	0.8	0.4	5.7	12.7	16.7	22.3	24.0	24.9	22.5	15.4	8.9	5.8	13.3
1992	1.8	1.1	6.6	11.7	14.7	19.7	24.0	26.5	21.0	15.2	9.5	4.5	13.0
1993	2.6	2.0	4.1	9.9	16.1	19.8	22.8	23.4	19.3	13.9	10.7	4.0	12.4
1994	1.1	0.6	3.7	12.8	17.8	20.8	26.5	27.4	21.9	16.6	10.2	3.8	13.6
1995	0.4	0.7	5.1	11.5	16.3	18.8	24.2	26.3	19.9	15.9	7.1	1.6	12.3
1996	1.2	-0.2	4.7	9.0	16.4	21.4	25.3	25.5	20.2	14.8	9.6	3.2	12.6
1997	1.1	0.3	6.2	11.4	17.6	21.6	24.3	25.7	21.1	14.1	10.2	4.8	13.2
1998	1.7	3.2	6.6	15.2	19.3	20.8	25.0	25.4	23.3	17.9	9.2	5.6	14.4
1999	1.2	0.3	7.3	11.9	17.3	21.3	24.5	26.5	24.4	16.3	10.0	3.1	13.7
2000	2.9	0.1	3.6	10.9	18.2	21.4	26.1	27.0	22.6	16.3	10.7	3.7	13.6
2001	0.5	1.2	5.0	12.4	18.5	21.0	26.7	25.8	21.2	16.1	8.9	3.9	13.4
2002	1.5	2.1	7.2	13.9	17.1	21.2	26.7	26.2	22.2	15.4	5.9	3.1	13.5
2003	0.6	1.8	4.8	12.9	18.8	21.5	22.4	25.7	22.8	14.4	12.6	4.4	13.6
2004	1.2	2.6	6.0	12.8	18.7	22.7	26.3	26.2	23.7	16.0	11.6	6.2	14.5
2005	1.0	1.6	4.2	12.6	16.4	23.0	24.7	26.0	23.8	16.9	9.2	0.5	13.3
2006	-0.2	1.4	3.9	10.4	17.8	21.8	24.4	27.4	21.7	17.2	10.9	4.9	13.5
2007	2.4	4.4	5.6	11.0	16.9	21.6	23.3	26.9	24.4	16.3	9.3	5.1	13.9
2008	0.3	-0.2	6.2	12.2	17.3	20.4	26.0	25.5	21.7	15.9	8.4	4.9	13.2

Appendix C (Continued)

Table C.2: Correlation coefficient of mean temperature between months

Month	Jan	Feb	Mar	Apr	May	Jun	Jul	Aug	Sep	Oct	Nov	Dec
1981	0.600	0.555	0.617	0.844	0.448	0.752	0.746	0.629	0.847	0.697	0.734	0.654
1982	0.622	0.676	0.706	0.805	0.665	0.653	0.669	0.535	0.766	0.708	0.710	0.526
1983	0.685	0.502	0.758	0.582	0.642	0.403	0.750	0.668	0.830	0.762	0.707	0.823
1984	0.364	0.554	0.637	0.798	0.774	0.510	0.658	0.727	0.794	0.709	0.696	0.819
1985	0.218	0.460	0.731	0.633	0.337	0.404	0.796	0.410	0.901	0.708	0.801	0.724
1986	0.247	0.385	0.601	0.789	0.311	0.158	0.818	0.786	0.650	0.863	0.548	0.403
1987	0.536	0.738	0.702	0.819	0.562	0.662	0.642	0.646	0.835	0.829	0.624	0.749
1988	0.540	0.344	0.744	0.834	0.676	0.702	0.516	0.496	0.671	0.804	0.695	0.637
1989	0.669	0.493	0.500	0.434	0.344	0.645	0.864	0.450	0.748	0.523	0.878	0.350
1990	0.515	0.720	0.604	0.578	0.703	0.437	0.818	0.627	0.627	0.855	0.586	0.810
1991	0.621	0.591	0.798	0.725	0.859	0.662	0.475	0.653	0.701	0.791	0.606	0.651
1992	0.633	0.436	0.732	0.614	0.477	0.577	0.839	0.567	0.805	0.754	0.608	0.755
1993	0.495	0.365	0.729	0.885	0.651	0.770	0.852	0.529	0.794	0.670	0.773	0.722
1994	0.687	0.303	0.488	0.626	0.565	0.597	0.727	0.799	0.774	0.718	0.661	0.698
1995	0.506	0.462	0.615	0.732	0.478	0.710	0.774	0.636	0.688	0.653	0.387	0.550
1996	0.464	0.657	0.694	0.885	0.841	0.523	0.891	0.795	0.725	0.504	0.647	0.504
1997	0.702	0.514	0.429	0.683	0.619	0.702	0.518	0.760	0.841	0.667	0.389	0.565
1998	0.680	0.593	0.725	0.846	0.415	0.742	0.729	0.545	0.578	0.727	0.815	0.658
1999	0.443	0.687	0.623	0.755	0.365	0.589	0.876	0.773	0.472	0.805	0.655	0.733
2000	0.590	0.588	0.633	0.528	0.672	0.712	0.378	0.561	0.847	0.719	0.693	0.679
2001	0.620	0.487	0.811	0.784	0.674	0.731	0.669	0.797	0.821	0.518	0.674	0.613
2002	0.329	0.665	0.585	0.492	0.448	0.633	0.771	0.758	0.910	0.896	0.411	0.720
2003	0.322	0.681	0.655	0.619	0.578	0.667	0.492	0.620	0.873	0.605	0.611	0.735
2004	0.693	0.637	0.742	0.501	0.633	0.617	0.665	0.645	0.276	0.705	0.770	0.660
2005	0.136	0.294	0.619	0.613	0.527	0.770	0.486	0.769	0.694	0.851	0.750	0.712
2006	0.510	0.431	0.671	0.539	0.440	0.743	0.598	0.716	0.672	0.454	0.535	0.593
2007	0.066	0.325	0.794	0.596	0.455	0.707	0.052	0.717	0.713	0.750	0.822	0.584
2008	0.590	0.177	0.892	0.767	0.644	0.673	0.767	0.800	0.881	0.746	0.802	0.428
AVG	0.498	0.511	0.673	0.689	0.564	0.623	0.669	0.658	0.741	0.714	0.664	0.645

Appendix C (Continued)

Table C.3: The standard deviation of temperature during that period

Month	Jan	Feb	Mar	Apr	May	Jun	Jul	Aug	Sep	Oct	Nov	Dec
1981	2.256	2.461	2.842	3.616	3.234	2.719	2.108	2.880	3.307	2.979	3.063	2.318
1982	3.341	2.484	3.479	4.586	3.506	2.362	1.715	1.574	2.629	3.142	3.660	2.218
1983	2.536	1.658	3.540	2.996	3.641	1.898	2.078	1.729	3.011	3.927	3.186	3.611
1984	1.832	2.715	2.342	4.318	3.446	1.801	1.698	1.957	2.589	3.285	3.432	4.253
1985	2.412	2.047	2.697	2.941	1.861	1.608	2.763	1.336	3.367	3.543	4.603	3.068
1986	1.874	2.154	2.740	4.720	2.138	1.653	2.996	2.161	2.288	3.432	2.728	2.208
1987	2.858	2.895	3.919	4.608	3.120	2.697	1.969	1.650	3.632	3.098	3.381	2.736
1988	2.282	2.025	2.700	3.863	3.177	2.095	1.660	1.706	1.752	2.909	3.102	1.974
1989	3.410	2.890	2.586	2.711	2.002	2.240	2.836	1.728	3.098	2.890	4.980	1.978
1990	3.149	3.724	2.862	3.472	2.862	2.285	2.350	2.298	2.646	2.909	2.763	3.192
1991	1.845	2.696	3.330	3.887	4.655	2.400	2.071	2.397	2.621	2.601	2.671	3.258
1992	2.581	1.559	2.562	3.056	2.282	1.753	2.033	1.622	3.585	2.688	3.028	4.135
1993	2.436	3.096	3.261	4.497	2.672	2.484	2.641	1.761	2.537	2.835	3.853	2.681
1994	2.592	2.121	2.686	3.471	2.998	1.859	1.528	1.960	2.672	3.249	3.357	3.822
1995	2.007	1.449	3.349	4.035	2.426	2.030	2.576	1.837	2.235	2.543	2.685	2.287
1996	2.471	2.590	3.879	5.048	3.723	2.196	3.240	2.311	2.271	2.975	3.988	2.567
1997	1.902	2.251	2.686	2.794	3.467	2.268	1.653	2.287	3.614	3.250	2.944	3.321
1998	2.277	2.828	3.004	4.754	2.343	2.473	1.719	1.304	1.811	3.018	3.839	1.965
1999	1.633	2.533	4.060	3.297	1.976	1.995	3.069	2.230	1.927	3.882	3.405	2.729
2000	3.176	1.953	3.070	2.614	2.557	2.285	1.631	1.137	3.535	3.316	3.306	2.688
2001	2.315	2.285	3.683	3.894	2.512	2.340	1.690	2.164	3.120	2.844	2.201	2.326
2002	1.859	2.274	2.921	3.639	1.876	2.272	2.046	2.752	3.371	3.868	2.579	3.304
2003	2.328	2.020	3.170	3.713	3.027	1.910	1.613	1.884	3.892	2.697	3.487	3.177
2004	2.208	3.230	4.073	3.472	2.808	2.451	1.929	1.962	2.126	3.118	3.025	3.266
2005	1.630	2.129	3.225	3.901	2.140	2.153	1.485	1.842	2.452	3.270	2.897	1.942
2006	2.505	3.072	2.980	3.461	2.799	1.761	1.979	1.289	2.767	1.814	3.050	2.465
2007	1.508	2.522	4.030	3.518	2.358	2.196	1.101	2.029	2.811	2.538	3.129	2.675
2008	1.924	1.601	3.264	3.123	2.669	1.712	1.837	2.244	3.472	2.632	3.814	3.371
AVG	2.327	2.402	3.176	3.714	2.796	2.139	2.072	1.930	2.826	3.045	3.291	2.841

Appendix C (Continued)

Table C.4: Monthly mean rainfall (1981-2008)

Month	Jan	Feb	Mar	Apr	May	Jun	Jul	Aug	Sep	Oct	Nov	Dec
1981	3.70	2.28	1.68	3.53	9.31	10.92	8.84	7.21	6.62	9.64	6.04	3.08
1982	3.85	1.81	3.26	6.32	5.03	6.64	6.62	20.20	9.65	2.67	9.95	4.78
1983	3.00	5.39	3.34	10.11	5.96	5.49	20.88	6.88	14.03	5.16	7.73	4.46
1984	3.07	2.88	2.04	5.66	4.46	11.02	8.78	4.78	2.85	3.09	4.08	8.64
1985	2.21	2.93	2.09	6.17	9.47	12.22	17.71	2.98	12.94	4.59	9.07	5.56
1986	6.06	2.53	2.56	6.96	7.19	9.60	13.95	2.36	4.95	5.29	3.27	5.20
1987	4.25	4.01	4.35	2.53	7.98	5.53	13.31	6.06	4.45	7.40	3.14	3.38
1988	4.44	3.01	4.94	5.46	7.79	12.15	10.16	3.44	10.31	4.77	8.10	3.78
1989	4.54	5.02	3.65	7.28	5.92	8.90	11.86	10.71	23.72	3.31	7.41	3.74
1990	4.21	3.71	4.39	6.84	6.62	10.16	8.35	3.65	15.83	8.66	11.22	5.68
1991	4.80	5.07	4.53	5.61	6.30	10.60	9.36	6.16	11.90	6.14	6.26	4.76
1992	3.41	2.59	3.18	6.66	5.66	5.49	6.30	9.38	3.65	6.39	3.95	5.01
1993	3.70	5.50	2.19	4.49	4.85	13.29	11.13	11.75	12.99	4.13	5.70	5.52
1994	2.82	3.44	2.24	2.85	6.39	5.16	2.03	2.09	12.07	2.85	3.55	4.48
1995	6.65	3.01	4.07	7.00	10.02	4.97	20.80	4.67	5.07	3.57	11.65	3.34
1996	3.34	2.55	5.95	1.08	4.08	10.43	3.69	12.12	5.30	3.54	6.60	6.69
1997	4.07	3.12	1.99	4.54	11.07	5.75	12.53	5.03	5.53	4.69	9.36	4.57
1998	3.83	2.04	2.70	7.52	9.60	9.29	12.97	10.91	13.96	11.69	6.04	3.39
1999	4.86	3.59	3.15	6.01	7.30	11.08	7.32	5.59	15.34	4.66	6.54	5.87
2000	2.56	4.03	4.41	6.35	4.13	6.66	5.66	3.12	11.81	5.23	5.30	3.85
2001	7.67	4.44	4.93	1.66	3.88	13.44	4.06	7.46	6.50	6.61	5.55	4.72
2002	9.75	2.52	6.41	6.16	6.12	2.81	14.75	4.54	4.64	9.36	13.34	3.69
2003	4.54	2.17	5.47	12.62	2.93	7.55	12.22	13.49	3.99	3.76	8.89	7.89
2004	3.65	7.70	2.39	7.30	12.47	11.68	13.17	13.48	13.09	12.41	5.34	4.82
2005	5.18	4.17	3.90	1.77	4.06	5.86	12.63	9.70	7.80	5.36	5.25	7.62
2006	3.97	2.46	3.70	3.09	7.11	3.45	18.29	1.72	8.00	4.00	6.99	4.71
2007	2.32	2.42	2.73	1.05	5.72	12.10	10.29	7.62	5.95	4.94	5.57	7.49
2008	1.86	1.89	2.11	2.24	6.04	6.22	4.54	6.57	6.42	4.56	7.01	5.13
AVG	4.23	3.44	3.51	5.32	6.70	8.52	10.79	7.28	9.26	5.66	6.89	5.07

Appendix C (Continued)

Table C.5: Correlation coefficient of mean rainfall between months

Month	Jan	Feb	Mar	Apr	May	Jun	Jul	Aug	Sep	Oct	Nov	Dec
1981	0.468	0.317	0.348	0.047	0.087	0.132	0.619	0.155	-0.053	0.148	0.045	-0.025
1982	-0.251	0.056	-0.104	0.116	0.435	0.183	0.276	0.201	0.196	0.370	0.013	0.214
1983	0.452	0.406	0.070	-0.113	0.084	0.280	0.516	0.210	0.090	0.002	0.396	-0.094
1984	0.268	-0.132	0.123	-0.016	0.281	0.112	0.452	0.275	0.432	-0.072	-0.080	0.078
1985	0.299	0.256	-0.004	0.028	0.089	0.131	0.105	0.118	0.288	0.159	0.111	-0.012
1986	0.283	-0.034	0.010	0.014	0.038	0.171	-0.015	-0.020	-0.112	0.095	0.232	0.187
1987	0.057	0.630	0.112	0.051	0.218	0.127	0.270	0.183	0.462	0.075	-0.130	0.373
1988	0.230	0.177	-0.019	0.267	0.012	0.140	0.089	0.111	0.156	0.214	0.162	0.211
1989	0.141	0.232	-0.110	0.050	0.072	-0.025	0.191	0.142	0.255	0.169	-0.082	0.260
1990	0.088	0.144	-0.147	-0.030	0.189	0.164	0.134	0.022	0.493	0.030	0.085	0.327
1991	0.523	0.193	0.085	0.076	-0.040	0.077	0.312	-0.020	0.036	0.167	-0.096	-0.275
1992	0.128	-0.028	0.107	-0.220	0.224	0.140	0.335	0.203	0.012	0.382	0.033	0.027
1993	0.031	0.008	0.156	0.158	0.044	-0.033	0.516	-0.031	0.170	0.175	-0.067	0.096
1994	0.090	0.080	0.122	-0.067	0.256	0.346	-0.028	0.473	0.631	0.009	0.066	0.188
1995	0.442	0.286	0.135	-0.099	0.183	0.333	-0.120	0.165	-0.068	0.145	0.182	0.210
1996	0.511	0.591	0.340	-0.103	-0.049	0.331	-0.010	0.430	-0.080	-0.157	-0.099	0.170
1997	0.357	0.020	-0.074	0.399	0.093	-0.058	0.173	0.519	-0.009	0.291	0.067	0.336
1998	-0.022	0.082	-0.105	0.323	0.189	0.146	0.270	-0.117	0.255	0.540	0.538	0.063
1999	0.470	0.333	-0.073	0.173	-0.041	0.109	0.104	0.056	0.051	0.167	-0.040	-0.145
2000	-0.016	-0.004	0.059	0.093	-0.084	0.154	0.059	0.198	0.157	-0.082	0.073	0.334
2001	0.318	0.396	0.215	-0.015	0.391	0.165	0.309	0.411	0.122	-0.017	0.087	0.075
2002	-0.056	0.234	-0.030	-0.026	0.220	-0.099	0.040	-0.083	-0.078	0.374	0.239	0.139
2003	0.319	-0.018	0.104	0.148	-0.029	0.456	0.195	0.135	0.269	0.395	0.091	0.170
2004	-0.032	0.252	-0.086	0.146	0.146	-0.074	-0.043	0.567	0.018	0.109	-0.029	0.257
2005	0.354	0.478	0.133	-0.135	0.066	0.543	0.057	-0.130	0.107	-0.037	0.057	0.095
2006	0.262	-0.131	0.253	0.174	0.015	0.004	0.630	0.031	0.329	0.126	0.121	0.253
2007	0.506	0.106	0.351	0.038	-0.122	-0.074	0.234	0.090	0.037	-0.053	0.166	0.143
2008	0.314	-0.068	-0.230	-0.053	0.037	-0.022	0.002	-0.056	0.192	0.091	0.157	0.100
AVG	0.233	0.174	0.062	0.051	0.107	0.138	0.203	0.151	0.156	0.136	0.082	0.134

Appendix C (Continued)

Table C.6: The standard deviation of rainfall during that period

Month	Jan	Feb	Mar	Apr	May	Jun	Jul	Aug	Sep	Oct	Nov	Dec
1981	8.843	3.623	3.314	4.564	15.693	16.127	24.648	13.112	12.554	15.808	7.659	3.769
1982	3.748	2.404	6.328	12.403	8.523	12.194	8.277	38.532	18.267	6.409	14.391	5.598
1983	3.451	5.701	5.497	15.937	17.772	14.758	29.642	15.851	26.923	9.766	11.859	5.242
1984	2.933	5.446	2.103	15.605	11.739	18.753	13.913	13.894	4.934	6.544	11.593	9.157
1985	3.099	4.163	3.195	9.993	20.289	22.197	28.850	6.645	16.077	7.267	8.494	6.431
1986	5.974	3.256	5.942	13.632	9.946	19.427	23.800	5.505	11.720	9.301	4.630	7.588
1987	4.507	6.102	5.969	5.977	15.705	12.175	21.574	12.764	9.196	21.211	5.466	5.000
1988	5.333	4.298	7.026	9.424	11.052	25.360	19.107	6.861	18.696	10.553	10.429	3.885
1989	6.421	6.849	5.904	12.929	8.118	17.133	21.908	23.948	39.064	5.417	14.991	5.303
1990	4.709	6.352	6.919	11.989	14.374	15.964	15.195	9.674	25.413	16.149	20.932	6.093
1991	3.751	2.963	5.117	6.835	12.185	15.170	12.324	11.502	22.437	8.833	7.360	4.265
1992	4.248	3.726	5.085	11.597	8.528	12.537	11.956	22.248	9.492	7.887	6.776	7.503
1993	4.973	7.631	4.053	5.891	10.187	20.660	16.369	18.388	23.889	8.386	10.371	6.780
1994	4.077	5.724	3.924	5.714	10.752	7.367	5.344	5.201	20.417	7.515	5.795	6.624
1995	7.381	4.022	5.895	10.488	15.260	9.026	28.255	12.159	10.547	6.527	13.146	3.722
1996	4.112	4.513	9.136	3.055	8.545	19.286	9.889	29.255	10.696	5.462	7.655	10.106
1997	4.633	4.144	2.930	6.701	21.390	16.485	17.557	13.606	10.116	8.881	15.832	5.610
1998	4.535	3.369	6.247	13.222	14.875	17.457	30.307	17.301	31.106	24.984	8.848	5.015
1999	5.686	3.613	5.639	9.119	18.950	19.521	18.387	10.576	37.125	10.035	9.660	6.487
2000	3.483	4.553	5.589	10.123	7.676	14.158	13.307	6.257	25.707	9.026	9.973	4.249
2001	5.667	6.558	6.148	3.690	6.991	24.063	8.957	19.689	12.440	13.183	10.492	6.759
2002	10.668	2.671	10.085	11.720	9.441	6.955	43.804	14.483	12.333	13.725	13.198	5.506
2003	6.462	2.702	9.503	17.530	8.460	12.239	13.248	32.494	6.869	8.190	13.126	7.138
2004	4.229	9.299	4.389	18.071	21.302	27.925	49.381	27.156	21.099	36.015	8.582	12.938
2005	5.299	5.363	4.709	3.974	7.452	17.355	30.187	17.034	23.523	10.466	8.474	6.571
2006	5.600	3.584	5.214	6.019	11.024	8.497	30.480	7.403	14.095	8.868	9.015	5.731
2007	4.222	3.413	3.865	1.927	12.565	25.166	17.707	15.090	9.653	11.391	12.460	7.028
2008	3.036	2.046	2.887	4.254	10.899	20.645	10.426	11.533	15.399	9.244	9.361	7.402
AVG	5.039	4.575	5.450	9.371	12.489	16.736	20.529	15.649	17.850	11.323	10.377	6.339

Appendix C (Continued)

Table C.7: The summarize of statistical parameters for temperature generating model

Month	Correlation	Mean	Slope	SD
Jan	0.498	1.057	0.030	2.327
Feb	0.511	1.232	0.052	2.402
Mar	0.673	5.096	0.047	3.176
Apr	0.689	11.914	0.016	3.714
May	0.564	17.211	0.037	2.796
Jun	0.623	21.071	0.041	2.139
Jul	0.669	24.704	0.030	2.072
Aug	0.658	26.136	0.002	1.930
Sep	0.741	21.868	0.079	2.826
Oct	0.714	15.400	0.078	3.045
Nov	0.664	9.425	0.035	3.291
Dec	0.645	3.861	0.031	2.841

Table C.8: The summarize of statistical parameters for rainfall generating model

Month	Correlation	Mean	Slope	SD
Jan	0.233	4.225	0.024	5.039
Feb	0.174	3.438	0.002	4.575
Mar	0.062	3.513	0.034	5.450
Apr	0.051	5.316	-0.085	9.371
May	0.107	6.696	-0.030	12.489
Jun	0.138	8.516	-0.068	16.736
Jul	0.203	10.793	-0.055	20.529
Aug	0.151	7.275	-0.006	15.649
Sep	0.156	9.263	-0.091	17.850
Oct	0.136	5.659	0.036	11.323
Nov	0.082	6.890	0.011	10.377
Dec	0.134	5.066	0.041	6.339